ADAPTATION OF RAINFALL-RUNOFF MODELS FOR RUNOFF SIMULATION IN THE HUMID ZONES OF KENYA:

A CASE STUDY OF THE UPPER EWASO NGIRO DRAINAGE BASIN

BY

OLANG' LUKE OMONDI

A Thesis Submitted to the Graduate School in Partial Fulfillment of the Requirements for the Masters of Science Degree in Agricultural Engineering of Egerton University.

EGERTON UNIVERSITY

MAY, 2004

DECLARATION AND RECOMMENDATION

I hereby do declare that this thesis is my original work and that to the best of my knowledge it has not been presented for the award of any other degree in any other University.

SIGNED..**Date** 02/06/2004.

Luke Omondi Olang'

This thesis has been submitted with our approval as the University Supervisors.

1) **Dr. Japheth O. Onyando**
Department of Agricultural Engineering
Egerton University, Njoro.

SIGNED..**Date** 3/6/2004

2) **Dr. Mathew C. Chemelil**
Department of Agricultural Engineering
Egerton University, Njoro.

SIGNED..**Date** 3/6/2004

DEDICATION

First and foremost, this thesis is dedicated to my parents Mr. and Mrs. Ezra Olang Owuondo for continued support and encouragement throughout the study period. Secondlly, to Dan & Rachel Obiero for their love and support. Lastly, to Sheila Cecily for her patience and continuous love during the times of doing this work.

COPYRIGHT

ACKNOWLEDGEMENTS

First and foremost, thanks are to the Almighty GOD who makes all things possible. Secondly, I would like to appreciate the personal commitments, guidance as well as the continuous supervision of Dr. J. O. Onyando and Dr. M. C. Chemelil. Their regular discussions and articulate criticisms greatly contributed towards the completion of this work. I would also wish to thank UNESCO for their financial support through my supervisors. This arrangement enabled me to effectively carry out my project and to prepare the thesis. Many thanks also go to CETRAD in Nanyuki for their support during the period of data acquisition

Many thanks go to Dr. D. M. Nyaanga of the Department of Agricultural Engineering, Egerton University. His valuable suggestions and criticisms enabled me to put the whole work in focus. Special thanks also go to Dr. A. Kahi of the Department of Animal science, Egerton University for allowing me to use his computer facilities. To all my lecturers and colleagues in the Faculty of Engineering and Technology, and to the experts in the various departments of the university where I obtained assistance in one-way or another, let me say thank you very much for the support offered during the development of this thesis.

Last but not least, to Uncle Simon Guya Owuondo and Dr. Moses Onim of LAGROTECH consultants. Thank you very much for the financial support that enabled me to complete my studies. God bless you all.

ABSTRACT

The design and operation of water resource management structures require reliable runoff data. Such data are available from catchments gauged with automatic recording instruments such as water level recorders and divers. However, in Kenya, such data are rare due to the high costs associated with the acquisition and maintenance of the instruments. Consequently, there is need to explore ways to generate runoff data for effective catchment management. This research explored the generation of runoff data through the use of conceptual rainfall-runoff models. Two lumped models, namely the Nash cascade-Diskin infiltration model and the Nash cascade-Green and Ampt infiltration models were used in this study. The models were applied in five catchments in the upper Ewaso Ngiro drainage basin in Kenya. Forty-five rainfall-runoff events were used to calibrate and validate the models. The conceptual parameters of the models on one hand were optimized using optimization algorithms and the physical parameters of the models were obtained from catchments characteristics with the help of Geographical Information Systems (GIS). The models satisfactorily simulated direct runoff in the five gauged catchments. In order to apply the models to ungauged catchments of the same drainage basin, the models were regionalized by developing transfer functions relating the conceptual parameters of the models to the characteristics of the catchments. Transfer functions were then tested in the gauged catchments of upper Ewaso Ngiro basin for use in ungauged catchments. The results obtained indicated that the two models had high potential for use in direct runoff generation in ungauged catchments.

TABLE OF CONTENTS

LIST OF TABLES

LIST OF FIGURES

LIST OF ABBREVIATIONS AND SYMBOLS

^{0}C	Degrees Centigrade
5BC4	Sub-catchments 5b gauging station number 4
A3	Naromoru North catchment
A4	Naromoru South catchment
AP	Lower Teleswani catchment
AQ	Mid Ituuri catchment
AR	Lower Ituuri catchment
CD-ROM	Compact Disc Read Only Memory
CETRAD	Center for Training, Research and Development
DEM	Digital Elevation Models
DRSRS	Department of Resource Surveys and Remote Sensing
EFF	Nash and Sutcliffe Efficiency
FAO	Food and Agricultural Organization
GAI	Green Ampt Infiltration
GIS	Geographical Information Systems
LRP	Laikipia Research Programme
MWR	Ministry of Water Resources
NC	Nash Cascade
NCDI	Nash Cascade Diskin Infiltration
NCGAI	Nash Cascade Green Ampt Infiltration
PEP	Percentage Error of Peak
RS	Remote Sensing
TSSR	Total Sum of Squares of Residuals
UNESCO	United Nations Education, Scientific and Cultural Organization
US	United States
USDA	United States Development Agency
US-SCS	United States Soil Conservation Service
D_d	Drainage density
f_c	Minimum infiltration rate

f_o	Maximum infiltration rate
$g(t)$	Percolation rate
$h(t)$	Response function at time, t
k	Storage constant
n	Number of linear reservoirs in cascade
$P(t)$	Rainfall at time, t
P_e	Effective rainfall
$Q(t)$	Direct runoff rate at time, t
Q_i	Linear reservoirs
$q(t)$	Infiltration rate
R_F	Form factor
S_{ch}	Channel slope
S_{ca}	Catchment slope
S_m	Maximum soil storage capacity
S_o	Soil moisture content
S_{ov}	Overland slope
$y(t)$	Runoff at time, t

DEFINATION OF TERMS

Adaptation	Application of a model to the local conditions of the study area
Adoption	Careful selection and use
Catchment	Area basin that drains into a particular stream or lake
Calibration	Determination of model parameters as relates to the conditions of the study area
Validation	Verifying that the model parameters calibrated can reproduce same results
Model	A small or larger replication of the real prototype
Simulation	Artificial creation of hydrologic phenomena using a model
Optimization	Comparing amongst a set of the available options to find the best possible fit
Regionalization	Relating the conceptual parameters of the model to the catchments characteristics
Hydraulic conductivity	A property of the soil that determines its ability to allow water to pass through
Hydraulic head	the total energy head at a particular point in a medium

CHAPTER ONE: INTRODUCTION

1.1 Background

In the tropical countries, the rural communities encroach into the humid areas to open up new land for agriculture. In Kenya for instance, the humid areas cover about one third of the total area of the country and support a greater part of the rural population who earn their living through agriculture (Onyando, 2000). Due to the increasing population pressure in these areas in search of land for agriculture, there has been over-exploitation of the available resources, which in turn has resulted to increased environmental degradation.

One of the drainage basins in Kenya which has undergone extensive land use changes in the recent past is the Ewaso Ngiro drainage basin. This is due to intervention by the local communities to open up more arable land for subsistence and commercial agriculture, settlements amongst others. The problem is more pronounced in the upper catchments of the basin. This area has undergone severe land degradation due to soil erosion owing to the exposure of soil to erosion agents such as water and wind. Figure 1 shows part of the upper Ewaso Ngiro drainage basin which has been severely eroded by surface runoff.

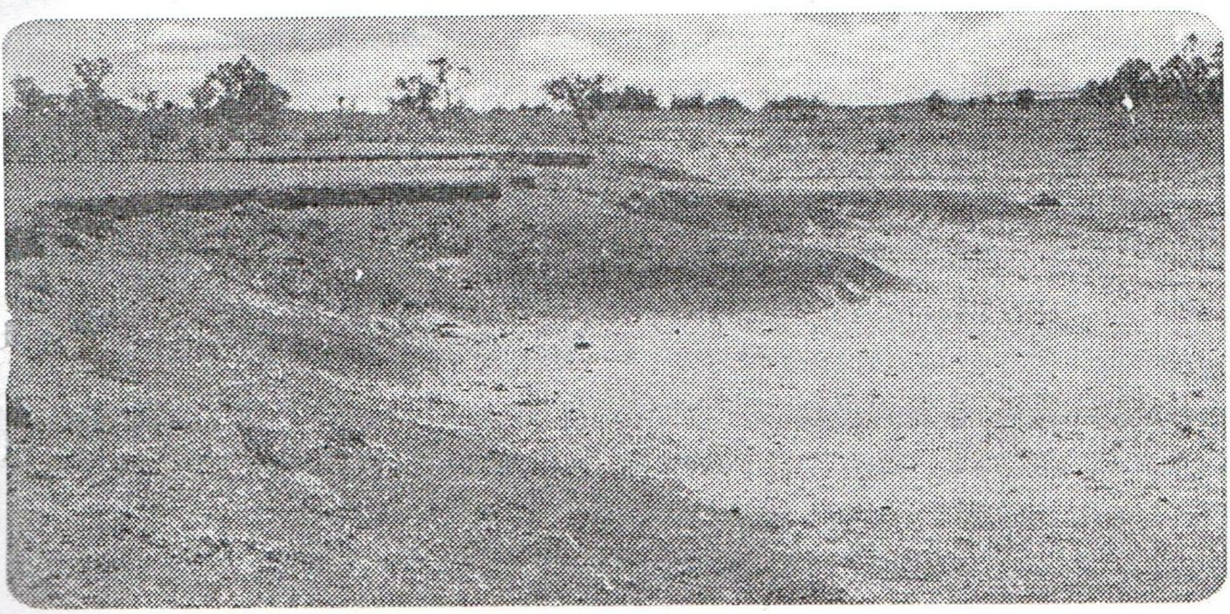

Figure 1 Land degradation in the upstream catchments of Ewaso Ngiro basin.

Since surface runoff is the major cause of erosion in this area, there is need to provide runoff data to control erosion and other forms of land degradation. Runoff data are essential for the design of water resource structures that are required for controlling the flow of water, both in the catchments and within the stream channels. Under normal circumstances, surface runoff data can be obtained from catchments gauged with automatic water level recorders. Such catchments however, are very few due to the high costs associated with the procurement, installation and maintenance of the automatic recording instruments. The few gauged catchments also do not have consistent rainfall-runoff data records due lack of proper maintenance of the gauging instruments.

Because of the high expenses involved in automatic gauging, only research catchments in Kenya have stage graphs from which surface runoff can be derived. Such catchments, however, operate only during periods of research after which they become non-operational due to lack of proper attendance. Examples of such catchments are Sambret and Lagan located at the eastern slopes of Mau ranges and Kimakia catchments on the eastern slopes of Aberdare ranges among others. In these rural catchments, Onyando and Sharma (1995) demonstrated that it was possible to simulate direct runoff using models.

Direct runoff data can be generated using rainfall-runoff models. These models have physical and conceptual parameters and require historical runoff data of the catchments for their calibration. Majority of these models have been widely used in the developed countries (Houghton-Carr, 1999 and Stewart *et al.*, 1999) but have limited application in the tropical countries such as Kenya (Onyando, 2000). For rainfall-runoff models to be used to simulate runoff process there is need to adapt them to the local conditions especially when applied in regions other than the ones they were developed in. This adaptation is attained through model calibration and validation (Duan *et al.*, 1992).

Calibration and validation is achieved by determining the physical and conceptual parameters of the model. Conceptual parameters are determined with the help of optimization algorithm (Sorooshian and Gupta, 1995) using observed rainfall and runoff data from the gauged catchments. Physical parameters of the models are determined from geophysical characteristics of the catchments with the help of GIS. Geophysical data of the catchments are obtained from soil maps, topographic maps, aerial photographs and satellite imagery.

After calibration, the model parameters are then validated before the models can be used to simulate runoff process in gauged catchments. However, for the models to be used to simulate runoff in ungauged catchments there is need to regionalize them. This is done by relating the conceptual parameters of the models to the catchments characteristics through regression analysis.

In this study, the Nash-Diskin (NCDI) and the Nash-Green Ampt (NCGAI) models were chosen and adapted in the small catchments of the upper Ewaso Ngiro drainage basin. The former is a combination of the Diskin Infiltration models for runoff generation (Diskin and Nazimov, 1995) and Nash cascade model for runoff routing (Chow *et al.*, 1988). The latter is a combination of the Green-Ampt infiltration model (Chow *et al.*, 1988) and the Nash cascade model for runoff routing. These two models were chosen for this study because they have few parameters but still represent the response of the catchments well.

This research was accomplished in the small upper catchments of the Ewaso Ngiro basin. This area has been undergoing rapid changes in land use systems in the recent past. Land degradation due to water is also eminent in this area and therefore the dire need for an effective catchment management system. Apart from that, the catchments in this area have historical rainfall-runoff data required for the calibration and validation of the models.

1.2 Statement of the Problem

The main problem in river basin management in Kenya is lack of reliable hydrological data, and especially runoff data, required for the designs of water resource structures. Lack of runoff data occurs in ungauged catchments. Inadequate and unreliable runoff data on the other hand occur in catchments that are either poorly managed and therefore have short-inconsistent runoff data or in non-operating gauged catchments with totally inaccurate runoff data.

1.3 Broad Objective

The main objective of this study was to adapt the NCDI and NCGAI conceptual rainfall-runoff models for direct runoff simulation from small catchments of the upper Ewaso Ngiro drainage basin.

Specific objectives

i) To calibrate and validate the NCDI and NCGAI conceptual models in the upper Ewaso Ngiro drainage basin.

ii) To simulate direct runoff using the calibrated and validated models in the chosen gauged catchments.

iii) To regionalize the models by developing transfer functions between the conceptual parameters of the models and the catchments characteristics.

1.4 Hypotheses

i) NCDI and NCGAI rainfall-runoff models, developed outside the humid tropics, cannot be calibrated and validated in the humid zones of Kenya.

ii) The calibrated rainfall-runoff models cannot simulate direct runoff in the gauged catchments.

iii) There is no relationship between the conceptual parameters of the model and the catchments characteristics.

1.5 Justification of the Study

Encroachment of the humid areas by the rural communities in search of better and fertile land for agriculture has resulted into over-exploitation of natural resources and consequently increased environmental degradation. Soil erosion, a major form of land degradation has continued to rise due to increased surface runoff as a result of the ever changing land use patterns. This has given rise to high magnitude floods which are destructive to the water conservation structures; especially those designed using unreliable and inadequate data.

Appropriate design of soil erosion control structures using reliable runoff data is a prerequisite to effective catchments management. Runoff data can be acquired from catchments that are gauged with the appropriate automatic runoff measuring instruments. These instruments however, are expensive to acquire and maintain in most catchments. The use of rainfall-runoff models therefore provides an alternative means for the production of runoff data. Rainfall-runoff models have been applied for runoff simulation in catchments such as Lagan located on the Eastern slopes of Mau ranges and Kimakia catchments located on the Eastern slopes of Aberdare Ranges. In these catchments, Onyando and Sharma (1995) and Onyando (2000) demonstrated that it was possible to generate surface runoff data through the use of rainfall-runoff models. The authors recommended further research in these areas with a view of adapting more models to be used for runoff data generation in ungauged catchments.

In this study, two conceptual models, NCDI and NCGAI were chosen and adapted in the small catchments of the upper Ewaso Ngiro drainage basin. Each of the two models has components for runoff generation and runoff routing. The Nash model was chosen for runoff routing because it has few parameters and still represent the response of the catchments in an effective manner (Nash and Sutcliffe, 1970). The Diskin and Green-Ampt infiltration models were used for this study since they have parameters that can easily be determined from the physical characteristics of the catchments. And because a catchment is a dynamic system that undergoes changes in its characteristics, there was need to analyze the spatial distribution of these characteristics so as to derive the physical parameters of the models. This was achieved with the help of GIS ArcView.

This research therefore, aids in the provision of a comprehensive runoff data base that should provide a baseline for the design of water resource structures. In gauged catchments, calibrated and validated rainfall-runoff models can be used to estimate missing runoff data. The models can also be used to provide runoff data in ungauged catchments in the same geographical location. This however, requires that the models be regionalized.

CHAPTER TWO: LITERATURE REVIEW

2.1 Hydrologic Models

Hydrologic models represent the behavior of a catchment in transforming a hydrologic input, rainfall into an output, runoff. These models are therefore mathematical expressions that simulate runoff in a manner similar to the way a catchment would operate on the same rainfall event. In developing hydrological models, assumptions are placed in applying the physical laws that govern the processes to simplify the larger and more complex catchment systems.

Hydrologic models fall under different categories according to the way they treat randomness of the hydrologic phenomena and spatial variation of the hydrologic process. These categories are highlighted in several hydrologic texts including Chow *et al.*, 1988; Shaw, 1996 and Singh, 1995. One of such classification adopted from Chow *et al.*, (1988) is shown in Figure 2.

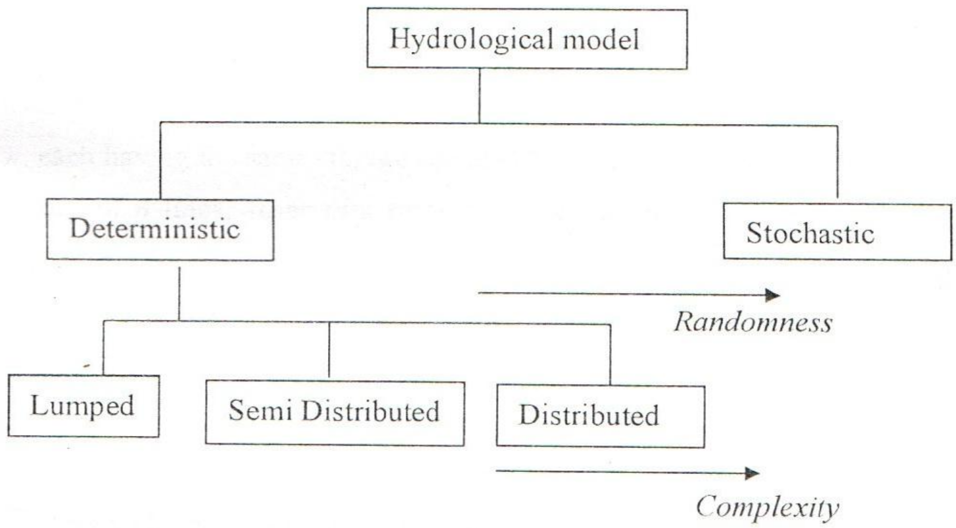

Figure 2 Classification of hydrologic models (Adapted from Chow et al., 1988)

The two major categories of hydrologic models in Figure 2 are stochastic and deterministic. Stochastic models are generally used for time series rainfall-runoff analysis while deterministic models are used to analyze rainfall-runoff process on event basis. Deterministic models have physical and conceptual parameters and can be classified as lumped, semi-distributed or distributed. Lumped models aggregate the parameters over the entire catchment and are therefore less complex in their application (Onyando, 2000). Distributed models aggregate the rainfall-runoff process at micro-scale, making them more complex and limited in applicability (Abbott *et al.*, 1986).

In semi-distributed models, aggregation is done based on hydrological similar events (Leavesley and Stannard, 1995). This method of aggregation is less complex than in distributed models but more representative than in lumped models. Aggregation based on hydrological similar units and catchment basis was used in the derivation of the parameters for the Nash Cascade-Diskin Infiltration and Nash Cascade-Green Ampt Infiltration rainfall-runoff models.

2.1.1 The NCDI model

NCDI model is a combination of Diskin infiltration model for runoff generation (Diskin and Nazimov, 1995) and Nash cascade model for runoff routing (Shaw, 1996). The model for runoff generation was tested by the authors and satisfactory results obtained (Diskin and Nazimov, 1995; 1996). The authors further demonstrated that the model could be applied under high water application rates. This makes the model suitable for use under the humid rainfall conditions.

Nash cascade model for runoff routing represents a catchment as a series of identical linear reservoirs n, each having the same storage constant k. The model routes a unit volume of inflow through a series of n linear reservoirs so as to yield a direct runoff hydrograph. Junil *et al.*, (1999) tested the Nash model in Su-Young river basin in South Korea. The results obtained were in good agreement with the observed runoff data. Onyando (2000) combined Diskin infiltration model and Nash cascade model for event based rainfall-runoff analysis using data from five catchments in Kenya and Germany. The simulation results obtained for this model compared satisfactorily to the observed rainfall-runoff data. However, since the catchments used were from different agro-climatic zones, it was not possible to obtain trends between the conceptual parameters of the model and catchment characteristics across the five catchments to establish its potential for use in the ungauged catchments. The authors thus recommended further work on this model with the aim of verifying its potential in simulating runoff in other humid areas of Kenya.

Structure of the NCDI Model

The schematic structure of the NCDI model is presented in Figure 3 (Diskin and Nazimov, 1995). From the figure, the Diskin Infiltration model for runoff generation starts with the inlet-regulating element that receives an input $P(t)$ and produces two outputs, $y(t)$ and $q(t)$. This element has a state variable $F(t)$, which determines the magnitude of the two outputs as shown in the figure.

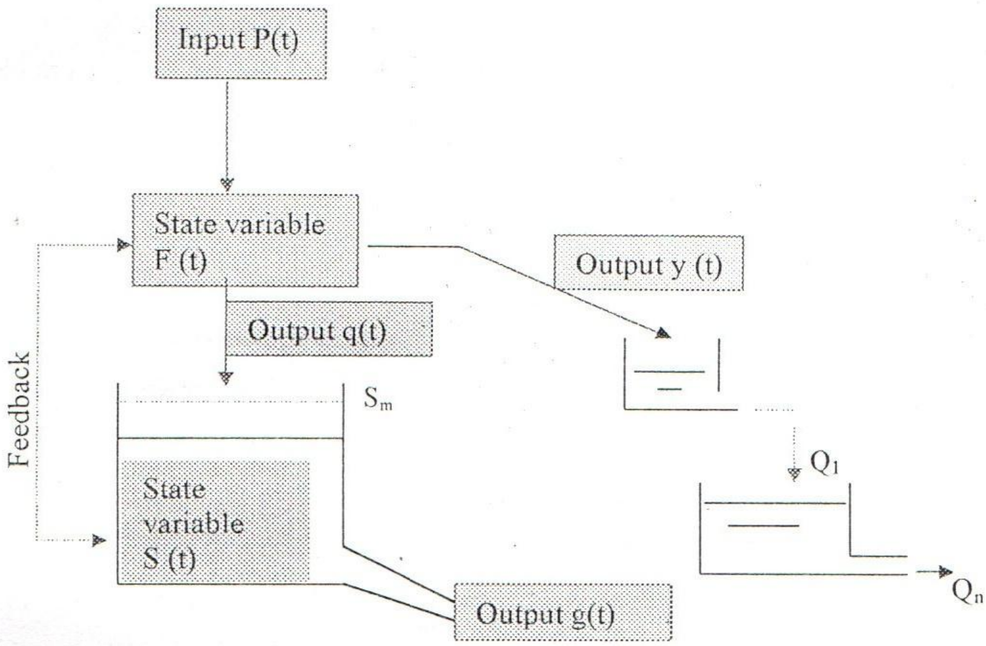

Figure 3 Schematic structure of the NCDI model (Adopted from Onyando, 2000)

The model also has the storage element which receives an input $q(t)$ and produces an output $g(t)$. It has a state variable $S(t)$ that determines the magnitude of $g(t)$. The state variable $S(t)$ has a maximum value of S_m. The state of the storage element is linked to the regulating element by a feedback path, which transmits information about the status of the element. Further linkage of the two state elements is through the output $q(t)$ (Diskin and Nazimov, 1995).

The Nash Cascade model for runoff routing starts with the output, $y(t)$ from the inlet-regulating element (Figure 3). The flow is routed through a series of linear reservoirs, Q_1, Q_2... Q_n assumed to represent the way the catchment transforms inflow into outflow.

In order to apply the Diskin Infiltration model for runoff generation, it is important to interpret the model in accordance with the infiltration process. The storage element is assumed to represent soil moisture $S(t)$ in excess of field capacity in the upper soil layer and varies from zero to a maximum value of S_m. Infiltration rate into this layer is defined by $q(t)$ while $g(t)$ represents the percolation rate. $P(t)$ represents the rainfall input and $y(t)$ is the resulting runoff.

The inlet regulation element is assumed to represent the soil surface. This determines the average infiltration capacity, $f(t)$ in accordance with the time value of the soil moisture storage of the upper soil zone. At complete depletion of the soil moisture storage, $S(t)$ equals to zero and the infiltration capacity, $f(t)$ is at its maximum value f. At maximum storage, $S(t)$ equals S_m and the infiltration capacity $f(t)$ will be at its minimum value of f_c. The inlet-regulating element on the other hand determines the portion of the rainfall input, $P(t)$ that becomes actual infiltration, $g(t)$ and that which constitutes the surface runoff, $y(t)$.

In order to apply this model, the required mathematical expressions are discussed below:

a) Surface-runoff component

Generation of surface runoff is achieved by using Diskin-Infiltration model. Diskin and Nazimov (1995) provided the mathematical expressions used for the generation of surface runoff. The main assumption in this model is that the storage element is a linear reservoir that produces an output proportional to the volume in storage.

The value of the output $g(t)$ can be expressed as:

$$g(t) = A \times S(t) \qquad 1$$

where A is a constant representing a model parameter.

The other assumption here is that the state variable of the inlet-regulating element $F(t)$ is determined by the value of $S(t)$ transmitted by a feedback loop to the inlet-regulating element. The two state variables are related by a decreasing linear relationship given by:

$$F(t) = B - C \times S(t) \qquad 2$$

where B and C are model parameters.

The outputs $g(t)$ and $y(t)$ from the inlet-regulating element depend on the state variable $f(t)$ and the input $P(t)$. This subdivision is done according to the current value of the infiltration capacity rate as specified in Equations (3) and (4).

$$q(t) = \begin{cases} P(t) \ \text{for} P(t) < f(t) \\ f(t) \ \text{for} P(t) > f(t) \end{cases} \qquad 3$$

$$y(t) = \begin{cases} 0 \ \text{for} P(t) < f(t) \\ P(t) - f(t) \ \text{for} P(t) > f(t) \end{cases} \qquad 4$$

The time value of the state variable $S(t)$ is dependent on the input $q(t)$ and the output $g(t)$. Based on the principles of conservation of mass, the relationship between these three variables can be expressed as:

$$dS/dt = q(t) - g(t) \qquad 5$$

where $g(t)$ and $q(t)$ are in run per unit time while S is in run. Plotting Equations (1) and (2) on the same coordination system, a linear relationship showing the variation of infiltration capacity, f and percolation rate, g with soil moisture, S are obtained as shown in Figure 4.

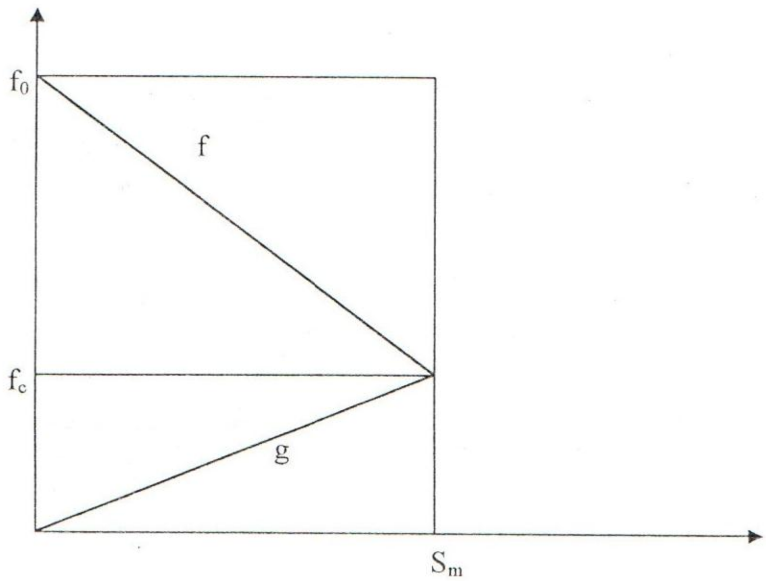

Figure 4 Functional relationship between infiltration capacity rate f, percolation rate g and storage S. Adopted from Diskin and Nazimov, 1995.

From Figure 4, it can be observed that an increase in the soil moisture content of the storage element causes a decrease in the infiltration capacity rate and an increase in the rate of percolation. The moisture content of the storage element increases as long as the infiltration capacity rate is more than the percolation rate until the maximum value is reached in which case

$$S(t) = S_m \text{ when } f(t) = g(t) = f_c \text{ and } ds/dt = 0 \qquad 6$$

From the equations presented above, three model parameters can be identified. These are the highest infiltration capacity f_o the smallest infiltration capacity f_c and the maximum storage S_m. These parameters can further be related to those expressed in Equations (1) and (2) as shown by

Equations (7) to (10). Since the maximum percolation rate g equals to f_c when storage is maximum. Substituting these values in Equation (1), we get:

$$A = \frac{f_c}{S_m} \qquad 7$$

From Equation (2), the relationship between B and f_o can be obtained at complete depletion of soil moisture storage

$$B = f_0 \qquad 8$$

Since $f(t)$ equals $g(t)$ when $S(t)$ equals S_m, then by solving Equations (1) and (2) simultaneously leads to an expression for C.

$$C = \frac{B - A \times S_m}{S_m} \qquad 9$$

If A and B from Equations (7) and (8) are substituted in Equation (9), an expression for C is obtained in terms of the model parameters f_o, f_c and S_m.

$$C = \frac{f_0 - f_c}{S_m} \qquad 10$$

Having expressed the three parameters A, B and C , in terms of the infiltration parameters of f_o, f_c and S_m, substituting these parameters into Equations (1) and (2) leads to expression for percolation $q(t)$ and infiltration capacity rate $f(t)$ shown by Equations (11) and (12).

$$g(t) = \frac{f_c \times S(t)}{S_m} \qquad 11$$

$$f(t) = \frac{f_o - (f_0 - f_c) \times S(t)}{S_m} \qquad 12$$

The equations given above can further be used to derive other equations to calculate the components for surface runoff generation (Diskin and Nazimov 1995).

b) Direct runoff routing

The Nash cascade model is used to route the flow generated by the Diskin Infiltration model. The routing equations are:

$$h(t) = \frac{1}{k\Gamma n}\left(\frac{t}{k}\right)^{t-1} e^{-\left(\frac{t}{k}\right)} \qquad 13$$

$$Q(t) = \int_{0}^{t} h(t-\tau) \times p_e(\tau) \times d\tau \qquad 14$$

where $h(t)$ is the response function at time $t(h^{-1})$, n is the number of linear reservoirs in cascade, $Q(t)$ is the direct runoff rate in units similar to P_e ,k is the storage constant and Γ is the gamma function.

2.1.2 The NCGAI Model.

The NCGAI is a combination of the Green-Ampt infiltration model for the generation of excess rainfall and Nash cascade model for routing the excess rainfall. Smith and Parlange (1978) applied Green-Ampt model for infiltration modeling and obtained results that were good enough in comparison to the observed values. Rawls and Brakensiek (1982, 1983) statistically analyzed Brooks-Corey and the Green-Ampt parameters across different soil textures. The results of the two model parameters varied collectively across the soil textural classes. The author also provided mean parameter values that could be used to obtain infiltration estimates in ungauged catchments.

Wesley *et al.*, (1992) compared the performance of the Green-Ampt model and Soil Conservation Service (SCS) curve number procedure in seven watersheds in the United States. Green-Ampt model delivered better results especially for precipitation that were greater than 25.4 mm. Obiero and Sharma (2002) estimated infiltration process using the Green-Ampt model in three small catchments of Lake Victoria basin in Kenya. The infiltration results obtained were poor when the soil input parameters obtained from USDA texture nomographs were used. However, improved results were obtained when the model parameters were derived through an optimization and validation exercise.

In the recent past, the Green-Ampt model has widely been used for estimating infiltration. This is because the model is physically based and therefore has parameters that can be derived from catchment characteristics (Brakensiek and Onstad, 1977). This property enables the model to be readily used for direct runoff generation in both gauged and ungauged catchments. Apart from that, Green-Ampt model is also suitable for estimating infiltration under rainy conditions thereby making it appropriate for use on catchment basis.

Green-Ampt infiltration model considers a rainfall event occurring in a catchment as a unit impulse input occurring in small duration of time, Δt. The catchment in turn responds by producing response function that takes the forms of infiltration and surface runoff. The model is therefore conceptualized as a homogenous soil profile with uniformly distributed soil moisture. The saturation process is visualized as the passage of a piston-wetting front through the soil profile as shown in Figure 5.

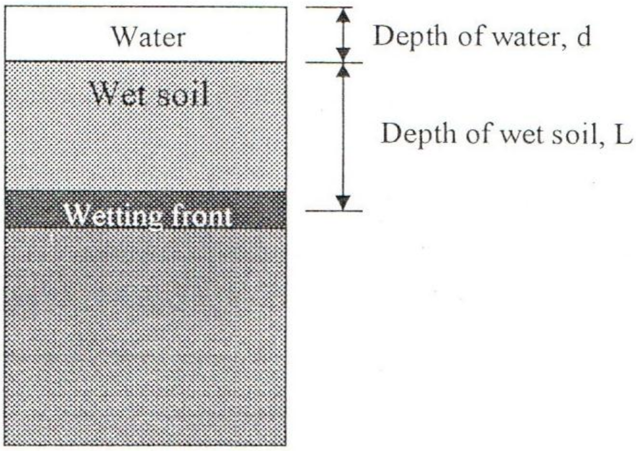

Figure 5 Conceptual profile for the GAI equation (Adopted from Wesley *et. al.*, 1992)

In Figure 5, the soil moisture ahead of the wetting front is assumed to be the antecedent moisture content while that behind equals to the effective porosity. The difference between the two gives the soil moisture variation in the soil column. As the saturation process continues downwards, the flux into the soil is calculated from Darcy's law expressed in Equation (15).

$$v = -K\frac{\partial h}{\partial z} = -K\frac{h_1 - h_2}{L} \qquad 15$$

Where the moisture flux, v has the dimension of length per unit time and occurs in the opposite direction to the infiltration process. K is the hydraulic conductivity and δh/δz is the hydraulic gradient. The units for K and the flux are the same. L is the length of the wetted soil column while h_i is the change in the hydraulic head within the soil column. At the soil surface, the hydraulic head equal to zero as the excess water is assumed to flow away as direct runoff. At a depth L, the hydraulic head equals to the sum of the wetting front suction head and depth of the wetted soil layer. Substituting these values, the infiltration f is obtained as.

$$f = K\frac{\varphi\Delta\theta + F}{F} \qquad 16$$

where L is given by $F/\Delta\theta$ with F being the cumulative infiltration and $\Delta\theta$ the change in the soil moisture content across the soil layer. The application of Green-Ampt model for infiltration estimation requires the parameter inputs of effective porosity P, hydraulic conductivity, K and the hydraulic head at the wetting front, φ. These parameters are physically based and can be derived from catchment characteristics.

Wesley *et al.*, (1992) deduced that good results, when using Green-Ampt Infiltration model, are attained with careful use and approximation of the parameters, especially where they are obtained physically from the soil characteristics. The authors further noted that good correlations existed between the observed and calculated values of effective porosity, while the hydraulic head at the wetting front and hydraulic conductivity did not correlate well due to their site specificity and high degree of variability within the catchments.

Because of this reason, this study chose to treat the hydraulic conductivity and the hydraulic head at the wetting front as conceptual parameters of the model. The mathematical expressions for adapting the Nash-Green and Ampt model as adopted from Chow *et al.*, (1988) are outlined in the next section.

(a) Generation of surface runoff

Green-Ampt Infiltration model generates runoff by removing infiltration abstractions from the total precipitation. The model assumes that abstractions due to interception and depression storage are negligible in comparison to infiltration. In this model, the infiltration rate is computed and compared with the rainfall intensity at every given time interval to determine the infiltration capacity of the soil. This process is repeated at each time interval throughout the rainfall event. The potential infiltration rate at any time interval is computed from the cumulative value of the infiltration at that particular time interval.

At the beginning of the storm, the value of the cumulative infiltration is taken as zero and the infiltration rate calculated using Equation (17).

$$f_t = k\left(\frac{\varphi\Delta\theta}{F_t} + 1\right) \qquad 17$$

As the rainfall continues, two cases are possible depending on the value of rainfall intensity obtained:

(a) If the value of the infiltration rate f_t is less than or equal to the rainfall intensity i_t then ponding does not occur during the whole rainfall interval and the cumulative infiltration at the end of the interval is calculated from Equation (18).

$$CF_{t+\Delta t} = K\Delta t + CF_T + \varphi\Delta\theta \ln\left[\frac{F_{t+\Delta t} + \varphi\Delta\theta}{F_t + \varphi\Delta\theta}\right] \qquad 18$$

(b) If the infiltration rate f_t is greater than the rainfall intensity i_t then ponding does not occur at the beginning of the rainfall interval. The cumulative infiltration at that interval is calculated from Equation (19).

$$CF'_{t+\Delta t} = CF_t + i_t\Delta t \qquad 19$$

The infiltration rate $f_{t+\Delta t}$ is again computed from Equation (17) and depending on its value, two cases are possible:

(i) If the value of the infiltration rate $f_{t+\Delta t}$ is greater than the rainfall intensity at that time interval then ponding does not occur throughout the rainfall interval.

(ii) But if the value of the infiltration rate $f_{t+\Delta t}$ obtained is less than or equal to rainfall intensity at that time interval, then ponding occurs during the interval. The cumulative infiltration at ponding is calculated from Equation (20) and the corresponding infiltration rate equals to the rainfall intensity.

$$CF_p = CF_t = \frac{K\varphi\Delta\theta}{i_t - K} \qquad 20$$

The excess rainfall values are then obtained by getting the differences between cumulative infiltration and cumulative rainfall depths at each time interval.

(b) Direct runoff routing

The equation for routing the flow using the Nash model remains the same as in the previous model. See Equations (13) and (14) of section 2.1.1.

The determination of the models' parameters entails the process of calibration and validation. And with this done, the model can then be used to simulate runoff process in gauged catchments.

For use in ungauged catchments, conceptual parameters of the models must be correlated to the catchment characteristics in a process called regionalization.

2.2 Regionalization

In the temperate countries, rainfall-runoff models have successfully been used to simulate runoff process in gauged catchments. However, to apply the models in ungauged catchments, the models need to be regionalized. Riggs (1990) defined regionalization as the process of relating the flow characteristics to the physical and climatic characteristics of the drainage basins. Regionalization process relates the conceptual parameters of the model to the catchments characteristics using valid transfer functions that are catchment specific.

In the recent past, the application of model parameters to ungauged catchments without regionalization has been a common practice amongst hydrologists. The limitation of this is that simulations are likely to be under or overestimated.

To effectively regionalize a hydrologic model, this process requires the application of many catchments, a property of which is difficult to find with many Kenyan catchments. Moreover, the geographic and climatic conditions need to be same since most model parameters are regionally specific and should be derived for every catchment. Pilgrim (1983) demonstrated that even in catchments of same climatic conditions but different geographic locations, differences still existed in the runoff process. This means that for regionalization process to be successful, the catchments of study need to be closely located next to each other.

Sefton and Howarth (1998) tried to link catchment characteristics to conceptual parameters of models using a stepwise procedure that is applicable to catchments with limited gauging stations. This same procedure was adopted by Onyando (2000) and used to test the potential of rainfall-runoff models for regionalization in some small catchments of Kenya and Germany. A similar approach was also used in this current study to regionalize the two rainfall-runoff models.

Regionalization Procedure

The stepwise procedure (Sefton and Howarth, 1998 and Onyando, 2000) adopted for this current study is as outlined below.

i) Identification of the catchment characteristics

The catchment characteristics to be used for regionalization need to be carefully identified and should have meaningful relationship to the conceptual parameters of the model. Because different models have different conceptual parameters and hence relate differently to the catchment characteristics, the process of regionalization usually has some bias towards the type of model used.

ii) Regression Analysis and Correlation

Regression models are chosen on the basis of statistical relationships. Four regression models that relate closely to the catchment characteristics are given in Equations (21) to (24).

(a) Linear Model: $MP = C_O + C_1 * CC$ 21

(b) Log-Linear model: $MP = C_O + C \ * \ln CC$ 22

(c) Power model: $MP = C_O * CC^{C1}$ 23

(d) Exponential Model: $MP = C_O * \exp(C_1 * CC)$ 24

where MP is the model parameter to be identified, C_o and C_1 are constants while CC represents the catchment characteristics.

iii) Determination of Transfer Functions

The determination of transfer functions involves three main steps. These include optimization of the model parameters, adjustment of the parameters and finally, the adjustment of the boundary conditions. In each of the stages, regression analysis is carried out to determine if any relationship exist between model parameters and catchments characteristics. The stages are carried out iteratively depending on the number and behavior of the conceptual parameters.

iv) Determination of regionalization efficiency

The process of regionalization is accompanied by errors produced at each stage of the process. The final step therefore involves the determination of regionalization efficiency. The regionalization efficiency is compared with the optimization efficiency at every stage for any difference. This process is continued until the difference between the two efficiencies is relatively small. Once that is achieved, the transfer functions are validated and generalized by testing them other catchments.

2.3 Geographical Information Systems (GIS)

Esri (1995) described GIS as a computer system capable of holding and using data that describes places on the earth's surface. There are several GIS softwares that exist. Each software permits spatial analysis of data apart from being able to handle larger quantities of raster data. GIS has found several applications in hydrology (Schultz, 1993), however, most important to this study is its ability to merge remote sensing data with Digital Elevation Models (DEM) thus allowing for the estimation of the parameters of the existing conceptual model. Moreover, because a catchment is generally a large and complex system, GIS is used in the management of spatial data. This allows the models to account for the spatial heterogeneity of hydrologic variables within the catchments.

In the recent past, the application of GIS in hydrology has been on the increase. Drayton *et al.*, (1992) used GIS to handle raster data for distributed modeling using the US-SCS model in the United States. Sanjay *et al.*, (2001) successfully employed GIS technique to estimate soil erosion in the Himalayas watersheds. Serwan and Kamaruzaman (2001) applied RS and GIS to model soil erosion in Langawiki Island in Malaysia.

The procedure involved in processing RS data using GIS depend on the particular software used since each has its unique extension enabling it to manage and analyze certain types of raw and higher forms of satellite imagery. However, most important to note that all GIS softwares allows for inter-transfer of processed, analyzed and other forms of data. The stages involved in processing RS data using GIS can be broadly divided into four as discussed below.

i) Acquisition of data and pre-processing

The data to be processed are acquired in the form of Tables, Toposheets and even in CD ROMs amongst others. The data is then keyed into the computer. Maps can also be directly digitized into suitable digital formats from Toposheets or as scanned images. Spatial data are captured during digitization and stored as vector coverages. Descriptive data in the form of character or numeric features are stored in tabular form using records and items. Spatial and descriptive data are interconnected using unique identifiers stored in both places. This enables the attribute data to be analyzed spatially.

ii) Management of the database

The data entered into the computer are retrieved, geo-referenced and displayed. This stage also includes conversion of spatial data from one form to another. For example, conversion of vector coverages to raster maps and vice versa, depending on the type of data available and being analyzed.

iii) Data manipulation and analysis

In this stage the data is manipulated and analyzed depending on the objective of the study. The analysis may proceed as single or combined themes. Single themes are used to transform spatial data into maps showing the distribution of the hydrologic variable. This is further used as input into the hydrologic model. Examples of single themes include the derivation of slope distribution from DEMs.

Combined thematic maps are achieved through spatial analysis. In this process thematic maps in raster format are combined through mathematical algorithms to produce higher ordered themes from which the parameters of the hydrologic modeling are extracted. An example here includes the combination of raster spatial data of soil types and land use types to produce spatial distribution of soil storage capacity.

iv) Presentation of the Results

The parameters extracted in stage 3 above are then used in hydrologic models. The modeling results are then displayed graphically in tabular form or in thematic maps.

2.4 Concluding Remarks

Unlike in the in the developed countries, rainfall-runoff models have not been widely used for runoff simulation in the developing countries. Because different categories of rainfall-runoff models exist, the choice on the model category to use is usually very important. In this study, lumped models were used to accomplish it. The NCDI model was one of the models chosen. This model has not been widely adapted in the humid tropics of Kenya. Onyando (2000) applied this model for runoff simulation in the Kenyan catchments and obtained satisfactory results. However, limited recommendations could be made on the future application of this model since it had not been tried out in catchments of varied climatic and geographic locations. It is with this in mind that the present study was instituted to establish the effectiveness of this model for runoff simulation in the humid tropics of Kenya.

The NCGAI model too was chosen for this study. The model also has had very limited application in Kenya. This model has parameters, which are physically based and can be determined from the soil textural classes. This study however, chose to optimize these parameters because of their high degree of variability in space and in time. This would thus allow for comparison to be made between the two approaches and appropriate recommendations arrived at.

CHAPTER 3: METHODOLOGY

3.1 The Study Area

The study area is located on the headwaters of Ewaso Ngiro drainage basin as shown in Figure 6.

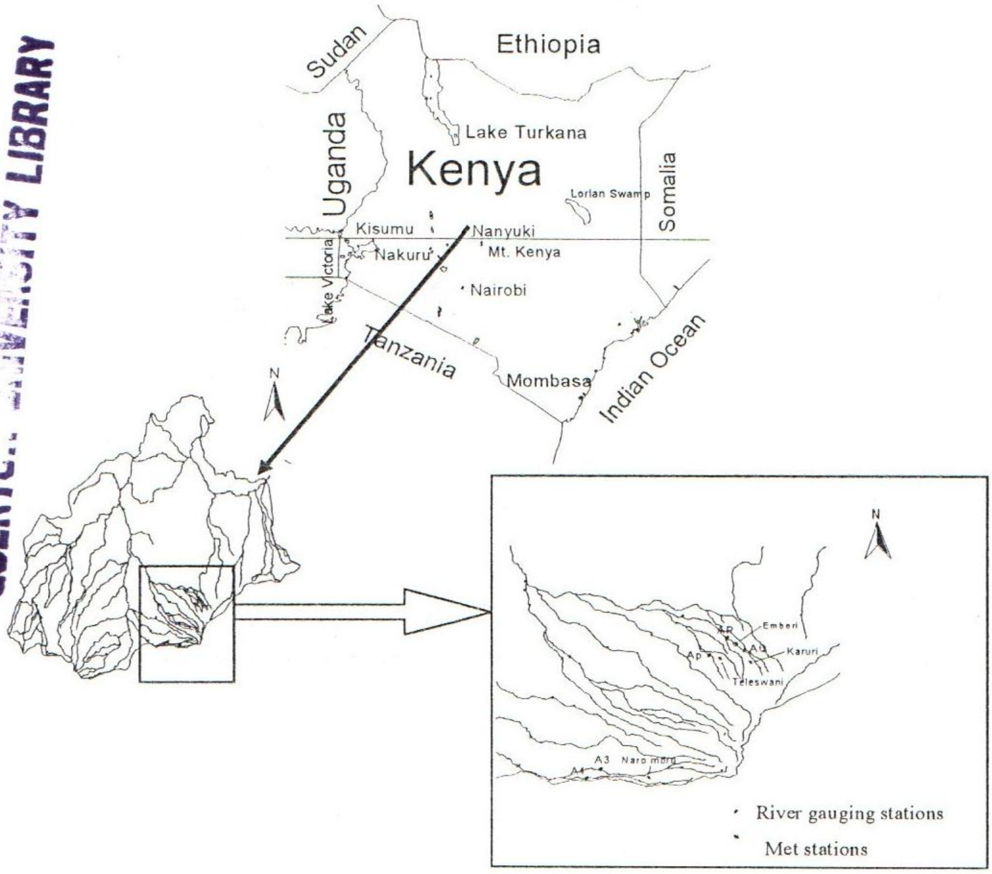

Figure 6 Location of the study area catchments in the upper Ewaso Ngiro basin.

The Ewaso Ngiro drainage basin in Figure 6 is drained by Ewaso Ngiro River with its source in Mt. Kenya and flows northeastwards through Lorian Swamp. The upper Ewaso Ngiro basin covers 15,151km^2 and lies between latitudes 0^0 20" South and 1^0 15" North and Longitudes 36^0 10" East and 38^0 00" East. The area has an altitude of about 2450m above mean sea level with mean annual temperatures of less than 12^0C, which decreases towards the top of the mountain (Braun, 1982 and Berger, 1989). The natural vegetation of the area is dry and moist forest, with the moisture increasing with the altitude. For the soils, the catchments are cut across by

Cambisols, Andosols, Invisols and Phaezems according to FAO-UNESCO classification system. The selected study catchments and their sizes are shown in Table 1.

Table 1 Sizes of the study catchments

Catchments	Approximate area in km^2
AQ-Mid Ituuri	6.5
AR-Lower Ituuri	11
AP-Lower Teleswani	13
A3-Naromoru North	21
A4-Naromoru South	26

The upstream catchments of the Ewaso Ngiro basin was chosen to accomplish the present study because soil erosion due to runoff was identified as a major problem (Ministry of Water and Development, 1992). Land degradation has continued to be evident with the ever-increasing changes in land use. It has therefore become necessary to map and quantify soil erosion so as to provide a planning tool for soil conservation strategies. In addition, soil conservation research on appropriate catchments management is an on going activity in the study area (Goodchild, 1993; Mutunga, 1994 and Kihara, 1998) and therefore there is availability of continuous rainfall-runoff data that could be used to calibrate the models.

3.2 Data Acquisition

The data acquired for this study included rainfall, stream flow, and geophysical data. They were acquired for the five catchments under study.

3.2.1 Rainfall Data

The rainfall data were obtained from automatic rainfall recorders located within the catchments. The meteorological stations located on the upstream of the catchments were used as shown in Table 2.

Table 2 Meteorological stations in the study catchments

Meteorological Station	Catchments Represented	
	Name	Symbol
Karuri	Lower and Mid Ituuri	AQ
Embori	Lower Ituuri	AR
Naromoru	Naromoru North	A3
Teleswani	Lower Teleswani	AP
Naromoru	Naromoru South	A4

From Table 2, each catchment was represented by one rain gauge station. This representation was not sufficient enough in catchments A3 and A4 considering the large sizes of the catchments and the areal rainfall patterns within the humid tropics. The rain gauges used however, provided reliable and consistent rainfall data. Other information obtained from the meteorological stations included the duration of the rainfall event, times and dates of their occurrence and the cumulative rainfall amounts.

3.2.2 Stream flow Data

Stream flow data required for this work were obtained from the Ministry of Water Resources (MWR) of Kenya and from Centre for Training, Research and Development (CETRAD). The rating equations usually used to change stage graphs to discharges were also acquired as given in the Table 3.

Table 3 Rating equations for the study catchments

Catchments Name	Catchments ID	Rating Equation	Continuous data
Lower Ituuri	AR	$Q=3.6702*H^{1.7198}$	1997-2001
Naro Moru South	A4	$Q=6.1291*(H-0.5)^{2.6446}$	1997-2001
Naro Moru North	A3	$Q=18.1176*(H+0.079)^{3.6485}$	1997-2001
Mid Ituuri	AQ	$Q=3.6702*H^{1.7198}$	1997-2001
Lower Teleswani	AP	$Q=3.6702*H^{1.7198}$	1997-2001

3.2.3 Geophysical Data

Geophysical data were obtained as satellite data and topographic sheets. Remote sensing data were obtained from the DRSRS in collaboration with CETRAD. Additional information was obtained from the ground survey taken along transects made through the catchments during the fieldwork. The geophysical data obtained included:

1) **Land use and land cover data**

Land use data included the extents of the various agricultural practices carried out in the area, settlements patterns amongst others. Land use data were collected from ground surveys carried out in the catchments and from literature available at CETRAD.

2) **River-gauging stations and stream network data**

Coordinates of river gauges were acquired to enable the identification and plotting of the stations on maps.

3) **Soil data.**

These were also obtained in soft form from CETRAD. The data included the different soil types in the catchments and their spatial distribution within the catchments.

3.3 Data Analysis

3.3.1 Rainfall Data

The meteorological station representing each gauging station in the catchment was established and the rainfall events that caused runoffs within the catchments noted. The individual rainfall amounts were calculated from the cumulative rainfall depths for every catchment and the rainfall hyetograph plotted. A typical rainfall hyetographs is shown in the Figure 7.

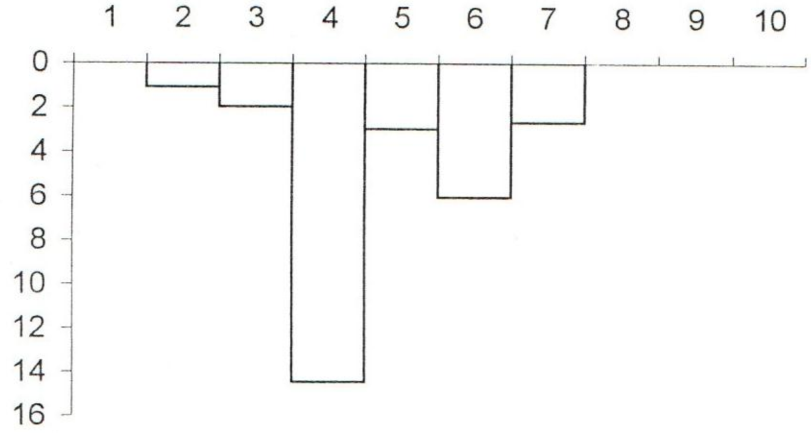

Figure 7 Rainfall hyetograph of 6/19/97 for Lower Ituuri catchment

At least ten hyetographs from each meteorological station were prepared and matched with the corresponding runoffs events recorded on the same dates at the stream gauges. This provided information of the observed rainfall-runoff processes for the catchment.

3.3.2 Stream Flow Data

Stream flow data were important for the derivation of direct runoff produced by a given rainfall event. Since not all the rainfall events produced runoff at the catchments output, the stream flow data were carefully sorted out to match with the days when corresponding rainfall events occurred. In some cases, the stream flow data for some days when rainfall occurred in the catchment were either missing or unavailable. Under such cases, the stream flow data were neglected.

The selected gauge heights were therefore matched with the days when the rainfall event occurred and used to derive the total stream flow discharges using the rating equations. Ten runoff events were derived for each catchment and the direct runoff hydrograph obtained from total discharge hydrograph as outlined below.

(1) Total discharge Hydrograph

The total discharge hydrographs were derived for each runoff event by plotting the total discharge against time shown in Figure 8.

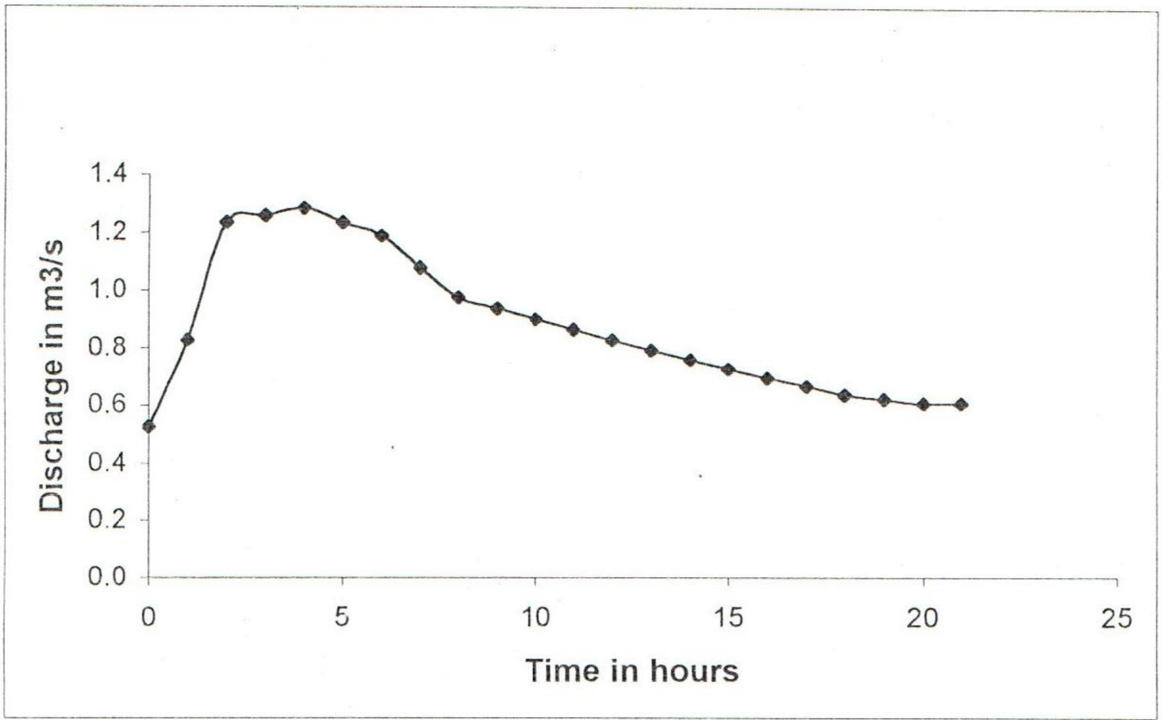

Figure 8 Total discharge hydrograph for Naromoru North catchment

To obtain the direct runoff hydrograph, the base flow was separated from the total discharge hydrograph(s) shown in Figure 8 as outlined below.

(2) Separation of base flow

The total discharge hydrograph represents the combined effects of both the base flow and direct runoff recorded at the catchments outlet. In order to obtain the runoff hydrograph, the base flow is separated from the total discharge hydrograph. Several methods of base flow separation have been outlined in Shaw (1996). The Log-linear relationship between the total flow rate and time is the most commonly used method of base flow separation. This method requires a continuous stage graph of the stream over a period of few years. The hydrographs are then examined for portions of the recession curves running into base flow contributions at different points to determine a master depletion curve for a particular stream. This method of base flow separation is the best. However, it depends strongly on the availability and consistency of the previously observed data, which was not available for the streams in the study catchments.

Instead, the linear relationship between total flow rate and time was employed in the separation of base flow. Apart from the unavailability of consistent data, this method of base flow separation was used because the sorted rainfall events chosen to accomplish this study occurred at different times and therefore the contribution of groundwater flow could not be exactly established. In the linear method of base flow separation; the lowest point of the greatest curvature, before the rising limb and after the recession, was identified in the total discharge hydrograph. Joining the two points with a straight line so that the area of the hydrograph below this line represented the base flow whereas the area above is due to the direct runoff then developed a linear relationship.

(3) Direct Runoff Hydrograph

Figure 9 gives the observed direct runoff hydrograph that was obtained by separating the base flow from the total discharge hydrograph.

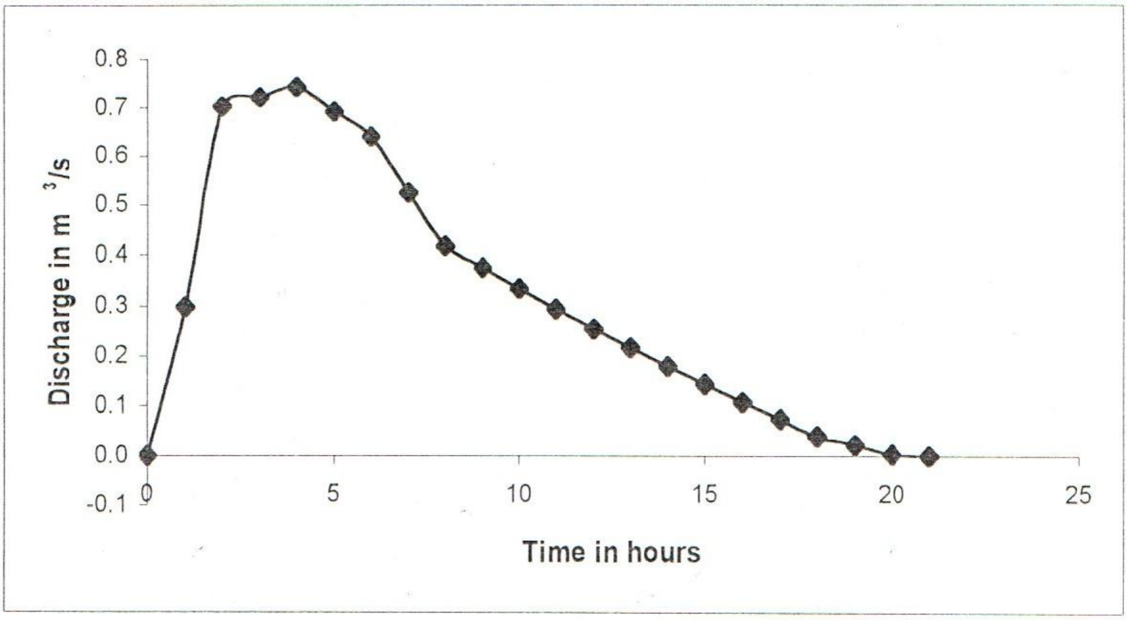

Figure 9 Direct runoff hydrograph for the Naromoru South catchment.

With the rainfall hyetograph and runoff hydrograph established, the geophysical characteristics of the catchments that affect the rainfall and runoff process were then determined.

3.3.2 Geophysical Data

Geo-physical data are important in the derivation of the physical parameters of the model required for regionalization. Such data include soils data, land use and land cover data and topographic data amongst others.

(a) Topographic maps

Topographic data such as the catchment slope S_{ca}, overland slope S_{ov}, catchments area A_c, length of the main stream L, length to the centroid of the catchments L_{ca}, catchments form $L*L_{ca}$, form factor R_F, drainage density D_d and the ratio of the catchments area to the equivalent circular area R_K were obtained from topographic maps. Some of the results are presented in Table 4.

Table 4 Physical characteristics of the study catchments

Catchment	S_{ca}(%)	S_{ov} (%)	A (km^2)	R_F
Lower Ituuri	72.1	6.05	11	4.66
Naro Moru South	5.11	3.03	26	2.60
Naro Moru North	2.62	1.66	21	4.52
Mid Ituuri	3.04	2.65	6.5	3.16
Lower Teleswani	5.32	4.10	13	5.19

The data in Table 4 were important in the development of transfer functions for every catchment. The general catchment slope S_c and the overland slope S_o were obtained by taking the difference in altitude between the upper section of the catchment and the lower. Form factor R_F on the other hand was calculated as a product of the catchment area A and the length on the main stream L.

(b) Soils data

The soil data were obtained from satellite imagery with the help of GIS-ArcView. The soils in the catchment were analyzed and categorized according to the FAO-UNESCO soil classification system as shown in Figure 10.

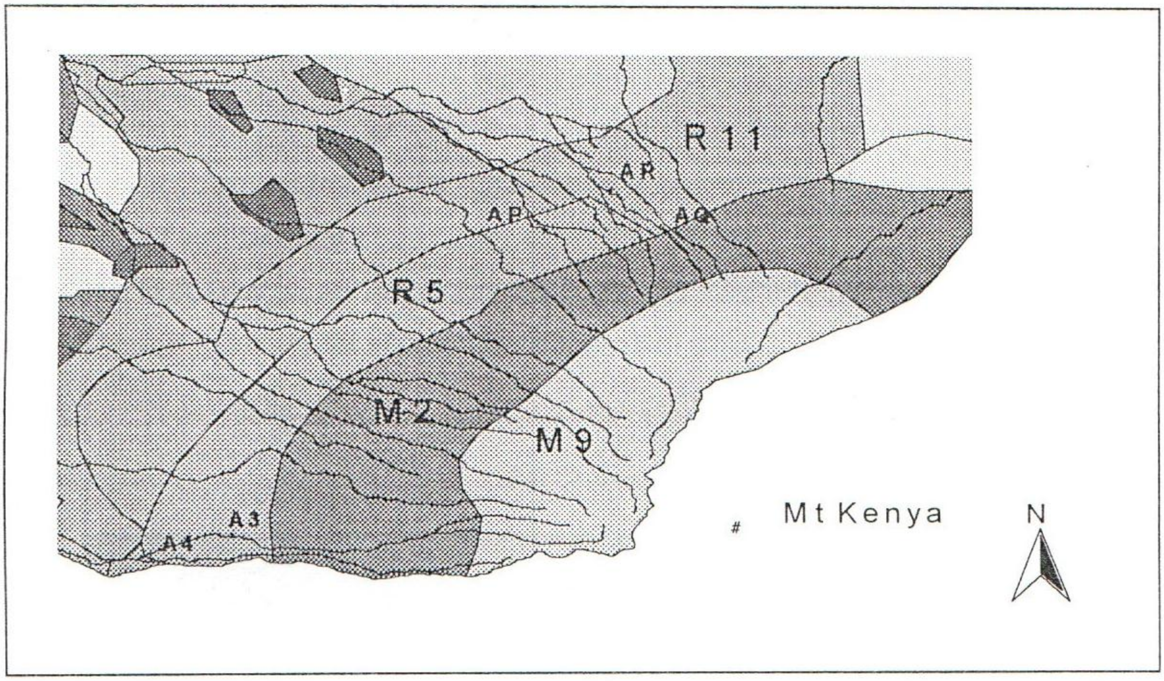

Figure 10 Spatial distributions of the soil types within the area of study.

The soils in Figure 10 were converted to USDA system of soil classification. With the USDA classification, it was then possible to derive the soil parameters using Clapp and Hornberger (1978) conversion procedure. The details of the soils for the study catchments are given in Table 5.

Table 5 Classification of the soil types within the catchments

ID	FAO-UNESCO classification	USDA classification	Description of the soil characteristics
R11	Phaezems	Clay	Very deep and well drained
R5	Luvisols	Clay	Moderate-very deep and well drained
M2	Andosols	Clay loam-Clay	Very deep and well drained
M9	Cambisols	Loam-Clay loam	Imperfectly drained, shallow to moderately deep with outcrops.

Table 5 describes the soil characteristics used to obtain the geo-physical parameters of the models. In Andosols for example, the soil textural classes fall between clay-loams to clay. The value of the effective porosity was obtained by establishing the average weighted values of the parameter values obtained from soil textural classes (Chow *et al.*, 1988).

(c) Land Use and Land Cover data

The main land cover within the catchments was forest. Towards the North-Western side of the study catchments there was the encroachment of modern small-scale farming shown in Figure 11.

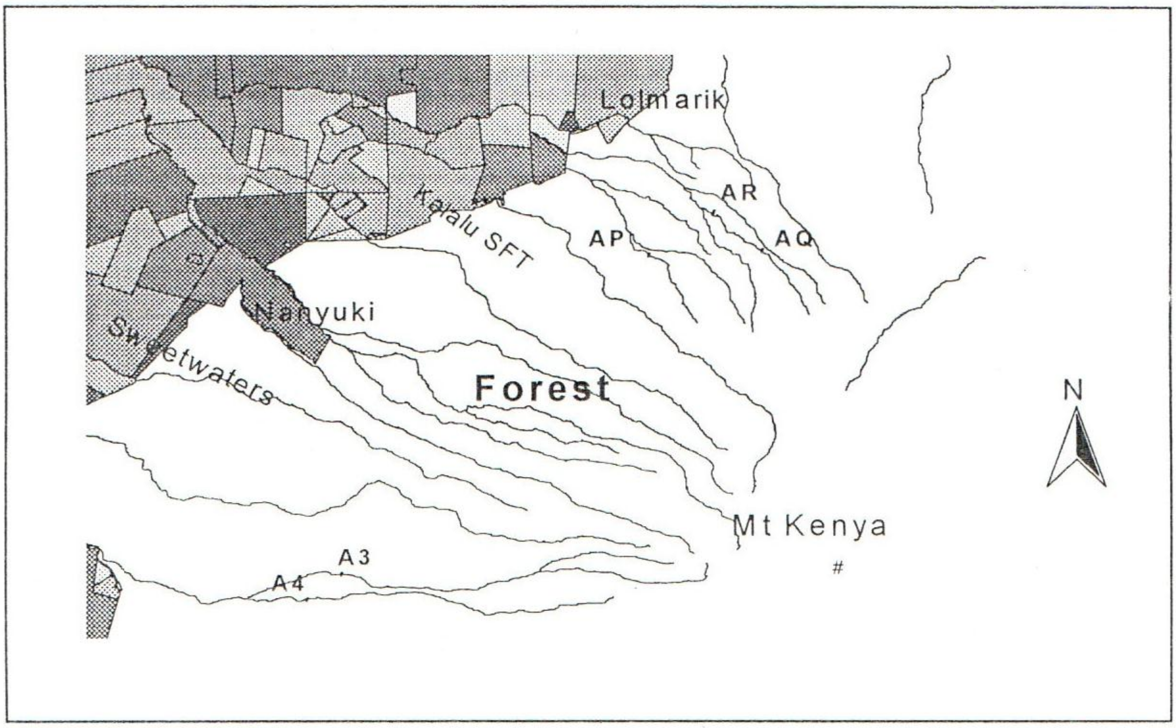

Figure 11 Spatial distribution of the Land cover and land uses in the study area

This information was important in the evaluation of the spatial extents of the different land use systems and their effects on the runoff process.

3.3 Derivation of the Model Parameters

To derive the parameters of the models, the area of the catchments were first calculated from the satellite data. The catchments areas were digitized and delineated along the catchments divide, as was shown by the position of the contours. This was done to allow for the aggregation of the physical parameters of the models based on areas of hydrological similar units (Leavesley and Stannard, 1995).

3.4.1 Physical Parameters

The physical parameters of the model were derived from geophysical data. The geophysical data were captured and processed into digital and manageable forms and derived with the help of GIS-ArcView.

(a) The NCDI model

For the NCDI model the only physical parameter was soil storage capacity (S_m). This was determined as a product of the effective porosity and depth root zone. The effective porosity for the different soil types were obtained from the soil textural classes presented by Rawls and Brakensiek (1983), while root depths were derived based on land use of the study catchments (Onyando, 2000).

With the help of GIS, values of S_m were determined through overlaying the coverages of soil types and land use containing attribute values of effective porosity tabulated in Table 6.

Table 6 Parameters of the NCDI model

Catchment	Soil types	Area in Pixels	Porosity	Root depth (mm)	Maximum S_m (mm)	Mean S_m	Total Area (km^2)
Mid-Ituuri	L-CL	2889	0.461	1250	65.0	87.5	6.5
(AQ)	CL-C	4333	0.470		102.5		
Lower	C	6500	0.475	1250	112.5	107	13.0
Teleswani	CL-C	7944	0.470		102.5		
(AP)							
Lower	C	2078	0.475		112.5	85.83	
Ituuri	CL-C	4156	0.470	1250	102.5		11.0
(AR)	L-CL	5989	0.464		65.0		
Naromoru	C	1167	0.475		112.5	87.25	
North	CL-C	12368	0.470	1250	102.5		21.0
(A3)	L-CL	9800	0.464		65.0		
Naromoru	C	2889	0.475		112.5	103.5	
South	CL-C	18778	0.470	1250	102.5		26.0
(A4)	L-CL	7222	0.464		102.5		

Key: L=Loam; CL=Clay Loam; C=Clay

(b) The NCGAI Model

The only geophysical parameter in this model was the effective porosity. The area of the catchments with similar soil types were measured and divided into pixels of 900m^2 each. The total porosity per pixel was obtained for each soil type within the catchment and tabulated in Table 7.

Table 7 Physical parameters of the NCGAI model for catchment A3

Soil Type	Area (pixels)	Porosity
Clay	316	0.475
Clay-Clay Loam	4156	0.470
Loam- Clay Loam	5989	0.464

3.4.2 Conceptual Parameters

The conceptual parameters for the models were determined with the help of optimization algorithms. The Shuffled Complex Evolution (SCE-UA) procedure for global optimization (Duan *et al.*, 1995) was adopted since it is more general and efficient for a broad class of problems (Sorooshian and Gupta, 1992). The sorted rainfall-runoff events for each catchment were divided into two equal sets. The first set was used for model calibration and the other set for validation.

The antecedent moisture content of the catchments S_o was treated as a conceptual parameter in both the models. Other parameters also treated as conceptual parameters in the NCGAI model are the hydraulic conductivity K and the wetting front suction head φ. The details of the conceptual parameters chosen for optimization in the NCDI and NCGAI models are given in the Tables 8 & 9, respectively.

Table 8 Conceptual parameters of the NCDI model

Parameter symbol	Description	Method of determination
S_o	Initial moisture content	Optimization algorithms
f_c	Minimum infiltration capacity	Optimization algorithms
f_o	Initial infiltration capacity	Optimization algorithms
n	Number of linear reservoir in cascade	Optimization algorithms
k	Storage constant of proportionality	Optimization algorithms

Table 9 Conceptual parameters of the NCGAI model

Parameter symbol	Description	Method of determination
S_o	Initial moisture content	Optimization algorithms
K	Hydraulic conductivity	Optimization algorithms
φ	Wetting front suction head	Optimization algorithms
n	Storage constant of proportionality	Optimization algorithms
k	Number of linear reservoirs	Optimization algorithms

The parameters K and φ in Table 9 were optimized because of their site specificity and high degree of variability within the catchments. With the physical and conceptual parameters of the models parameters determined, the two models were then used to simulate the rainfall-runoff events whose details are presented in Table 10.

Table 10 Results of the rainfall-runoff analysis for the catchments

Rainfall				Runoff				
Catchment	Date	Total (mm)	Duration (h)	Peak (m^3/s)	Time to peak (h)	Flow Time (h)	Time Lag (h)	Mean time lag (h)
A3	1/8/97	50.69	10	1.14	3	23	0.5	0.8
	1/21/97	43.98	18	0.352	5	23	1	
	3/26/97	28.30	6	0.217	3	15	0.5	
	3/30/97	28.20	6	0.742	5	22	2	
	4/7/97	24.00	8	5.952	3	21	0.5	
	10/8/01	22.60	7	8.945	4	29	1	
	9/18/01	44.20	11	0.133	6	21	1	
	9/16/01	18.30	5	0.371	3	22	0.5	
	9/14/01	25.60	5	0.217	3	15	0.5	
	8/28/01	52.40	6	0.310	4	29	0.5	
A4	3/31/97	50.69	10	0.464	5	17	2	1.72
	4/6/97	43.98	17	0.681	5	22	1	
	4/7/97	28.25	6	0.582	7	22	4	
	4/8/97	24.16	8	3.418	7	28	3	
	4/9/97	22.26	7	7.606	3	25	0.5	
	4/10/97	34.42	8	0.644	5	15	0.5	
	4/11/97	18.30	5	0.704	5	15	2	
	1/10/97	54.20	8	3.079	3	21	0.5	
	1/11/97	42.40	6	3.504	5	11	2	
AP	5/5/98	18.30	5	0.006	4	10	1	0.93
	10/4/98	42.40	6	3.540	5	11	2	
	1/12/98	49.38	7	0.212	4	25	1	
	7/14/99	52.40	6	0.192	3	25	0.5	
	5/5/98	23.30	5	0.005	3	9	1	
	10/4/98	15.70	5	0.010	3	10	0.5	
	7/9/99	4.50	3	0.006	2	5	0.5	
AR	4/3/97	21.00	3	0.315	2	23	0.5	1.10
	4/4/97	11.01	4	0.085	2	5	0.5	
	4/5/97	17.30	3	0.238	3	7	2	
	4/10/97	27.30	5	1.345	4	13	0.5	
	6/19/97	38.20	8	1.973	7	12	2	
	4/21/97	28.10	6	0.217	3	14	0.5	
	4/27/97	27.60	5	0.755	4	8	1	
	6/7/97	4.70	4	1.500	3	5	1	
	6/15/97	11.40	6	2.710	3	7	1	
	6/15/97	13.20	4	2.083	4	9	2	
AQ	4/3/97	1.60	4	0.430	4	8	0.5	1.06
	4/5/97	8.80	5	1.890	4	10	1	
	4/7/97	46.88	18	2.120	4	27	1	
	4/9/97	7.90	5	0.160	4	14	2	
	11/9/97	12.7	5	1.000	3	12	1	
	4/23/97	6.15	4	2.020	5	9	2	
	6/19/97	29.40	7	2.180	5	20	1	
	6/20/97	18.20	2	1.940	2	7	0.5	
	7/10/97	20.10	4	5.010	3	11	0.5	

The rainfall-runoff events given in Table 10 were obtained after a thorough analysis of the details of all the rainfall that produced runoff in the study catchments. Catchments A4 and A3 had the highest rainfall amounts compared to the others. Consequently, these catchments produced the highest direct runoff volumes. Since all the catchments had at least one rain gauge, the direct runoffs produced by a given rainfall event could easily be derived from stream gauges. In catchments AP, however only seven rainfall-runoff events could be obtained due to lack of proper maintainace of the gauging instruments.

3.5 Assessment of Model Performance

Assessing the performance of the models involves comparing the simulated and the observed results. This was done by visual observation through graphical displays and also by statistical techniques. Different statistical methods have been outlined and tested for analysis of models performance. Each statistical method depends on the objective of the study and the characteristics of runoff event under investigation.

In this study, the performance of the two models was tested as outlined by ASCE (1993). The authors recommended four methods for assessing the performance of single rainfall events. The objective function of Nash and Sutcliffe (1970) in Equation (24) was used for analyzing the shape of the hydrographs.

$$EFF = \frac{\sum_{i=1}^{n}(Q_{OI} - Q_{AV})^2 - \sum_{I-1}^{N}(Q_{OI} - Q_{SI})^2}{\sum_{I=1}^{N}(Q_{OI} - Q_{AV})^2} \qquad 24$$

where EFF is the Nash and Sutcliffe efficiency, Q_{oi} and Q_{si} are the measured and simulated runoffs respectively, n is the number of observation and Q_{av} is the average measured runoff.

ASCE (1993) also recommended three other methods for assessing the model performance. These include the percentage deviation of runoff volume D_v for runoff volume assessment, expressed in Equation (25).

$$D_V = \frac{(V_M - V_P)}{V_M} \times 100 \qquad 25$$

where D_v is the percentage deviation of runoff volume, V_m is measured runoff volume and V_p is simulated runoff volume. For evaluating peak discharges, Equation (26) was used.

$$PEP = \frac{(Q_{PS} - Q_{PO})}{Q_{PO}} \times 100 \qquad 26$$

where *PEP* is the percentage error of peak, Q_{ps} is simulated peak flow rate; Q_{po} is observed peak flow rate.

The shape of the hydrograph was assessed using the total sum of squares of the residual (TSSR). Equation (27) gives the expression for this criterion.

$$TSSR = \sum_{i=1}^{n} (Q_{oi} - Q_{si})^2 \qquad 27$$

The symbols in this Equation (27) here have the same meaning as those of Equation (24) for hydrograph shape analysis. This assessment criterion is the dimensional form of Equation 24 and is hence not frequently used. Values of *TSSR* close to zero indicate a perfect fit of the simulated and observed hydrographs.

3.6 Determination of Transfer Functions

To regionalize the models, the catchments characteristics closely related to the conceptual parameters were determined with the help of GIS. Transfer functions were then developed in a series of optimization steps. At every step, the conceptual parameters were correlated to the physical parameter(s) through regression analysis. The physical parameter that gave the highest correlation coefficient was used in deriving the regression equation.

3.6.1 NCDI Model

The conceptual parameters to be regionalized and the physical parameters for developing transfer functions are shown in Table 11. Also shown in the same Table are the geophysical parameters from which physical parameters are obtained.

Table 11 Geo-physical and physical parameters for NCDI model

Conceptual Parameter	Geo-physical characteristics	Physical parameter
	Catchments area	Drainage density (D_d)
	Drainage network	
f_o and f_c	Main channel slope	Channel slope (S_c)
	Catchment area slope	Overland slope (S_o)
	Catchment area	Catchment area (A)
n and k	Stream length	Length of main stream (L)
	Catchment shape	Length to the centriod of the
	Main stream length	catchment (L_{ca})
	Catchment shape	Catchment form (L* L_{ca})
	Main stream length	
	Catchment area	Form factor (R_F)
	Main stream length	
	Catchment area	Catchment area/circular area
	Catchment shape	

3.6.2 NCGAI Model

In this model, the hydraulic conductivity and the wetting front suction head were treated as conceptual parameters. However, since these parameters are physically based, no transfer functions were developed for the two parameters. Instead, the optimized values obtained were compared with the physical values obtained from the soil textural classes (Chow *et al.*, 1988). The accuracy of optimization was estimated using the percentage deviation of the optimized value from the soil textural values. The Percentage deviation for hydraulic conductivity K and wetting front suction head φ were calculated using Equations (28) and (29) respectively.

$$(\frac{K_{OP} - K_{SC}}{K_{SC}}) * 100 \tag{28}$$

$$(\frac{\varphi_{OP} - \varphi_{SC}}{\varphi_{SC}}) * 100 \tag{29}$$

where the subscripts *op* and *sc* represents the optimized and soil textural values respectively. The optimized parameter values with percentage deviation greater than forty percent were considered outliers and were therefore regionalized. The result obtained during the analyses are outlined in the next section

CHAPTER FOUR: RESULTS AND DISCUSSION

4.1 Calibration and Validation

In calibrating the models, split sampling procedure was used. The rainfall-runoff data for each catchment was divided into two sets. The first set for calibration and the other for validation, as shown in Table 12.

Table 12 Calibration and validation data

Catchments ID	Catchment Name	No. of Events	Calibration	Validation
A3	Northern Naromoru	10	5	5
A4	South Naromoru	9	5	4
AP	Lower Teleswani	7	4	3
AQ	Mid Ituuri	9	5	4
AR	Lower Ituuri	10	5	4

Catchment AP had the lowest number of rainfall-runoff events compared to the others as shown in Table 12. However, the data were sufficient together with the others for calibraticn and validation.

4.1.1 The NCDI Model

In the NCDI model four parameters were optimized. The description and boundaries of the conceptual model parameters optimized for every storm are given in Table 13.

Table 13 Initial boundaries of the NCDI model

Parameter	Description	Min. value	Max. Value	Initial value	Units
n	No. of linear reservoirs in cascade	1	7	4	-
k	Storage constant	0.3	5	2	h
f_o	Max. infiltration capacity rate	10	65	20	mm/h
f_c	Min. infiltration capacity rate	0	10	1.5	mm/h

The optimization process was carried out between the boundaries given in Table 13. The choice of the boundary values were done using the approach adopted by Onyando (2000). The mean values of the optimization values obtained are given in Table 14.

Table 14 Optimized parameters for the catchments for NCDI model

Catchments	No. of storm events	Mean values of the optimized parameters				
		n	k	f_o	f_c	S_o
A3	10	3.37	2.42	28.90	4.96	25.30
A4	9	4.16	2.18	41.64	5.61	23.54
AP	7	5.76	0.90	38.19	5.73	25.94
AQ	9	4.62	0.68	33.87	3.95	25.29
AR	10	6.12	0.67	32.62	4.42	28.83

From the Table 14, S_o is a catchment parameter that changes on storm basis. However, the mean values of this parameter in the catchments were close to each other. This indicates that the moisture content variation within the catchments just before the storm was relatively small since the catchments were located in the same geographical area and also had similar land use patterns, land cover and soil types.

The highest value of the initial infiltration capacity f_o was obtained in catchment A4. Many factors could have contributed to this. The main reason is that part of catchment A4 is situated next to an urban centre with heavy settlements alongside. This difference, in land use and land cover, could have contributed to the surface sealing and crusting in this part of the catchment thereby reducing the rate of infiltration and the water holding capacity of the soils. Catchment AQ recorded the lowest infiltration capacity f_c compared to the others possibly because of the presence of Cambisols (loam to loam-clay) which had the lowest infiltration rate compared to others.

In the Nash model parameters, the storage constant k which is dependent on the size of the catchment, and the values of the linear reservoirs in cascade n were highest in the largest catchment, A4 and lowest in the smallest catchment, AR respectively.

4.1.2 The NCGAI Model

Four parameters of this model were optimized as given in Table 15. Also given in the same Table are the boundary conditions of the parameters.

Table 15 Optimization boundaries of the NCGAI model

Parameter	Description	Min. value	Max. Value	Initial value	Units
n	No. of linear reservoirs in cascade	1	7	4	-
k	Storage constant	0.3	5	2	h
K	Hydraulic conductivity	0.3	3.0	0.8	mm/h
φ	Wetting front suction head	350	50	245	mm
S_o	Initial soil moisture content	0.01	0.467	0.22	-

In the case of n and K, the same boundary values used in the previous model were adopted. As for the Green-Ampt parameters, the boundaries were chosen depending on the general hydraulic properties of the soils in the study catchments. During optimization, the inverse relationship between hydraulic conductivity and the hydraulic head of the wetting front was taken into consideration. The mean optimization values obtained for the catchments are given in Table 16.

Table 16 Results of the optimized parameters for the catchments using NCGAI model

Catchments	Number of storm events	Mean values of the optimized parameters				
		n	k	K	φ	S_o
A3	10	5.12	1.681	1.01	219.67	0.314
A4	9	6.28	1.0031	0.97	207.82	0.289
AP	7	5.57	0.91	1.17	248.51	0.400
AQ	9	4.69	0.872	1.39	159.78	0.312
AR	10	5.2	0.804	0.79	253.32	0.295

The values of the initial moisture content S_o in the Table 16 were taken as a ratio of the effective porosity. Because of the different soil types within the study catchments, the variables K and φ were aggregated based on areas of hydrological similarities to account for the various spatial extents of the different soil types. The mean weighted value of K and φ was obtained for the catchments and used in optimization process. The values of the parameters K and φ obtained in Table 16 were compared with the mean weighted values obtained by Rawls *et al.* (1983) from a detailed study of different soil texture in the United States.

4.2 Runoff Simulation

4.2.1 The NCDI model

The optimized parameters of the NCDI model were used to simulate the runoff events of the catchments. The sample results for typical simulations are presented in Figures (12) to (16). The other results are in the Appendix.

(i) Catchment A3

(a) Rainfall

(b) Runoff

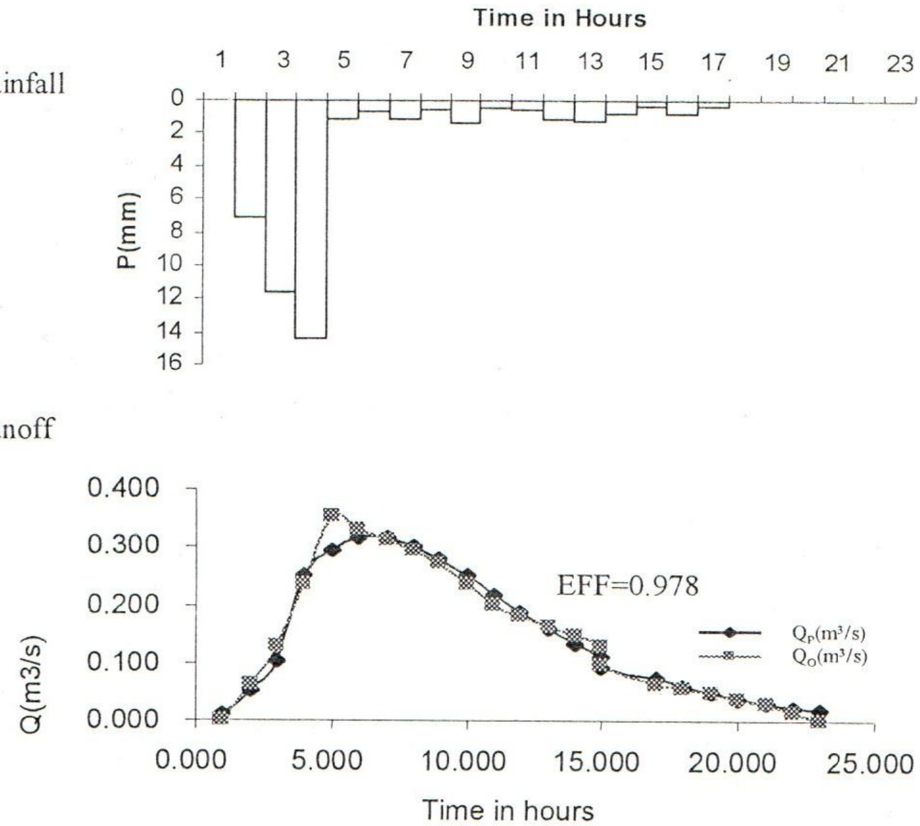

Figure 12 Predicted and observed hydrographs of 21/01/97 for A3 in NCDI model

Figure 12 shows the rainfall event and the corresponding direct runoff hydrograph of both the simulated (Q_p) and observed (Q_o). Also shown in the same figure is the efficiency *EFF*, which is 0.978. This value of the EFF obtained is reasonably high since perfect simulation has a value equal to 1.

(ii) **Catchment A4**

(a) Rainfall

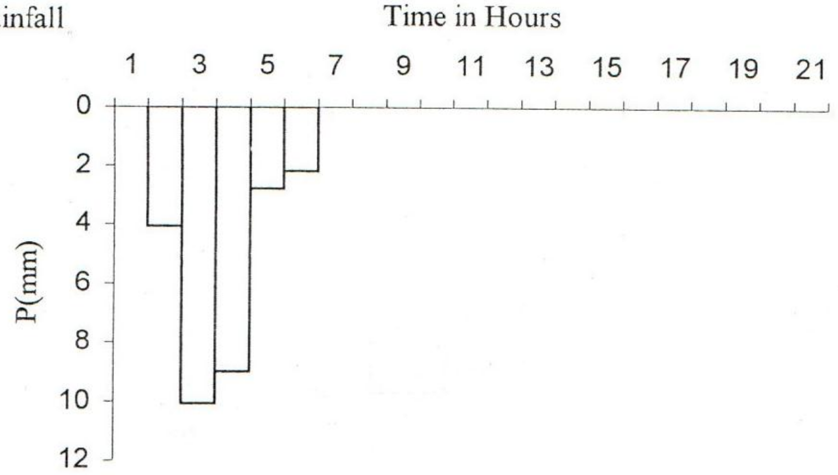

(b) Runoff

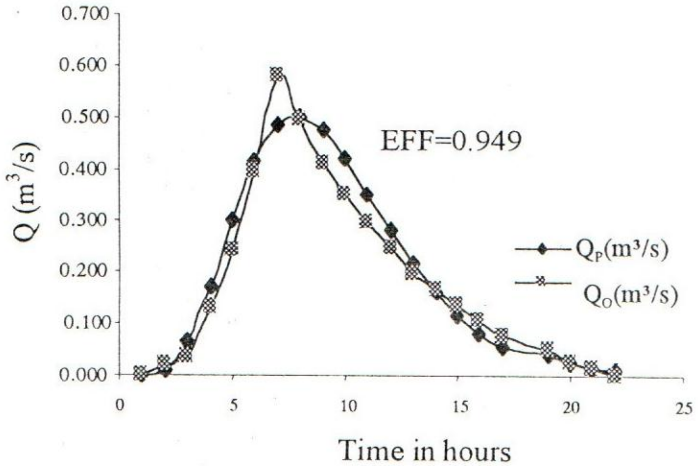

Figure 13 Predicted and observed hydrographs of 4/07/97 for A4 in NCDI model

The simulated hydrograph in Figure 13 was also satisfactory from visual inspection and from the value of EEF obtained. However, the lag time and time to peak obtained by the model were relatively lower compared to the observed data. One typical hydrographs for catchment AP is presented in Figure 14.

(iii) Catchment AP

(a) Rainfall

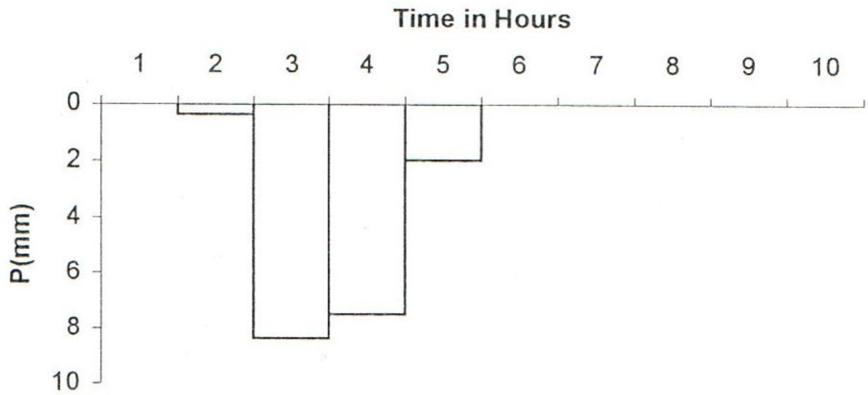

(b) Runoff

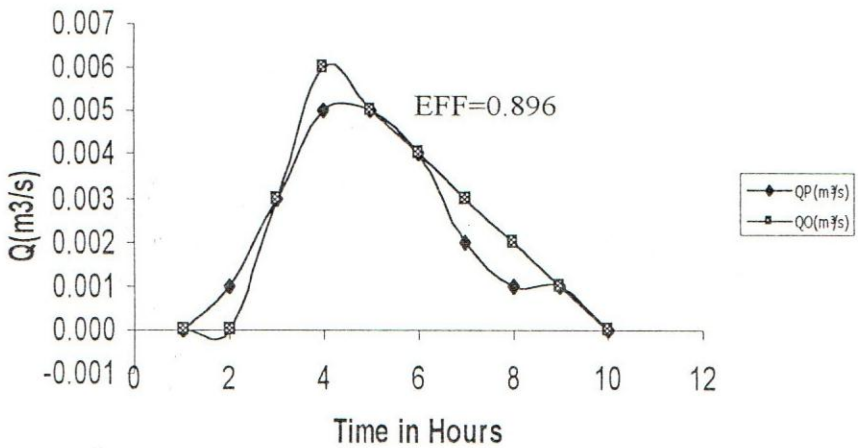

Figure 14 Predicted and observed hydrographs of 5/05/97 for AP in NCDI model

The result shown in Figure 14 indicates satisfactory simulations as depicted by the hydrographs and the efficiency. Similarly, catchments AQ also gave satisfactory results as given in Figure 15.

(iv) Catchment AQ

(a) Rainfall

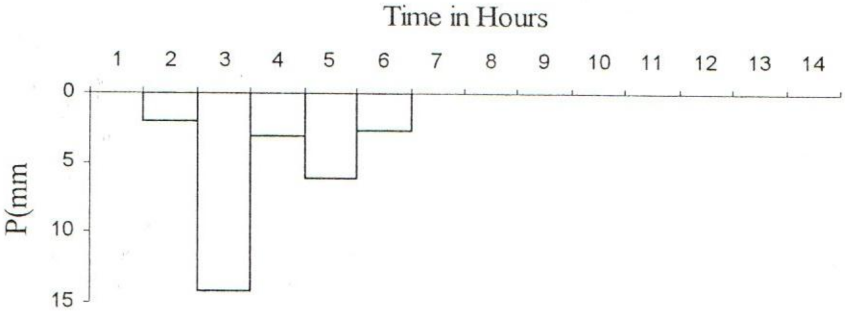

(b) Runoff

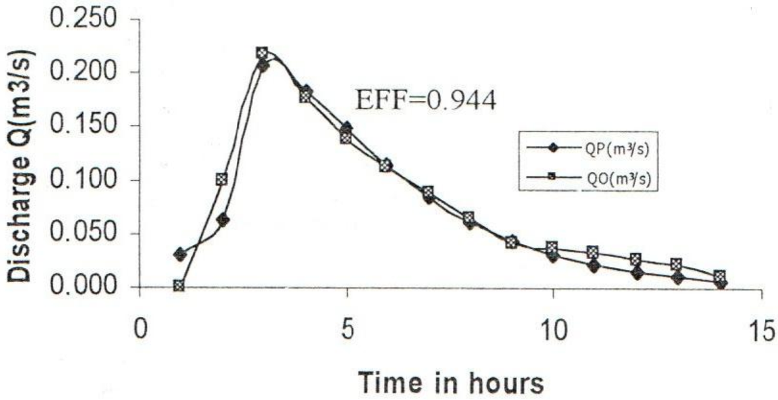

Figure 15 Predicted and observed hydrographs of 21/04/97 for AQ in NCDI model

Simulation process was done satisfactorily by the model for the runoff event in the Figure 15. The model predicted well the peak runoff rate. In this catchment, small lag time values were obtained as can be seen by the difference between peaks of the rainfall and runoff. This in physical terms could imply that the catchment had high moisture content thereby reducing the rate of infiltration thereby producing direct runoff almost immediately.

(v) **Catchment AR**

(a) Rainfall

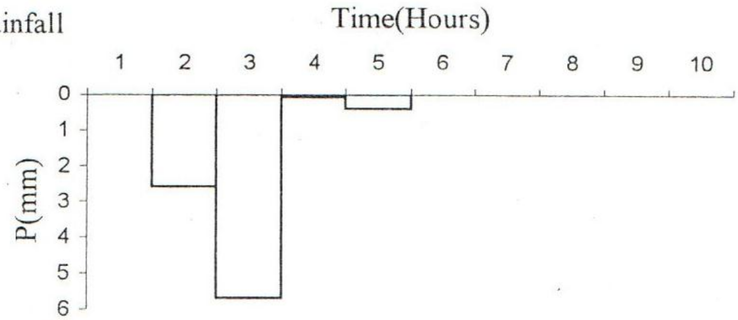

(b) Runoff

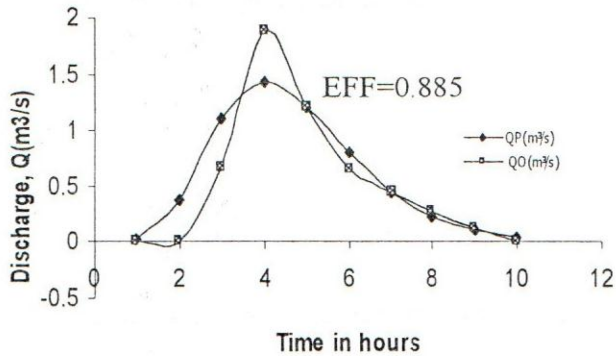

Figure 16 Predicted and observed hydrographs of 5/04/97 for AR in NCDI model

The results for catchment AR are presented in Figure 16. In this case, the simulated hydrograph compared reasonably well with the observed one although the hydrograph shape was slightly different, other hydrograph parameters like time to peak and duration were well simulated.

Overall Assessment of Model Performance

Apart from visual inspection of the observed and predicted hydrographs, statistical analysis was also carried out according to ASCE (1993) to verify the accuracy of the simulations. The mean statistical values obtained are given in Table 17.

Table 17 Mean values of the NCDI statistical model performance parameters

Catchment	No. of events	D_v (%)	*PEP (%)*	*SSR*	*EFF (%)*
A3	10	2.841	4.930	0.085	88.40
A4	9	1.646	14.88	0.350	81.10
AP	7	2.360	-8.39	0.003	87.74
AQ	9	-0.550	-29.64	0.240	73.87
AR	10	1.733	18.74	0.210	78.92

The values in Table 17 were obtained by lumping the mean statistical values obtained for every simulated runoff event in the catchment. The percentage deviations of the runoff volumes D_v obtained were close to zero indicating good simulation by this model. In catchment AQ the value of D_v obtained was negative. This indicates that the runoff volume was over simulated by the model.

The most important parameter used to evaluate the performance of the models was the Nash and Sutcliffe efficiency (EFF). Values of this parameter close to 100% indicate a perfect fit while those close to zero indicate that the model performed not better than the mean values of the observed runoff data. The mean values of the *EFF* obtained in Table 17 were all above 70% indicating an acceptable performance of the model (ASCE, 1993).

4.2.2 The NCGAI Model

The optimized parameters were used to simulate runoff processes using NCGAI model. The results for selected rainfall events for each catchment are shown in Figures 17 to 21 and in Appendix 7.2.

(i) Catchment A3

(a) Rainfall

(b) Runoff

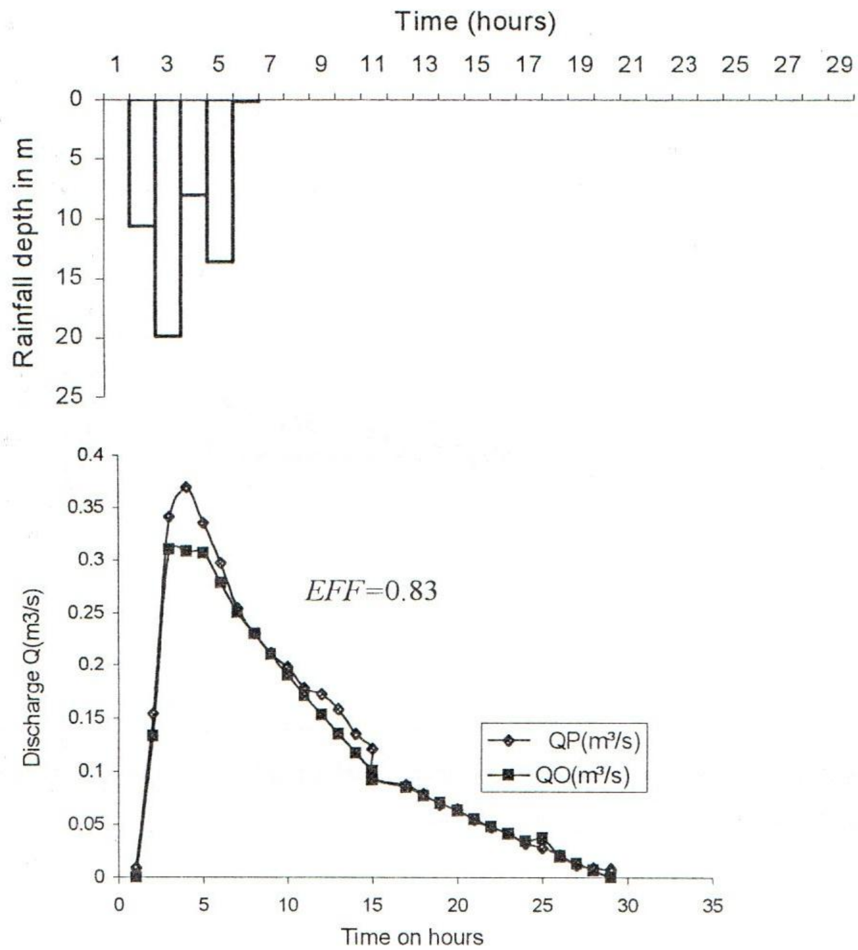

Figure 17 Predicted and observed hydrographs of 28/08/97 for A3 in NCGAI model

Simulation of runoff in catchment A3 (Figure 17) was reasonable. The predicted hydrograph slightly over predicted the peak runoff rate and the runoff volumes. However, these differences were quite small as shown by the hydrographs and the value of *EFF* obtained.

(ii) Catchment A4

(a) Rainfall

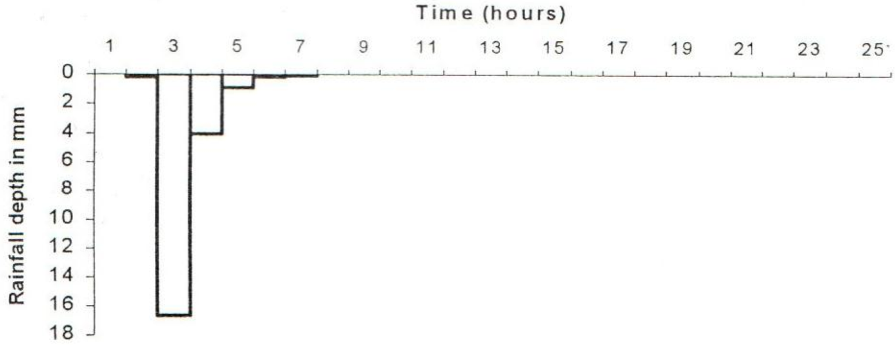

(b) Runoff

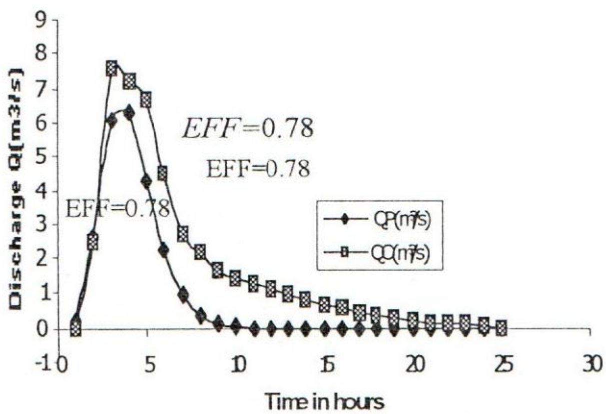

Figure 18 Predicted and observed hydrographs of 10/04/97 for A4 in NCGAI model

For this runoff event in Figure 18, the simulation process was fairly successful. Time of the runoff to peak was estimated well by the model, however, peak runoff rate and the runoff volumes were over-estimated by the NCGAI model. The overall *EFF* of 0.78 for this simulation was however, acceptable.

iii) Catchment AP

(a) Rainfall

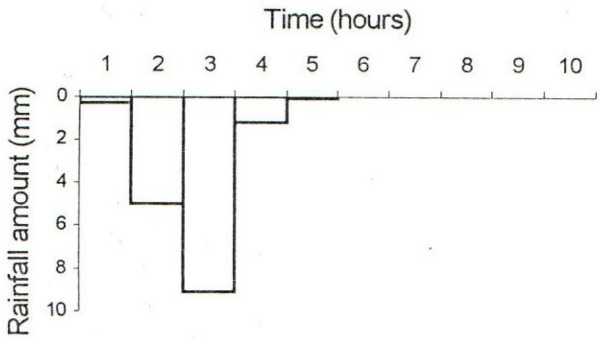

(b) Runoff

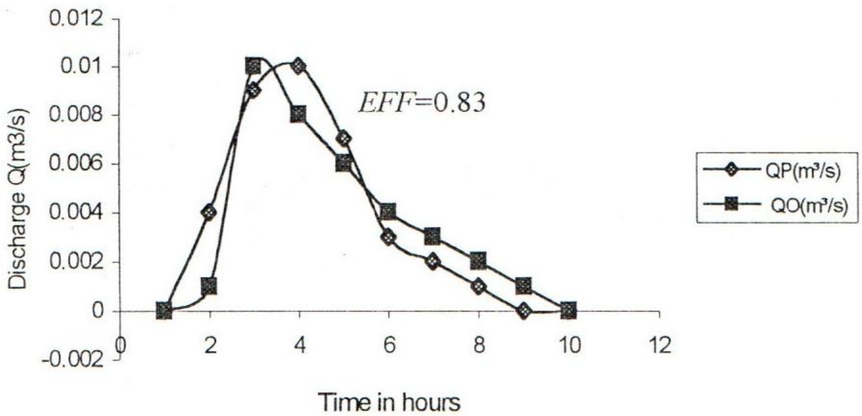

Figure 19 Predicted and observed hydrographs of 10/04/98 for AP in NCGAI model

The *EFF* obtained for this simulation was 0.830 and the predicted hydrograph was reasonable in terms of estimating the runoff volumes and times to peak of the runoff process. From Figure 19, the predicted hydrograph slightly lagged the observed hydrograph. The model therefore underestimated this parameter.

iv) Catchment AQ

(a) Rainfall

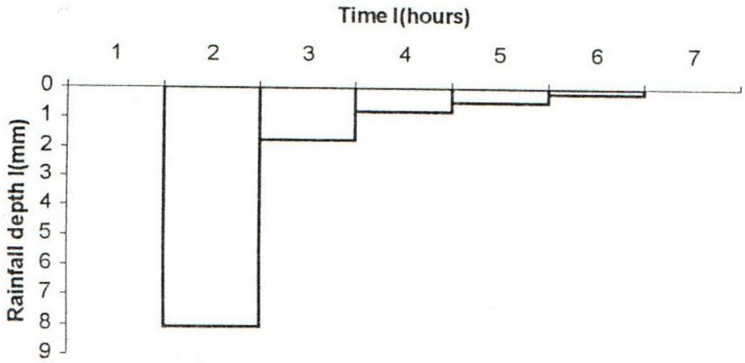

(b) Runoff

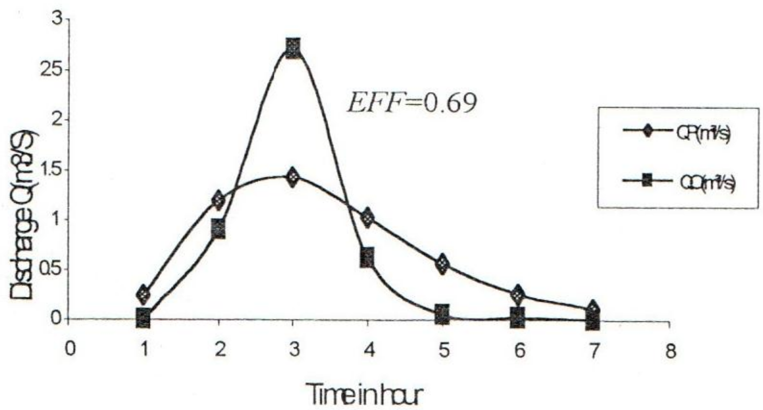

Figure 20 Predicted and observed hydrographs of 15/06/97 for AQ in NCGAI model

The predicted hydrograph in Figure 20 over predicted the peak runoff for this event. However, the runoff volume and the times to peak of the runoff process were well estimated. The discrepancy could have been caused by the rainfall not covering the entire catchment as the hydrographs indicated.

v) **Catchment AR**

(a) Rainfall

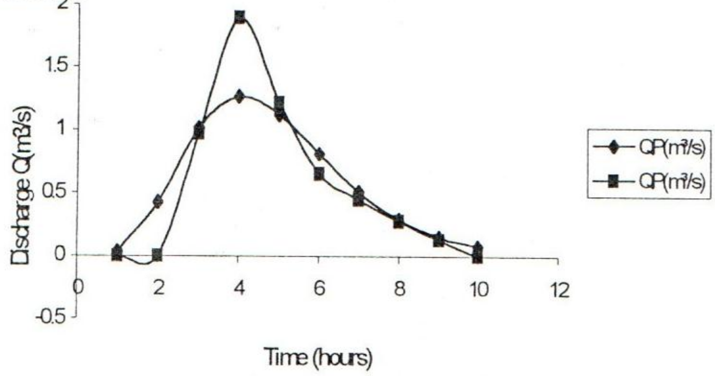

(b) Runoff

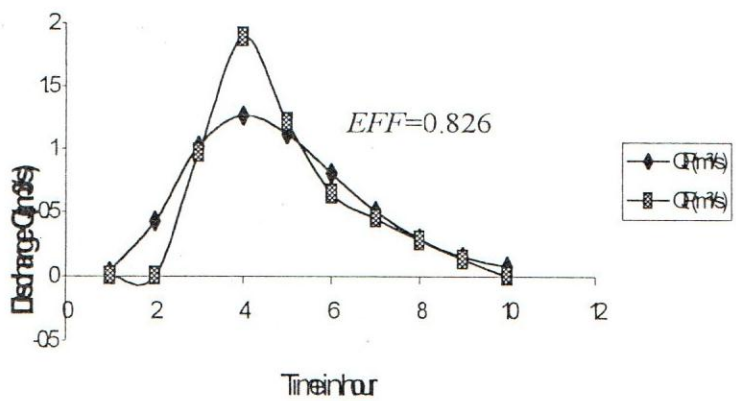

Figure 21 Predicted and observed hydrographs of 5/04/97 for AR in NCGAI model

The model also successfully simulated the runoff event in Figure 21. Times to peak of the runoff, time lag and the total runoff volumes were well predicted by the model. The model, however, over predicted the peak runoff in this catchment. From the value of *EFF* obtained, the simulation process was acceptable.

Overall assessment of the model performance

The predicted and observed hydrograph given in the Figures 17-21 indicate that the simulation results of the NCGAI model were acceptable by visual inspection. In order to verify these simulation results, statistical inspection was carried out according to the procedure outlined by ASCE (1993). The *EFF* values obtained for the catchments were greater than 0.6 as shown in Table 18.

Table 18 Mean values of the performance parameters of the NCGAI model

Catchment	No. of Events	D_v (%)	*PEP (%)*	*SSR*	*EFF (%)*
A3	10	45.48	30.12	0.0911	78.45
A4	9	22.65	19.26	2.00	76.80
AP	7	37.71	21.97	0.872	73.45
AQ	9	-9.36	-5.51	0.534	60.00
AR	10	19.40	23.3	1.97	73.27

From Table 18, the model simulated well the percentage runoff volumes in all the catchments except in catchment A3 where the mean value for the percentage runoff deviation, D_v was slightly high. Generally, low runoff volumes were obtained in this catchment due to the longer times of runoff recession exhibited by the catchment. Also, in this catchment, the value of the percentage error to peak, *PEP* was the highest compared to others due to the geographical location of this catchment relative to the others.

In general, the NCGAI model could not properly estimate peak flows for the catchments. However, the Nash and Sutcliffe efficiency obtained were for all the simulations were greater than 60% in all catchments indicating a good fit between the simulated and the observed data (ASCE, 1993).

4.3 Regionalization

4.3.1 The NCDI Model

In the first step of regionalization, the parameters of the model were optimized using the optimization algorithms. The results obtained are shown in Table 19.

Table 19 Parameters of the NCDI model after the initial optimization

Catchments	f_o	f_c	N	k	T_L	EFF
A3	28.90	4.96	3.37	2.42	8.16	0.884
A4	41.64	5.61	4.16	2.18	9.07	0.811
AP	38.19	5.73	5.76	0.9	5.18	0.877
AQ	33.87	3.95	4.62	0.68	3.14	0.734
AR	32.62	4.42	6.12	0.67	4.10	0.789

Mean *EFF*=0.819

The infiltration parameters f_o and f_c are interdependent in a similar way as the routing parameters. This means that an increase in one parameter causes a decrease in the other without causing a significant decrease in the *EFF*. Because of this, the adjustment process was done such that one parameter was held constant while the other successively adjusted through optimization as outlined in the following subsections.

1st Adjustment

The first adjustment was carried out on the infiltration parameters. The mean optimized value of f_c for the five catchments was used. The parameter f_c was held constant and the other parameters optimized. The results obtained shown in the Table 20.

Table 20 Parameters of the NCDI model after the first adjustment

Catchments	f_o	f_c	N	k	T_L	EFF
A3	11.34		3.07	1.42	4.359	0.816
A4	20.56		3.12	2.12	6.614	0.724
AP	28.19	4.934	4.72	1.19	5.617	0.793
AQ	23.87		4.42	3.28	14.49	0.686
AR	12.62		4.61	1.62	7.468	0.669

Mean *EFF*=0.738

The new parameters obtained in Table 20 were then used to simulate direct runoff in the study catchments. There was a reduction in the value of *EFF* from 0.819 to 0.738 due to the constant value of f_c used to eliminate interdependency between the infiltration parameters. The values of

f_o obtained were then correlated with the physical parameters for any relationship between them, as given in Table 21.

Table 21 First adjustment of the model parameters in NCDI model

Regression model	Catchments characteristic	*R* (correlation coefficient)	R^2
Log–linear	S_o	-0.823	0.677
Log–linear	S_c	-0.746	0.556
Log–linear	D_d	-0.688	0.473

The analysis indicated that maximum infiltration f_o correlated well with the overland slope *Sov* than the other two. A negative log-linear relationship was found to best fit this relationship as shown graphically in Figure 22.

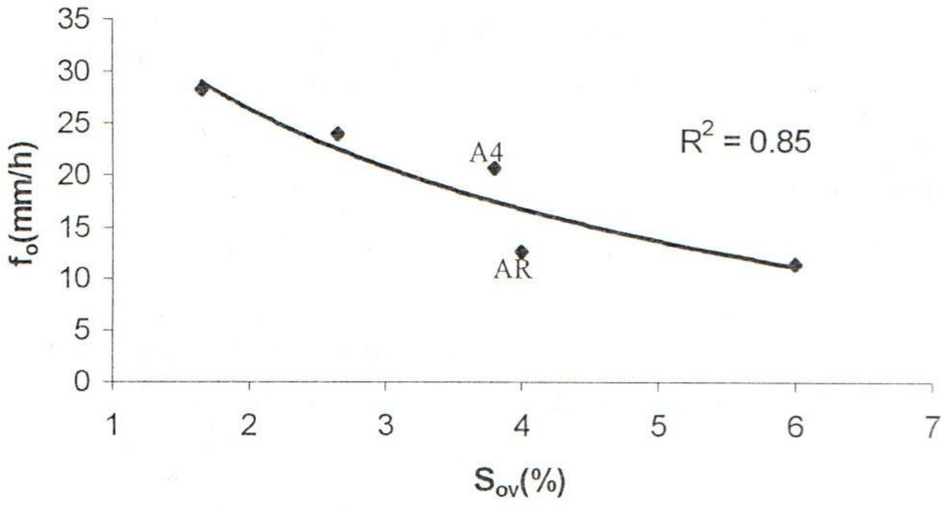

Figure 22 Relationship of f_o and S_o after the first adjustment.

From Figure 22, the two parameters related negatively with a correlation coefficient, *R* of 0.85. However, catchments A4 and AR deviated from the trend line and thus to improve their relationship, the second adjustment was necessary.

2nd Adjustment

The boundary conditions of the outlier catchments were adjusted by choosing new optimization boundaries (Table 22), which would closely orient them towards the trend line. Using the new boundaries, optimization was carried out and new parameter sets established. The parameters were then used to simulate runoff in the two catchments and new model derived parameters in Table 23 obtained..

Table 22 New boundaries for the outlier catchments in the NCDI model

Catchments	Lower boundary	Upper Boundary
A4	7	11
AR	8	10

Table 23 NCDI model parameters after the second adjustment

Catchments	f_o	f_c	n	k	T_L	*EFF*
A3	11.34		3.07	1.42	4.359	0.768
A4	**22.63**		**3.12**	**2.12**	**6.614**	**0.621**
AP	28.19	4.934	4.72	1.19	5.617	0.693
AQ	23.87		4.42	3.28	14.49	0.634
AR	**18.24**		**4.61**	**1.62**	**7.468**	**0.611**

Mean *EFF*=0.665

From Table 23, optimization with the new boundaries gave values of the mean *EFF* that reduced significantly from 0.738 to 0.665. This reduction was due to the errors introduced through change of boundary conditions. The new values of f_o obtained were then regressed with the overland slope S_{ov} as displayed graphically in Figure 23.

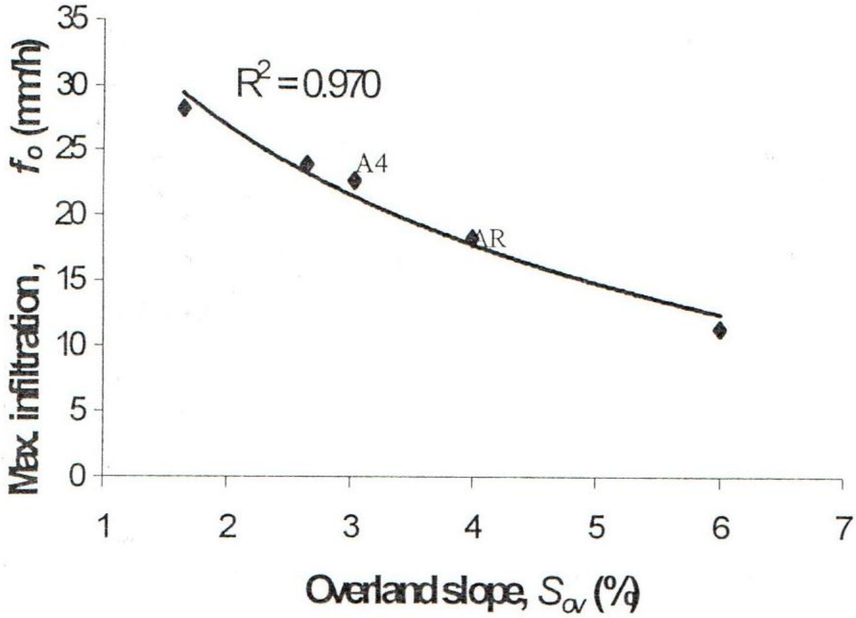

Figure 23 Relationship between f_o and S_o after second adjustment.

The correlation coefficient of the two parameters after the second regression was 0.97. This value was considered good enough in this study and therefore used to develop the transfer function given by Equation 30.

$$f_o = -13.148 \ln S_o + 36.019 \qquad 30$$

This equation gives an inverse relationship between f_o and S_o. This in physical sense indicates that as the slope steepness of the catchment increases, the rate of infiltration reduces.

With the development of the transfer function, the runoff generation parameters were considered regionalized. The regionalized parameter values were then used in adjusting the runoff routing parameters n and k in the third and forth adjustments.

3^{RD} Adjustment

The runoff routing parameters were first adjusted with the developed transfer function derived from Equation 30. Optimization was then carried out to determine new sets as given in Table 24.

Table 24 Parameters of the NCDI model after the third adjustment

Catchments	f_o	f_c	n	K	T_L	EFF
A3	12.46095		3.807	1.102	4.1953	0.648
A4	21.42286		2.142	1.712	3.6671	0.601
AP	29.39482	4.934	3.721	1.219	4.5359	0.643
AQ	23.20078		2.942	1.286	3.7834	0.614
AR	17.792		4.112	2.262	9.2995	0.589

Mean EFF=0.619

Through the use of the regionalized parameters of f_o and f_c, the value of EFF reduced from 0.665 to 0.619. This reduction is however considered relatively diminutive since the transfer function developed and used had a very high correlation value. The runoff routing parameters derived through optimization were regressed with the catchments characteristics for any relationship. The results of this regression are given in Table 25.

Table 25 Correlation coefficient, R for n and k in the NCDI model.

Regression model	Catchments characteristics	R values for n	R values for k
Log-linear	D_d	0.874	0.805
Log-linear	S_{ca}	0.866	0.752
Log-linear	S_{ov}	0.899	0.719
Log-linear	A	0.941	0.801
Log-linear	L	0.907	0.742
Log-linear	L_{ca}	0.911	0.785
Log-linear	$L*L_{ca}$	0.921	0.787
Linear	R_F	0.9664	0.768

From Table 25, the parameter n had the highest correlation than k. The best relationship was obtained between n and R_F as shown by the values of the correlation coefficient, R obtained. The graphical relationship between these two parameters and the catchment characteristics is further illustrated in Figures 24(a) and (b) for k and n respectively.

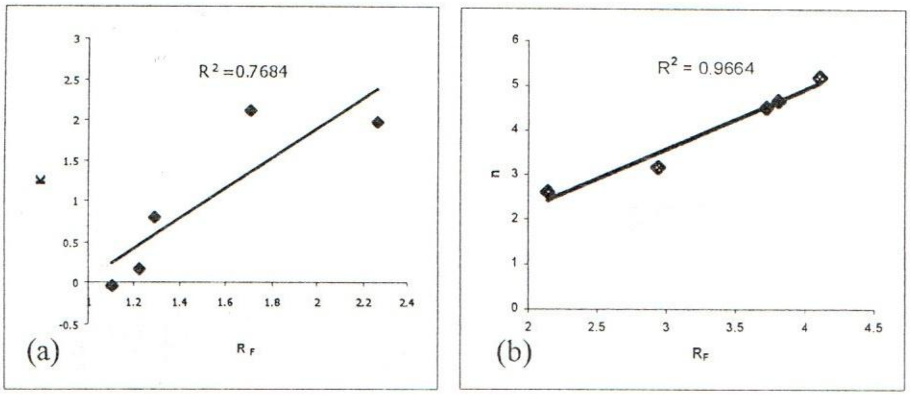

Figure 24 Relationships of k & n and the form R_F in the NCDI model.

Because the parameter n relates well with the catchments characteristics compared to k, the parameter k was therefore used to break the interdependency. The mean value of k for the five catchments was taken as the constant value and the next adjustments carried out.

4TH Adjustment

After optimization was carried out using the constant value of k, the results obtained were as given in Table 26.

Table 26 Parameters of the NCDI model after the fourth adjustment

Catchments	f_o	f_c	n	k	T_L	EFF
A3	12.46095		4.507		6.83381	0.626
A4	21.42286		5.124	1.5162	7.76900	0.567
AP	29.39482	4.934	2.121		3.21586	0.613
AQ	23.20078		3.242		4.91552	0.602
AR	17.792		4.712		7.14433	0.561

Mean EFF=0.594

The mean value of the *EFF* in Table 26 reduced from 0.619 to 0.594 due to the error introduced by the interdependency. Despite this reduction however, the values of the parameters were now more regionally specific and catchment based. The graphical relationship between n and R_F is illustrated in the Figure 25.

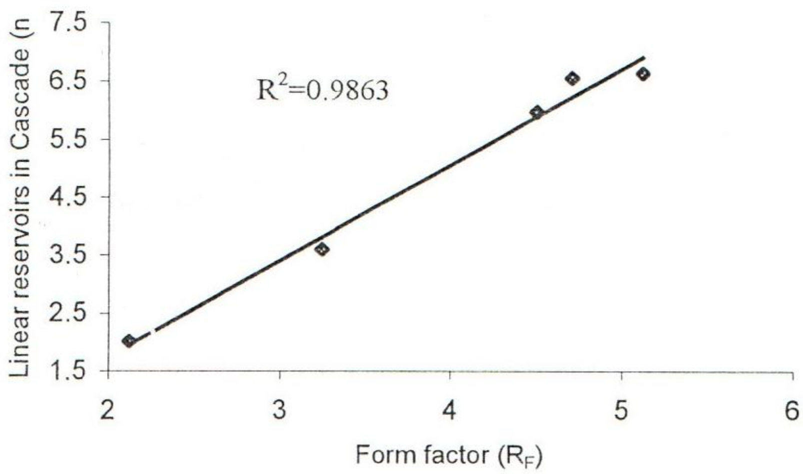

Figure 25 Graphical relationship between n and form factor R_F

The correlation coefficient of the two parameters in Figure 25 was 0.9863. This value was good enough and therefore the transfer function between the routing parameter n and form factor R_F was developed as expressed in Equation 31.

$$n = 1.6631 * R_F - 1.5867 \qquad 31$$

The determination of transfer functions for the routing parameters Equations (31) marks the regionalization of this model. The transfer functions developed were then be evaluated and validated in the gauged catchments before being used in the ungauged catchments.

<u>Evaluation of the Regionalization Procedure</u>

Using the values obtained from the transfer functions, simulations were again carried out to obtain new sets of fully regionalized parameters for the catchments. The results are given in Table 27 for the NCDI model.

Table 27 Regionalized parameters and the mean regional efficiencies in the NCDI model

Catchments	f_o	f_c	n	k	T_L	*EFF*
A3	12.46095		5.9871		9.0776	0.582
A4	21.42286		6.6648	1.5162	10.105	0.527
AP	29.39482	4.934	2.0081		3.0447	0.591
AQ	23.20078		3.6001		5.4585	0.580
AR	17.792		6.5800		9.9766	0.531

Mean *EFF*=0.5622

The overall mean *EFF* reduced from 0.594 to 0.562. The mean *EFF* values for each catchment at every stage of regionalization are summarized in Table 28.

Table 28 Mean EFF for the study catchments at various stages in the NCDI model

Catchment	Initial EFF	Adjust.1 EFF	Adjust.2 EFF	Adjust.3 EFF	Adjust.4 EFF	Region. EFF
A3	0.884	0.816	0.768	0.648	0.626	0.582
A4	0.811	0.724	0.621	0.601	0.567	0.527
AP	0.877	0.793	0.693	0.643	0.613	0.591
AQ	0.734	0.686	0.634	0.614	0.602	0.580
AR	0.789	0.669	0.611	0.589	0.561	0.531
Mean	**0.819**	**0.738**	**0.665**	**0.619**	**0.594**	**0.562**

From Table 28, the value of the mean *EFF* reduced after every stage of regionalization. This is because regionalization process constrains the model parameters so as to relate them with the physical characteristics of the catchments. In doing that, there is loss of accuracy. Nevertheless, the process of regionalization makes the model more versatile for use in runoff simulation in ungauged catchments.

4.3.2 The NCGAI Model

In this model, the optimized Green-Ampt infiltration model parameters of K and φ were regionalized. It is important to note that because of the high degree of variability of these two parameters within the catchments (Wesley *et al.*, 1992), this study chose to optimize the parameters. The results obtained were compared with the values obtained by Rawls *et al.* (1983), which are normally used for estimating Green-Ampt parameters, based on soil texture.

Because optimization of the parameters K and φ in the Green-Ampt model were done using a single weighted value, the soil textural values obtained by Rawls *et al.* (1983) were also weighted against the total catchments area and their obtained. The results of this coparison are given in Table 29.

Table 29 Comparison of the optimized infiltration parameters and soil textural values

Catchments	Mean values of the optimized parameters		Range of weighted values from soil textural classes		Deviation (±)	
	K (mm/h)	φ (mm)	K (mm/h	φ (mm)	K (%)	φ (%)
A3	1.01	219.67	1.27	217.7	20.47	0.905
A4	0.97	207.82	1.35	239.8	28.15	13.33
AP	1.17	248.51	0.5	287.0	-134.0	13.41
AQ	1.39	159.78	1.28	217.4	8.59	26.50
AR	0.79	253.32	1.00	216.2	21.00	-17.16

From the table, the optimized values of suction head wetting front, φ and the values obtained from the soil textural classes compared well within the study catchments. The percentage deviation of less than 30% was obtained. This parameter was thus considered successfully optimized and regionalized. Negative values of wetting front suction head in catchment AR indicate that the obtained optimized value of the parameter was slightly higher than that of the soil textural classes.

As for the hydraulic conductivity, the percentage deviation between the mean weighted optimized values and the mean weighted value obtained from soil textural classes were relatively small in all the catchments except in AP. In this catchment, the percentage deviation of the hydraulic conductivity was very high. Moreover, a negative deviation was obtained indicating a higher value of the optimized hydraulic conductivity. The value of *K* in this catchment was therefore adjusted as outlined below.

First Adjustment

In order to adjust the outlying value of *K* in catchment AP close to the expected soil textural class value, the boundaries of the hydraulic conductivity was constrained as shown in Table 30.

Table 30 New boundary conditions of *K* for the outlier catchments in NCGAI model

Catchment	Parameter	Min. value	Max. Value	Initial value
AP	*K*	0.1	0.75	0.2

This was done to reduce the value of the percentage deviation of the parameter *K* in this catchment. Optimization was carried out and the new sets of parameter obtained used to simulate runoff in the same catchment. The results obtained are given in Table 31.

Table 31 Parameters of the NCDI model after the first adjustment

Catchments	Mean values of the optimized parameters		Range of weighted values from soil textural classes		Deviation (±)	
	K (mm/h)	φ (mm)	K (mm/h	φ (mm)	K (%)	φ (%)
A3	1.01	219.67	1.27	217.7	20.47	0.905
A4	0.97	207.82	1.35	239.8	28.15	13.33
AP	**0.66**	**340.21**	**0.5**	**287.0**	**-32.00**	**-18.54**
AQ	1.39	159.78	1.28	217.4	8.59	26.50
AR	0.79	253.32	1.00	216.2	21.00	-17.16

The value of the hydraulic conductivity *K* obtained in the Table 31 reduced significantly from 1.17 to 0.66. This value obtained was accepted since any further boundaries adjustment gave negative deviation values of wetting front suction head. With this done, the hydraulic conductivity, *K* and wetting front suction head, φ were hence considered regionalized.

As for the Nash model, runoff routing parameters *n* and *k* were optimized using the regionalized values of the infiltration parameters and the results obtained given in the Table 32.

Table 32 Parameters of the NCGAI model after initial optimization

Catchments	Mean values of the optimized parameters				T_L =(*n***k*)	%*EFF*
	K	φ	*n*	*k*		
A3	1.01	219.67	5.12	1.681	8.607	74.45
A4	0.97	207.82	6.28	1.003	6.299	72.80
AP	0.66	340.21	5.57	0.910	5.069	71.45
AQ	1.39	159.78	4.69	0.872	4.090	60.00
AR	0.79	253.32	5.20	0.804	4.181	72.27

Mean *EFF*=70.19

The mean *EFF* value reduced from 72.39 to 70.19 (Table 32) due to the errors introduced by using the regionalized values of the infiltration parameters.

In order to regionalize the Nash routing parameters, the parameter *k* was held constant to break the interdependency between the two. This parameter was held constant because it was less sensitive than the parameter *n* which correlated much better with the catchments characteristics (Table 33). The constant value of *k* used was obtained by finding the mean values of the parameter in the five catchments under study.

Table 33 Values of correlation coefficient, *R* for n and k in the NCGAI model

Regression model	Catchments characteristics	R values for n	R values for k
Log-linear	D_d	0.914	0.821
Log-linear	S_c	0.801	0.724
Log-linear	S_o	0.923	0.768
Log-linear	A	0.949	0.821
Log-linear	L	0.912	0.787
Log-linear	L_{ca}	0.932	0.845
Log-linear	$L*L_{ca}$	0.941	0.827
Linear	R_F	0.971	0.868

The catchment characteristic R_F produced the highest correlation with the parameter n as compared to k (Table 33). The parameter n was therefore correlated to the catchments characteristic in a series of adjustments outlined below.

<u>**Second Adjustment**</u>

With the value of k held constant, the optimization was conducted and a new set of parameters presented in Table 34 established.

Table 34 Parameters of the NCGAI model after second adjustment

Catchments	Mean values of the optimized parameters				T_L =(n*k)	%EFF
	K	φ	n	k		
A3	1.01	219.67	6.718		6.7645	65.21
A4	0.97	207.82	5.021		6.7361	69.45
AP	0.66	340.21	4.357	1.054	5.0139	68.82
AQ	1.39	159.78	5.769		5.5535	54.65
AR	0.79	253.32	5.653		5.9582	64.37
					Mean *EFF*=64.50%	

The mean value of the *EFF* in Table 34, reduced from 70.19% to 64.50% due to the errors introduced by using a constant value of *k*. The relationship between *n* and R_F illustrated graphically is as shown in Figure 26.

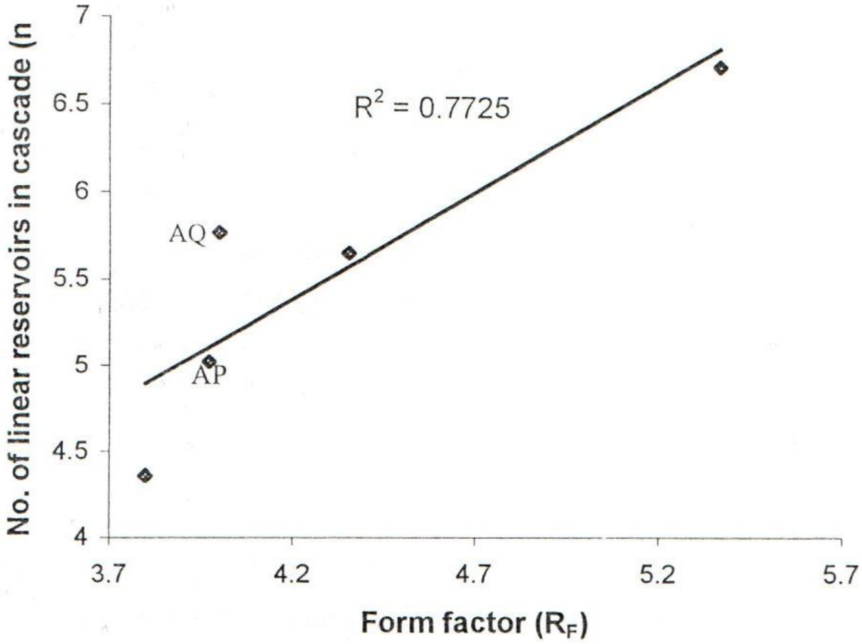

Figure 26 Graphical relationship of *n* and R_F in NCGAI model after the 1st adjustment

The two parameters correlated relatively well in all the catchments, as shown by the correlation coefficient obtained in Figure 25, except in catchments AP and AQ. The two outlying catchments were therefore adjusted in the next section.

Third Adjustments

The optimization boundaries for the two-outlier catchments were constrained as shown in the Table 35.

Table 35 New boundary conditions for two-outlier catchments in NCGAI model

Catchments	Lower boundary	Upper Boundary
AP	0.8	3
AQ	1.0	4

The boundaries in Table 35 were chosen in a manner to confine the values of the two parameters towards the trend line. Optimization was then carried out using these new boundaries and the results obtained given in Table 36.

Table 36 Adjusted Parameters of AP and AQ in the NCGAI model

Catchments	Mean values of the optimized parameters				T_L (n*k)	%EFF
	K	φ	n	k		
A3	1.01	219.67	6.718		7.0808	65.21
A4	0.97	207.82	5.021		5.2921	69.45
AP	**0.66**	**340.21**	**4.617**	1.054	**4.8663**	**58.97**
AQ	**1.39**	**159.78**	**5.334**		**5.6220**	**51.13**
AR	0.79	253.32	5.653		5.9582	64.37

Mean *EFF*=61.82%

After the third adjustment, the value of the *EFF* reduced from 64.50% to 61.82% due to errors caused by change of boundaries in the two catchments. However, the correlation coefficient of the parameter n and the catchment characteristic R_F improved to a value of 0.9215 as shown in the Figure 27.

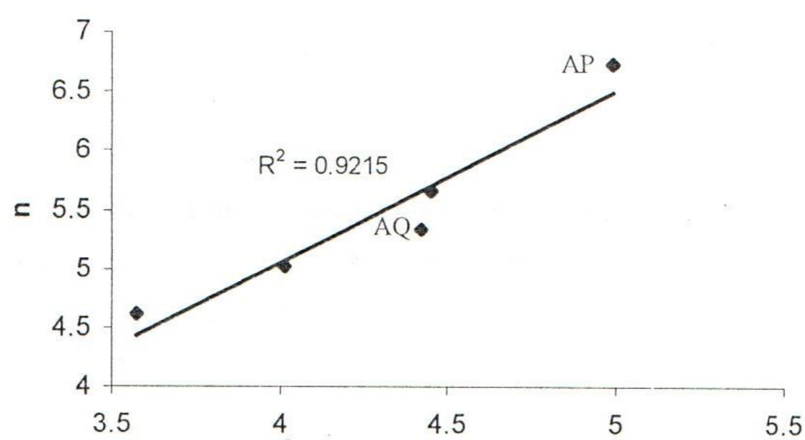

Figure 27 Graphical relationship of n and R_F in NCGAI model after the 2nd adjustment

The value of the correlation coefficient obtained in Figure 27 was considered good enough. The transfer function in Equation 32 was therefore developed between the routing parameter n and the form factor R_F.

$$n = 1.4397 * R_F - 0.7095 \qquad 32$$

Using this equation, new sets of the parameter n were established and optimization carried out with the mean regionalization efficiency obtained given in Table 37.

Table 37 Regionalized and the mean *EFF* values in the NCGAI model

Catchments	Mean values of the optimized parameters				T_L (n*k)	%EFF
	K	φ	n	k		
A3	1.01	219.67	7.898651		8.32518	62.011
A4	0.97	207.82	6.429604		6.77680	64.321
AP	0.66	340.21	6.079873	1.054	6.40818	55.915
AQ	1.39	159.78	6.700560		7.06239	49.213
AR	0.79	253.32	6.976709		7.35345	61.747

Mean EFF=58.64%

After this stage this model was considered fully regionalized. The mean regionalization efficiency *EFF* finally reduced to 58.64%. The regional values above were then used to estimate the model parameters from the catchments characteristics.

4.3.3 Comparison of the Nash Cascade Transfer Functions

The Nash Cascade model was used for runoff routing in the two models. Because the same runoff routing model was adopted in the same catchments of study, ideally the values of the transfer functions developed should be the same. For comparison purposes the transfer functions for Nash routing model in NCDI and NCGAI models are given in Equations (33) and (34) respectively.

$$n = 1.6631 * R_F - 1.5867 \qquad 33$$

$$n = 1.4397 * R_F - 0.7095 \qquad 34$$

A comparison of the two equations using values of R_F obtained from the study catchments gave the following estimates in Table 38.

Table 38 Comparison of the transfer functions for the NCDI and NCGAI models

Catchment	R_F	*n* values for the models	
		NCDI model	NCGAI model
A3	4.21	5.41	5.27
A4	4.54	5.96	5.74
AP	3.41	4.08	4.11
AQ	2.83	3.12	3.28
AR	1.80	1.41	1.80

In spite of using the same routing model, small differences were still inevitable in the regionalized values of the parameter n for both of the models. This was because the values of the runoff routing parameters obtained after optimization was a direct indication on the amount of rainfall excess generated and consequently routed in the catchments.

The two models, namely Diskin and the Green-Ampt models slightly quantified the infiltration processes differently depending on their parameters. This therefore meant that the rainfall excess produced and routed within the catchments using the Nash model was also slightly different as depicted in Table 38. Despite this, the values of n obtained in Table 38 closely approached each other indicating that regionalization was done successfully.

4.3.4 Testing of the Regionalized Model for use in ungauged Catchments

Due to the dire need to provide runoff data for appropriate catchment and river basin management practices such as flood mitigation, soil and water conservation amongst others, regionalization of rainfall-runoff models is unavoidable. Regionalization makes the models more versatile for use in runoff data generation in ungauged catchments. However, before regionalized models can be used, it is essential to test the applicability of the regionalized models using data from the gauged catchments.

(a) The NCDI model

Using the transfer functions, the regionalized NCDI model was tested using data from the study catchments to verify if the model could be used to generate reasonable runoff data in the ungauged catchments. Simulations were carried out using the regionalized model and the regionalized hydrographs compared with the observed hydrographs as shown in the Figure 28.

(a) Rainfall

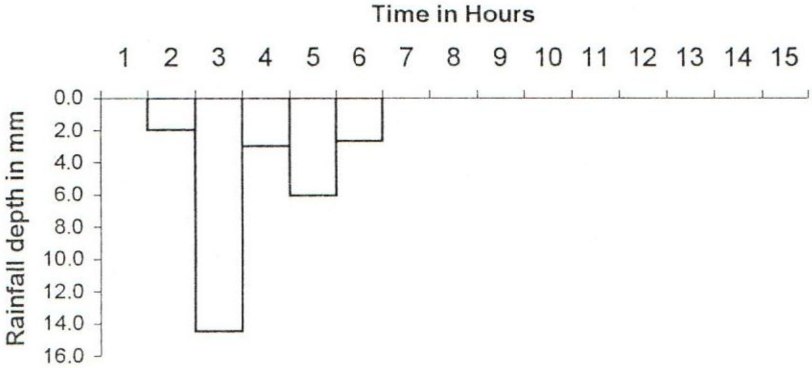

(b) Runoff

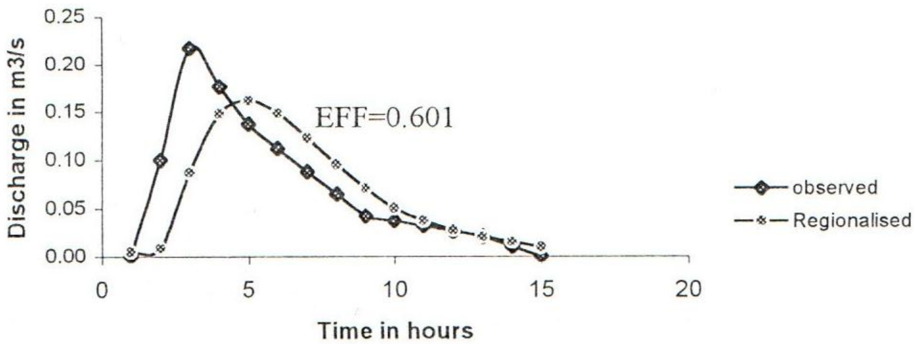

Figure 28 Observed and regionalized hydrographs for NCDI model for A3 catchment

The *EFF* of observed and regionalized runoff hydrographs in Figure 28 is about 0.601. This value is reasonable enough and implies that the regionalized parameters can be used to estimate surface runoff in ungauged catchments. For this particular runoff event, the regionalized hydrograph under estimated the peak runoff and the time lag. However, the runoff volumes were fairly estimated. Other parameters reasonably estimated by the regionalized model were the times to peak and the total duration of the runoff shown by the length of the hydrograph.

Generally, the regionalized NCDI model adequately simulated the runoff process. This model can therefore be used to simulate direct runoff in the neighboring-ungauged catchments with reliable rainfall and geophysical.

(b) The NCGAI model

The NCGAI model was first tested using data from the gauged catchments. Simulations were carried out using the model and the regionalized hydrographs compared with the observed hydrographs shown in Figure 29.

(a) Rainfall

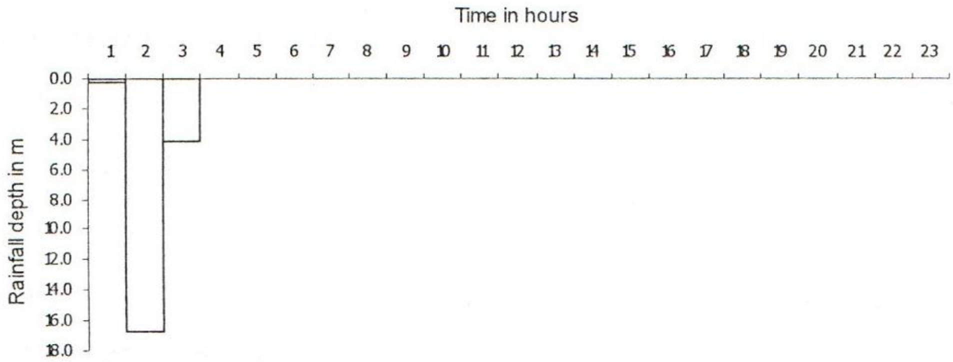

(b) Rainfall

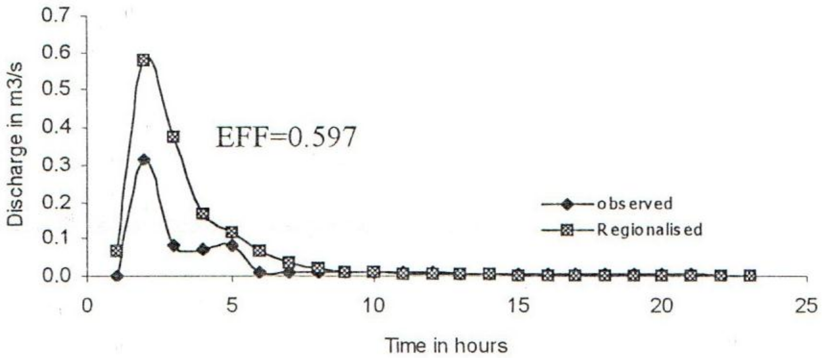

Figure 29 Observed and regionalized hydrographs for NCGAI model

Generally, the regionalized NCGAI model estimated well the observed hydrograph. From Figure 29, the model also estimated well the time lag and duration of the runoff. Nevertheless, the model can also be used to estimate direct runoff in the neighboring-ungauged catchments with reliable rainfall and geophysical data.

CHAPTER FIVE: CONCLUSIONS AND RECOMMENDATIONS

5.1 Conclusions

Since most catchments in Kenya are not gauged with appropriate instruments for runoff measurements, the use of rainfall-runoff models provide a possible alternative. Two rainfall-runoff models were adapted in this study to simulate runoff processes in a humid zone in Kenya. The models were calibrated with conceptual model parameters successfully determined from optimization algorithms. GIS-ArcView was used to derive the geo-physical parameters of the models. This was done through the identification of hydrologically similar units in a GIS environment.

In the NCDI model, the minimum and maximum infiltration rates were treated as conceptual parameters. The hydraulic conductivity and the wetting front suction head were also treated as conceptual parameter in the Green-Ampt model. These parameters, though physically based, were more site specific and had high degree of spatial variability within the catchment. Because of this reason, this study chose to optimize them and satisfactory results were obtained.

After calibration, the models were validated using data obtained from the gauged catchment of the upper Ewaso Ngiro basin and used to simulate runoff process. The NCDI model and the NCGAI models satisfactorily runoff simulations in the catchments under study. The NCDI model, however, gave better simulations with runoff events, which occurred for very long period of time. Such runoff events were dominant in catchments A3 and A4 due to their large sizes. NCGAI model on the other hand, produced better results with the shorter runoff events. Such events were dominant in catchments AP, AQ and AR. In general, the NCDI model was more consistent and produced better results compared to the NCGAI model.

Regionalization process was done effectively. The catchments characteristics were established from the catchments data and transfer functions that related the conceptual parameters to the catchment characteristics obtained. In the NCDI model, a transfer function for the maximum infiltration capacity was successfully developed. And for the NCGAI model, the Green-Ampt model parameters were treated as conceptual and then optimized. The results obtained were also satisfactory.

5.2 Recommendations

The models adopted for this research namely the NCDI and NCGAI models can be used to estimate and modify missing runoff events in gauged catchments with reliable rainfall data. As for the ungauged catchments, the model parameters can be established from the catchments characteristics, using transfer function developed in the regionalization process. This study reasonably developed transfer functions for the runoff generation models. However, the routing model gave two transfer functions for the same study area. Further tests should be carried out on regionalization to ascertain the transfer functions. This is important in to enable data generation in ungauged catchments of Kenya.

REFFERENCES

Abbott, M.B., Bathurst, J.C., Cunge, J.A., O'Conell, P.E. and Rasmussen, J., 1986. An Introduction to the European hydrological system-Systeme hydrologique European, "SHE", 2: Structure of a physically based distributed modeling system. J. hydrol. 87: 61-77.

ASCE Task Committee, 1993. Criteria for evaluation of watershed models. J. of Irrigation and Drainage Engineering, ASCE, 119(3):429-442.

Berger, P., 1989. Rainfall and Agroclimatology of the Laikipia plateau, Kenya. African Studies series vol. 7. Geograghica Bernensia and Geophysical society of Berne, University of Berne, Berne Switzerland.

Brakensiek, D.L. and C.A. Onstad, 1977. Parameter Estimation of the Green-Ampt Infiltration Equation. Water Resour. Res. 13(6): 1009-1012.

Braun, H. M., 1982. Agro-climatic zone map of Kenya, 1:1000000. Kenya Soil Survey, Ministry of agriculture, Nairobi Kenya.

Chow, V.T; Maidment, D.R. and Marys, L.W., 1988. Applied Hydrology. International edition. Mc Graw – Hill Book Company, New York.

Clapp, R. B. and Hornbereger, G. M, 1978. Empirical equations for some Hydraulic properties. Water resource. Res. 14(4): 601-604.

Diskin, M.H. and Nazimov, N., 1995. Linear reservoir with feedback regulated inlet as model for the Infiltration process. J. Hydrology. 172:313 – 330.

Diskin, M.H. and Nazimov, N., 1996: Ponding time and infiltration capacity variation dump steady rainfall. J. Hydrol. 178: 369-380.

Drayton, R. S., Wilde, B. M., and Harris, J. H. K., 1992: Geographical Information System approach to distributed modeling, Hydrological Processes, Vol. 6, 361-368.

Duan, Q., Sorroshian, S., and Gupta, V., 1992: Effective and efficient Global optimization for conceptual Rainfall-runoff models. Water resourc. res 28(4):1015-1031.

ESRI, 1995. Understanding GIS. Environmental System Resources Institute, Redlands.

Funke, R., Schumann, A.H. and Schultz, G. A. 1998: Regionale Parameterisierung eines hydrologischen Niederschlab-Abflub-Modells fur Mittelgebirgsverhaltnisse. Abschlubberitcht an die Deutsche Forschungsgemeinschaft. Unpubli.

Goodchild, M.F., 1993. Data models and data quality: Problem and prospects. In: M.F. Goodchild, L. T. Styaert and B.O. Park (Eds), Environmental Modeling with GIS. Oxford University of Berne, Berne, 69pp.

Houghton-Carr, H.A., 1999. Assessment criteria for simple conceptual daily rainfall-runoff models. Water Resorc. Res. 21 (12): 1841-1850.

Junil, P., Kang, S. I. and Singh, P. V., 1999. Comparison of simple runoff models used in Korea for small watersheds, Hydrol. process. 13, 1527-1540.

Kihara, F. I., 1998. An investigation into the soil loss Problem in the upper Ewaso Ngiro basin. Msc. thesis, University of Nairobi.

Leavesley, G.H. and Stannard, L.G., 1995. The precipitation runoff modeling system-PRMS. In: Computer Models of watershed Hydrology. Singh, V.P (Ed.) Chp 9.

Ministry of water development, 1992. The study on the National Master Water Plan-Sectorial Report (B); Hydrology. Ministry of Water Development, Nairobi.

Mutunga, C.N., 1994. The influence of vegetative cover on Runoff and Soil loss- a study in Kukogodo, Laikipia District, Msc. Thesis, University of Nairobi.

Nash, J.E. (1957): The form of the instantaneous Unit Hydrograph, IASH Publication no. 45, Vol. 3-4, pp. 114 – 121.

Nash, J.E. and Sutcliffe, J.V., 1970. River flow forecasting through conceptual models part 1 – a discussion of principles. J. Hydrol. 10: 282 – 290.

Obiero , J. P. O. and Sharma, T. C., 2002: Evaluation of Infiltration using the Green-Ampt Model for Catchments in Kenya, East Africa. J. Engineering in Agriculture and the Environment. Vol. 2 No. 1 2002.

Onyando, J.O and Sharma, T.C., 1995. Simulation of direct runoff volumes and peak rates for rural catchments in Kenya, East Africa. Hydrol. Sci. J. 40(3): 367 – 380.

Onyando, J.O., 2000. Rainfall – Runoff Models for ungauged catchments in Kenya. Ph.D. Thesis Ruhr University, Germany.

Pilgrims, D. H., 1983. Some problems in transferring hydrological relationships between small and large drainage basins and between regions. J. Hydrol. 65: 49-72

Rawls, W. J. and D. L. Brakensiek, 1982. Estimating Soil Water Retention from soil Properties. Journal of Irrigation and Drainage Division, ASCE 108(IR2).

Rawls, W. J. and D.L. Brakensiek, 1983. Procedure to Predict Green-Ampt Infiltration Parameters. *In:* Advances in Infiltration. Proceedings of the National Conferences on Advances in Infiltration, ASAE, Chicago, Illinois.

Rawls, W.J. and D.L. Brakensiek, 1985. Prediction of Soil Water Properties for Hydrologic Modeling. *In:* Watershed Management in the 80's, E. B. Jones and T.J. Ward (Editors). ASCE, Newyork, pp. 293-299.

Riggs, H. C., 1990. Estimation of flow characteristics at ungauged sites. In: Regionalisation in Hydrology (Proceedings of the Ljubljana Symposium, April 1990). IAHS Publ. no. 191:159-169.

Sanjay, K. J., Sudhir, K., and Varghese, J., 2001. Estimation of soil erosion for a Himalayan watershed using GIS. Water Resources Management 15:41-54.

Schultz, G.A., 1993. Application of GIS and remote sensing in Hydrology. Hydro GIS 93: Application of Geographic Information Systems in Hydrology and water Resources. Proc. of the Vienna Conference, 1993. IAHS Publ. No. 211: 127 – 140.

Sefton, C.E.M. and Horwarth, S.M., 1998: Relationships between dynamic response characteristics and physical descriptors of catchments in England and Wales. J. Hydol. 211:1-16.

Serwan, M. J. B., and Kamaruzuman W. Y., 2001: Modeling of Soil Erosion in the tropical environments using Remote Sensing and geographical Information Systems. Hydrological sciences- Journal des sciences Hydrologiques, 46(2).

Shaw, E.M., 1996. Hydrology in Practice. Third edition. Chapman and Hall. London.

Singh, V.P., 1995(ed.) Computer models for watershed Hydrology. Water resources publication. Colorado.

Smith, R.E., and J.Y. Parlange, 1978. A parameter efficient hydrologic infiltration model, Water Resour. Res., 14 (3), 533-538.

Sorooshian, S. and Gupta, V.K., 1995. Model calibration. In: Computer Models of watershed Hydrology. Chp 2. Pp 23-68. Ed. Singh, V.P.

Stewart, M. D., Anderson, M.G., Price, D. A. and Burt, T. P., 1999. Modeling floods in hydrologically complex lowland river reaches. 223: 85-106.

Wesley P. James, John Warriner, and Michael Reedy, 1992. Application of the Green-Ampt Infiltration Equation to Watershed modeling. American Water Resources Association. Water Resources bulletin. Vol.28, No. 3.

APPENDICES

Simulated and Regionalized Hydrographs for the Models

1 Catchment A3

Date	Time (h)	P (mm)	NCDI Model			NCGAI model		
			QP (m^3/s)	QO (m^3/s)	Qregion.	QP (m^3/s)	QO (m^3/s)	Qregion.
1/8/9		0.000	0.009	0.000	0.005	0.001	0.000	0.001
		0.200	0.522	0.487	0.505	0.458	0.487	0.473
		16.700	0.985	1.140	1.063	1.140	1.140	1.140
		14.100	1.040	1.028	1.034	1.061	1.028	1.045
		8.900	1.007	0.920	0.964	0.924	0.920	0.922
		6.100	0.926	0.817	0.872	0.818	0.818	0.818
		3.140	0.824	0.719	0.772	0.718	0.719	0.719
		0.650	0.715	0.625	0.719	0.626	0.625	0.626
		0.800	0.610	0.536	0.625	0.534	0.536	0.718
	10	0.100	0.513	0.451	0.926	0.447	0.451	0.626
	11	0.000	0.426	0.370	0.824	0.373	0.370	0.534
	12	0.000	0.351	0.334	0.715	0.331	0.334	0.447
	13	0.000	0.287	0.300	0.610	0.305	0.300	0.373
	14	0.000	0.233	0.266	0.513	0.267	0.266	0.331
	15	0.000	0.188	0.233	0.426	0.231	0.233	0.305
	15	0.000	0.151	0.201	0.351	0.200	0.201	0.267
	17	0.000	0.121	0.170	0.287	0.170	0.170	0.231
	18	0.000	0.097	0.140	0.233	0.140	0.140	0.200
	19	0.000	0.077	0.110	0.188	0.110	0.110	0.170
	20	0.000	0.061	0.081	0.071	0.080	0.081	0.140
	21	0.000	0.048	0.054	0.051	0.055	0.054	0.110
	22	0.000	0.038	0.026	0.032	0.025	0.026	0.026
	23	0.000	0.030	0.000	0.015	0.000	0.000	0.000

Date	Time (h)	P(mm)	NCDI Model			NCGAI model		
			QP (m^3/s)	QO (m^3/s)	Qregion.	QP (m^3/s)	QO (m^3/s)	Qregion.
1/21/97		0.000	0.010	0.000	0.015	0.001	0.000	0.001
		7.100	0.052	0.062	0.057	0.020	0.062	0.063
		11.600	0.103	0.128	0.116	0.166	0.128	0.160
		14.400	0.249	0.235	0.256	0.218	0.235	0.298
		1.200	0.295	0.352	0.350	0.351	0.352	0.425
		0.700	0.316	0.332	0.412	0.328	0.332	0.430
		1.200	0.317	0.312	0.317	0.305	0.312	0.391
		0.600	0.302	0.292	0.310	0.220	0.292	0.354
		1.400	0.278	0.273	0.300	0.243	0.273	0.342
	10	0.480	0.249	0.235	0.350	0.280	0.235	0.337
	11	0.600	0.218	0.198	0.228	0.148	0.198	0.248
	12	1.200	0.187	0.180	0.180	0.132	0.180	0.215
	13	1.300	0.158	0.162	0.182	0.121	0.162	0.196
	14	0.800	0.132	0.145	0.155	0.114	0.145	0.173
	15	0.300	0.109	0.128	0.143	0.118	0.128	0.157
	15	0.800	0.090	0.094	0.128	0.085	0.094	0.123
	17	0.300	0.073	0.062	0.103	0.073	0.062	0.093
	18	0.000	0.059	0.054	0.084	0.052	0.054	0.076
	19	0.000	0.047	0.046	0.067	0.046	0.046	0.063
	20	0.000	0.037	0.038	0.056	0.040	0.380	0.138
	21	0.000	0.030	0.030	0.046	0.032	0.030	0.042
	22	0.000	0.023	0.015	0.037	0.016	0.015	0.026
	23	0.000	0.030	0.000	0.015	0.000	0.000	0.000

Date	Time (h)	P(mm)	NCDI Model			NCGAI model		
			QP (m^3/s)	QO (m^3/s)	Qregion.	QP (m^3/s)	QO (m^3/s)	Qregion.
3/26/97		0.000	0.030	0.000	0.050	0.005	0.000	0.021
		2.000	0.124	0.100	0.009	0.075	0.100	0.102
		14.500	0.190	0.217	0.087	0.174	0.217	0.221
		3.000	0.204	0.176	0.147	0.179	0.176	0.221
		6.100	0.186	0.137	0.162	0.122	0.137	0.186
		2.700	0.152	0.112	0.148	0.064	0.112	0.147
		0.000	0.117	0.088	0.122	0.028	0.088	0.111
		0.000	0.085	0.065	0.095	0.011	0.065	0.080
		0.000	0.060	0.042	0.071	0.004	0.042	0.055
	10	0.000	0.041	0.037	0.050	0.001	0.037	0.042
	11	0.000	0.027	0.032	0.037	0.000	0.032	0.032
	12	0.000	0.018	0.026	0.027	0.000	0.026	0.024
	13	0.000	0.012	0.021	0.020	0.000	0.021	0.019
	14	0.000	0.007	0.010	0.015	0.000	0.010	0.011
	15	0.000	0.030	0.000	0.015	0.000	0.000	0.000

Date	Time(h)	P(mm)	NCDI Model			NCGAI model		
			QP(m^3/s)	QO(m^3/s)	Qregion.	QP(m^3/s)	QO(m^3/s)	Qregion.
3/30/97		0.000	0.044	0.000	0.345	0.000	0.000	0.097
		4.100	0.211	0.296	0.011	0.290	0.296	0.276
		10.100	0.571	0.702	0.286	0.602	0.702	0.716
		9.000	0.724	0.722	0.472	0.827	0.722	0.867
		2.800	0.774	0.742	0.640	0.745	0.742	0.911
		2.200	0.747	0.690	0.683	0.689	0.690	0.875
		0.000	0.674	0.640	0.691	0.642	0.640	0.822
		0.000	0.580	0.526	0.660	0.526	0.526	0.704
		0.000	0.481	0.419	0.581	0.419	0.419	0.580
	10	0.000	0.388	0.376	0.495	0.377	0.376	0.503
	11	0.000	0.306	0.335	0.430	0.336	0.335	0.436
	12	0.000	0.237	0.294	0.368	0.296	0.294	0.372
	13	0.000	0.181	0.255	0.314	0.251	0.255	0.314
	14	0.000	0.136	0.216	0.264	0.212	0.216	0.261

15	0.000	0.102	0.179	0.220	0.187	0.179	0.217
15	0.000	0.075	0.142	0.183	0.140	0.142	0.170
17	0.000	0.055	0.107	0.144	0.102	0.107	0.129
18	0.000	0.040	0.073	0.112	0.071	0.073	0.092
19	0.000	0.029	0.040	0.082	0.041	0.040	0.058
20	0.000	0.021	0.021	0.055	0.020	0.021	0.035
21	0.000	0.015	0.004	0.036	0.003	0.004	0.016
23	0.000	0.030	0.000	0.015	0.000	0.000	0.000

Date	Time(h)	P(mm)	NCDI Model			NCGAI model		
			QP(m^3/s)	QO(m^3/s)	Qregion.	QP(m^3/s)	QO(m^3/s)	Qregion.
4/7/97	1	0.000	0.351	0.000	0.214	0.112	0.000	0.169
	2	6.200	1.695	2.181	0.116	1.345	2.181	1.879
	3	0.600	3.024	5.952	1.359	3.205	5.952	4.873
	4	11.300	4.842	5.592	3.074	3.975	5.592	5.769
	5	2.700	5.176	5.245	3.942	3.522	5.245	5.782
	6	1.700	4.998	4.029	4.254	2.546	4.293	5.030
	7	1.000	4.511	3.438	3.879	1.607	3.438	4.218
	8	0.500	3.880	2.791	3.453	0.920	2.791	3.459
	9	0.000	3.220	2.203	2.867	0.490	2.203	2.746
	10	0.000	2.597	1.872	2.341	0.247	1.872	2.232
	11	0.000	2.049	1.560	1.896	0.119	1.560	1.796
	12	0.000	1.587	1.267	1.517	0.055	1.267	1.423
	13	0.000	1.211	0.991	1.201	0.025	0.991	1.105
	14	0.000	0.912	0.812	0.936	0.011	0.812	0.871
	15	0.000	0.679	0.641	0.734	0.005	0.641	0.675
	15	0.000	0.501	0.552	0.565	0.002	0.552	0.543
	17	0.000	0.366	0.464	0.447	0.001	0.464	0.436
	18	0.000	0.266	0.379	0.349	0.000	0.379	0.343
	19	0.000	0.192	0.295	0.273	0.000	0.295	0.264
	20	0.000	0.138	0.144	0.209	0.000	0.144	0.159
	21	0.000	0.030	0.000	0.015	0.000	0.000	0.000

Date	Time(h)	P(mm)	NCDI Model			NCGAI model		
			QP(m³/s)	QO(m³/s)	Qregion.	QP(m³/s)	QO(m³/s)	Qregion.
10/8/01	1	0.000	0.033	0.000	0.035	0.000	0.057	0.031
	2	0.200	0.868	0.000	0.008	0.200	0.847	0.481
	3	16.700	3.724	2.774	0.276	16.700	2.559	6.508
	4	4.100	7.176	8.945	5.802	4.100	4.068	7.523
	5	0.960	9.186	8.940	5.124	0.960	4.639	7.212
	6	0.200	9.161	8.936	6.222	0.200	4.325	7.211
	7	0.100	7.727	6.769	5.855	0.100	3.525	5.994
	8	0.000	5.781	4.965	5.204	0.000	2.609	4.640
	9	0.000	3.952	4.051	4.150	0.000	1.797	3.488
	10	0.000	2.519	3.241	3.302	0.000	1.170	2.558
	11	0.000	1.518	2.528	2.478	0.000	0.728	1.813
	12	0.000	0.874	1.903	1.837	0.000	0.437	1.263
	13	0.000	0.484	1.558	1.314	0.000	0.254	0.902
	14	0.000	0.260	1.243	0.970	0.000	0.144	0.654
	15	0.000	0.135	1.116	0.704	0.000	0.080	0.509
	15	0.000	0.069	0.995	0.555	0.000	0.044	0.416
	17	0.000	0.034	0.878	0.442	0.000	0.023	0.344
	18	0.000	0.017	0.766	0.367	0.000	0.012	0.290
	19	0.000	0.008	0.658	0.306	0.000	0.006	0.245
	20	0.000	0.004	0.554	0.258	0.000	0.003	0.205
	21	0.000	0.002	0.464	0.216	0.000	0.002	0.171
	22	0.000	0.001	0.377	0.181	0.000	0.001	0.140
	23	0.000	0.000	0.293	0.149	0.000	0.000	0.110
	24	0.000	0.000	0.212	0.119	0.000	0.000	0.083
	25	0.000	1.000	0.134	0.090	0.000	0.000	0.306
	26	0.000	0.000	0.059	0.313	0.000	0.000	0.093
	27	0.000	0.000	0.032	0.037	0.000	0.000	0.017
	28	0.000	0.000	0.005	0.086	0.000	0.000	0.023
	29	0.000	0.030	0.000	0.015	0.000	0.000	0.000

Date	Time(h)	P(mm)	NCDI Model			NCGAI model		
			QP(m³/s)	QO(m³/s)	Qregion.	QP(m³/s)	QO(m³/s)	Qregion.
9/18/01	1	0.000	0.009	0.000	0.008	0.000	0.001	0.005
	2	1.300	0.042	0.061	0.002	1.300	0.063	0.367
	3	4.200	0.073	0.133	0.353	4.200	0.138	1.224
	4	4.800	0.091	0.132	1.102	4.800	0.130	1.564
	5	11.700	0.096	0.131	1.344	11.700	0.130	3.350
	6	11.600	0.153	0.130	3.257	11.600	0.128	3.817
	7	7.700	0.135	0.130	3.307	7.700	0.129	2.850
	8	1.300	0.114	0.119	2.806	1.300	0.118	1.114
	9	1.000	0.093	0.109	1.210	1.000	0.107	0.630
	10	0.400	0.073	0.090	1.002	0.400	0.087	0.413
	11	0.200	0.057	0.071	0.443	0.200	0.071	0.211
	12	0.000	0.043	0.053	0.332	0.000	0.056	0.121
	13	0.000	0.032	0.040	0.135	0.000	0.040	0.062
	14	0.000	0.024	0.031	0.101	0.000	0.032	0.047
	15	0.000	0.017	0.026	0.047	0.000	0.026	0.029
	15	0.000	0.013	0.021	0.036	0.000	0.021	0.023
	17	0.000	0.009	0.015	0.020	0.000	0.012	0.014
	18	0.000	0.006	0.011	0.015	0.000	0.011	0.011
	19	0.000	0.005	0.007	0.009	0.000	0.005	0.007
	20	0.000	0.003	0.004	0.007	0.000	0.004	0.004
	21	0.000	0.030	0.000	0.015	0.000	0.000	0.000

Date	Time(h)	P(mm)	NCDI Model			NCGAI model		
			QP(m³/s)	QO(m³/s)	Qregion.	QP(m³/s)	QO(m³/s)	Qregion.
9/16/01	1	0.000	0.028	0.000	0.033	0.000	0.000	0.015
	2	0.400	0.131	0.146	0.007	0.146	0.146	0.144
	3	8.400	0.224	0.371	0.114	0.371	0.371	0.363
	4	7.500	0.272	0.340	0.243	0.341	0.340	0.384
	5	2.000	0.279	0.311	0.267	0.311	0.311	0.370
	6	0.000	0.258	0.286	0.286	0.286	0.286	0.351
	7	0.000	0.223	0.261	0.274	0.260	0.261	0.320
	8	0.000	0.184	0.237	0.258	0.237	0.237	0.288
	9	0.000	0.146	0.213	0.233	0.210	0.213	0.254
	10	0.000	0.113	0.190	0.207	0.192	0.190	0.223

11	0.000	0.085	0.168	0.182	0.167	0.168	0.193
12	0.000	0.063	0.146	0.157	0.145	0.146	0.164
13	0.000	0.046	0.125	0.134	0.126	0.125	0.139
14	0.000	0.033	0.109	0.113	0.108	0.109	0.118
15	0.000	0.024	0.093	0.096	0.095	0.093	0.100
15	0.000	0.017	0.078	0.081	0.083	0.078	0.084
17	0.000	0.012	0.062	0.069	0.062	0.062	0.067
18	0.000	0.008	0.047	0.054	0.046	0.047	0.051
19	0.000	0.006	0.033	0.042	0.032	0.033	0.037
20	0.000	0.004	0.018	0.031	0.017	0.018	0.022
21	0.000	0.003	0.004	0.020	0.003	0.004	0.009
22	0.000	0.030	0.000	0.015	0.000	0.000	0.000

Date	**Time(h)**	**P(mm)**	**NCDI Model**			**NCGAI model**		
			QP(m^3/s)	**QO(m^3/s)**	**Qregion.**	**QP(m^3/s)**	**QO(m^3/s)**	**Qregion.**
9/14/01	1	0.000	0.030	0.000	0.042	0.005	0.000	0.019
	2	2.000	0.124	0.100	0.009	0.075	0.100	0.102
	3	14.500	0.190	0.217	0.085	0.174	0.217	0.221
	4	3.000	0.204	0.176	0.147	0.179	0.176	0.221
	5	6.100	0.186	0.137	0.161	0.122	0.137	0.186
	6	0.000	0.152	0.112	0.148	0.064	0.112	0.147
	7	0.000	0.117	0.088	0.122	0.028	0.088	0.111
	8	0.000	0.085	0.065	0.095	0.011	0.065	0.080
	9	0.000	0.060	0.042	0.071	0.004	0.042	0.055
	10	0.000	0.041	0.037	0.050	0.001	0.037	0.042
	11	0.000	0.027	0.032	0.037	0.000	0.032	0.032
	12	0.000	0.018	0.026	0.027	0.000	0.026	0.024
	13	0.000	0.012	0.021	0.020	0.000	0.021	0.019
	14	0.000	0.007	0.010	0.015	0.000	0.010	0.011
	15	0.000	0.030	0.000	0.015	0.000	0.000	0.000

Date	Time(h)	P(mm)	NCDI Model			NCGAI model		
			QP(m³/s)	QO(m³/s)	Qregion.	QP(m³/s)	QO(m³/s)	Qregion.
8/28/01	1	0.000	0.041	0.000	0.045	0.009	0.000	0.024
	2	10.600	0.101	0.133	0.013	0.154	0.133	0.133
	3	19.900	0.265	0.310	0.108	0.341	0.310	0.334
	4	8.100	0.295	0.308	0.232	0.369	0.308	0.378
	5	13.600	0.302	0.306	0.270	0.335	0.306	0.380
	6	0.200	0.293	0.278	0.294	0.297	0.278	0.360
	7	0.000	0.275	0.250	0.285	0.254	0.250	0.328
	8	0.000	0.253	0.230	0.268	0.230	0.230	0.303
	9	0.000	0.227	0.210	0.249	0.211	0.210	0.277
	10	0.000	0.202	0.190	0.229	0.198	0.190	0.252
	11	0.000	0.177	0.171	0.210	0.178	0.171	0.227
	12	0.000	0.154	0.153	0.189	0.172	0.153	0.205
	13	0.000	0.133	0.135	0.172	0.158	0.135	0.183
	14	0.000	0.114	0.117	0.154	0.135	0.117	0.159
	15	0.000	0.100	0.100	0.135	0.121	0.100	0.139
	15	0.000	0.083	0.092	0.119	0.095	0.092	0.120
	17	0.000	0.070	0.085	0.101	0.087	0.085	0.107
	18	0.000	0.059	0.077	0.090	0.079	0.077	0.096
	19	0.000	0.049	0.070	0.079	0.069	0.070	0.084
	20	0.000	0.041	0.063	0.070	0.064	0.063	0.075
	21	0.000	0.035	0.055	0.062	0.054	0.055	0.065
	22	0.000	0.029	0.048	0.053	0.047	0.048	0.056
	23	0.000	0.024	0.041	0.046	0.041	0.041	0.048
	24	0.000	0.020	0.034	0.040	0.032	0.034	0.040
	25	0.000	0.016	0.027	0.033	0.028	0.037	0.035
	26	0.000	0.014	0.020	0.028	0.021	0.020	0.026
	27	0.000	0.011	0.013	0.022	0.012	0.013	0.018
	28	0.000	0.009	0.007	0.016	0.009	0.007	0.012
	29	0.000	0.030	0.000	0.015	0.000	0.000	0.000

2. Catchment A4

Date	Time(h)	P(mm)	NCDI Model			NCGAI model		
			QP(m³/s)	QO(m³/s)	Qregion.	QP(m³/s)	QO(m³/s)	Qregion.
3/31/97	1	0.000	0.008	0.000	0.010	0.002	0.000	0.005
	2	0.200	0.076	0.159	0.003	0.122	0.059	0.105
	3	16.700	0.197	0.121	0.092	0.283	0.121	0.203
	4	14.100	0.312	0.283	0.151	0.463	0.283	0.373
	5	8.900	0.385	0.464	0.287	0.408	0.464	0.502
	6	6.100	0.408	0.409	0.352	0.356	0.409	0.483
	7	3.140	0.391	0.355	0.365	0.301	0.355	0.442
	8	0.650	0.348	0.302	0.350	0.253	0.302	0.389
	9	0.800	0.294	0.252	0.317	0.226	0.252	0.335
	10	0.100	0.238	0.227	0.280	0.202	0.227	0.294
	11	0.000	0.187	0.202	0.246	0.155	0.154	0.236
	12	0.000	0.142	0.154	0.206	0.108	0.109	0.180
	13	0.000	0.106	0.109	0.163	0.064	0.065	0.127
	14	0.000	0.077	0.065	0.121	0.022	0.022	0.077
	15	0.000	0.056	0.022	0.082	0.012	0.011	0.046
	16	0.000	0.039	0.011	0.053	0.001	0.000	0.026
	17	0.000	0.030	0.000	0.015	0.000	0.000	0.000

Date	Time(h)	P(mm)	NCDI Model			NCGAI model		
			QP(m³/s)	QO(m³/s)	Qregion.	QP(m³/s)	QO(m³/s)	Qregion.
4/6/97	1	0.000	0.038	0.000	0.042	0.001	0.000	0.020
	2	7.100	0.192	0.140	0.010	0.140	0.140	0.155
	3	11.600	0.356	0.300	0.129	0.305	0.300	0.347
	4	14.400	0.494	0.480	0.243	0.481	0.480	0.544
	5	1.200	0.550	0.681	0.396	0.682	0.681	0.747
	6	0.700	0.552	0.592	0.539	0.594	0.592	0.717
	7	1.200	0.519	0.507	0.533	0.508	0.507	0.644
	8	0.600	0.464	0.426	0.518	0.429	0.426	0.566
	9	1.400	0.401	0.349	0.463	0.347	0.349	0.477
	10	0.480	0.336	0.300	0.404	0.289	0.300	0.407
	11	0.600	0.276	0.252	0.347	0.251	0.252	0.345

12	1.200	0.223	0.206	0.296	0.203	0.206	0.283
13	1.300	0.177	0.162	0.245	0.161	0.162	0.227
14	0.800	0.138	0.140	0.199	0.141	0.140	0.189
15	0.300	0.107	0.119	0.166	0.119	0.119	0.157
16	0.800	0.082	0.098	0.136	0.098	0.098	0.128
17	0.300	0.063	0.078	0.111	0.078	0.078	0.102
19	0.000	0.047	0.058	0.089	0.058	0.058	0.077
20	0.000	0.036	0.038	0.068	0.037	0.038	0.054
21	0.000	0.027	0.019	0.050	0.020	0.019	0.034
22	0.000	0.030	0.000	0.015	0.000	0.000	0.000

Date	Time(h)	P(mm)	NCDI Model			NCGAI model		
			QP(m^3/s)	QO(m^3/s)	Qregion.	QP(m^3/s)	QO(m^3/s)	Qregion.
4/7/97	1	0.000	0.000	0.000	0.001	0.000	0.000	0.000
	2	4.100	0.012	0.018	0.000	0.017	0.018	0.016
	3	10.100	0.065	0.036	0.012	0.038	0.036	0.047
	4	9.000	0.171	0.129	0.035	0.128	0.129	0.148
	5	2.800	0.301	0.242	0.110	0.243	0.242	0.285
	6	2.200	0.414	0.397	0.205	0.396	0.397	0.452
	7	0.000	0.483	0.582	0.329	0.582	0.582	0.640
	8	0.000	0.500	0.493	0.463	0.492	0.493	0.610
	9	0.000	0.474	0.410	0.454	0.411	0.410	0.540
	10	0.000	0.418	0.351	0.440	0.351	0.351	0.478
	11	0.000	0.349	0.296	0.393	0.298	0.296	0.408
	12	0.000	0.279	0.244	0.346	0.245	0.244	0.339
	13	0.000	0.214	0.195	0.290	0.195	0.195	0.272
	14	0.000	0.159	0.164	0.237	0.164	0.164	0.222
	15	0.000	0.115	0.133	0.194	0.135	0.133	0.178
	16	0.000	0.081	0.105	0.155	0.108	0.105	0.139
	17	0.000	0.056	0.077	0.122	0.078	0.077	0.103
	19	0.000	0.038	0.051	0.092	0.052	0.051	0.071
	20	0.000	0.026	0.026	0.066	0.024	0.026	0.042
	21	0.000	0.017	0.013	0.042	0.012	0.013	0.024
	22	0.000	0.030	0.000	0.015	0.000	0.000	0.000

Date	Time(h)	P(mm)	NCDI Model			NCGAI model		
			QP(m^3/s)	QO(m^3/s)	Qregion.	QP(m^3/s)	QO(m^3/s)	Qregion.
4/8/97	1	0.000	0.007	0.000	0.003	0.002	0.000	0.003
	2	0.600	0.129	0.110	0.002	0.055	0.110	0.102
	3	6.200	0.528	0.234	0.074	0.281	0.234	0.338
	4	11.300	1.146	0.587	0.261	0.673	0.587	0.814
	5	2.700	1.796	1.027	0.620	1.077	1.027	1.387
	6	1.700	2.306	2.053	1.040	1.345	2.053	2.199
	7	1.000	2.592	3.418	1.581	1.423	3.418	3.108
	8	0.500	2.648	2.550	2.118	1.335	2.550	2.800
	9	0.000	2.518	1.808	2.029	1.146	1.808	2.327
	10	0.000	2.264	1.501	1.898	0.917	1.501	2.020
	11	0.000	1.947	1.219	1.678	0.694	1.219	1.689
	12	0.000	1.615	1.031	1.439	0.502	1.031	1.405
	13	0.000	1.299	0.855	1.206	0.349	0.855	1.141
	14	0.000	1.018	0.722	0.986	0.235	0.722	0.921
	15	0.000	0.781	0.596	0.795	0.154	0.596	0.731
	16	0.000	0.587	0.506	0.629	0.099	0.506	0.582
	17	0.000	0.435	0.419	0.497	0.062	0.419	0.458
	19	0.000	0.317	0.362	0.386	0.038	0.362	0.366
	20	0.000	0.228	0.307	0.303	0.023	0.307	0.292
	21	0.000	0.162	0.253	0.236	0.014	0.253	0.230
	22	0.000	0.114	0.201	0.183	0.008	0.201	0.177
	23	0.000	0.079	0.150	0.140	0.005	0.150	0.131
	24	0.000	0.055	0.101	0.104	0.003	0.101	0.091
	25	0.000	0.038	0.075	0.075	0.002	0.075	0.066
	26	0.000	0.026	0.050	0.055	0.001	0.050	0.045
	27	0.000	0.017	0.025	0.038	0.000	0.025	0.026
	28	0.000	0.030	0.000	0.015	0.000	0.000	0.000

Date	Time(h)	P(mm)	NCDI Model			NCGAI model		
			QP(m^3/s)	QO(m^3/s)	Qregion.	QP(m^3/s)	QO(m^3/s)	Qregion.
4/9/97	1	0.000	2.289	0.000	2.691	0.168	0.000	1.287
	2	0.200	5.170	2.462	0.614	2.628	2.462	3.334
	3	16.700	6.297	7.606	3.238	6.086	7.606	7.708
	4	4.100	6.417	7.218	5.151	6.288	7.218	8.073
	5	0.960	5.996	6.658	5.790	4.259	6.658	7.340
	6	0.200	5.323	4.456	5.516	2.234	4.456	5.496
	7	0.100	4.568	2.718	4.451	0.987	2.718	3.860
	8	0.000	3.826	2.131	3.447	0.386	2.131	2.980
	9	0.000	3.147	1.611	2.698	0.138	1.611	2.301
	10	0.000	2.553	1.436	2.086	0.046	1.436	1.889
	11	0.000	2.048	1.269	1.683	0.014	1.269	1.571
	12	0.000	1.628	1.110	1.354	0.004	1.110	1.302
	13	0.000	1.284	0.958	1.106	0.001	0.958	1.077
	14	0.000	1.006	0.815	0.899	0.000	0.815	0.884
	15	0.000	0.784	0.679	0.732	0.000	0.679	0.718
	16	0.000	0.608	0.551	0.591	0.000	0.551	0.575
	17	0.000	0.470	0.429	0.473	0.000	0.429	0.450
	18	0.000	0.362	0.370	0.372	0.000	0.370	0.369
	19	0.000	0.277	0.312	0.301	0.000	0.312	0.301
	20	0.000	0.212	0.230	0.240	0.000	0.230	0.228
	21	0.000	0.162	0.152	0.186	0.000	0.152	0.163
	22	0.000	0.123	0.124	0.139	0.000	0.124	0.127
	23	0.000	0.094	0.097	0.108	0.000	0.097	0.099
	24	0.000	0.071	0.048	0.082	0.000	0.048	0.062
	25	0.000	0.030	0.000	0.015	0.000	0.000	0.000

Date	Time(h)	P(mm)	NCDI Model			NCGAI model		
			QP(m^3/s)	QO(m^3/s)	Qregion.	QP(m^3/s)	QO(m^3/s)	Qregion.
4/10/97	1	0.000	0.009	0.000	0.631	0.002	0.000	0.161
	2	1.300	0.090	0.056	0.003	0.058	0.056	0.066
	3	0.420	0.239	0.114	0.209	0.121	0.114	0.199
	4	0.800	0.388	0.364	0.119	0.365	0.364	0.400
	5	11.700	0.492	0.644	0.331	0.646	0.644	0.689
	6	11.600	0.535	0.608	0.475	0.609	0.608	0.709

7	7.700	0.527	0.571	0.521	0.570	0.571	0.690
8	0.900	0.483	0.107	0.536	0.107	0.107	0.335
9	0.000	0.419	0.500	0.304	0.501	0.500	0.556
10	0.000	0.349	0.431	0.489	0.435	0.431	0.534
11	0.000	0.281	0.364	0.380	0.368	0.364	0.439
12	0.000	0.220	0.267	0.375	0.269	0.267	0.350
13	0.000	0.168	0.174	0.284	0.181	0.174	0.245
14	0.000	0.126	0.085	0.225	0.085	0.085	0.151
15	0.000	0.030	0.000	0.015	0.000	0.000	0.000

Date	Time(h)	P(mm)	NCDI Model			NCGAI model		
			QP(m³/s)	QO(m³/s)	Qregion.	QP(m³/s)	QO(m³/s)	Qregion.
4/11/97	1	0.000	0.009	0.000	0.007	0.210	0.000	0.056
	2	0.400	0.090	0.065	0.055	3.285	3.219	1.676
	3	8.400	0.239	0.214	0.859	7.609	9.509	4.583
	4	7.500	0.389	0.304	2.004	7.861	7.381	4.500
	5	2.000	0.492	0.704	2.368	5.325	5.540	3.592
	6	0.000	0.536	0.611	2.116	2.792	3.090	2.286
	7	0.000	0.527	0.529	1.576	1.234	1.299	1.302
	8	0.000	0.483	0.197	1.112	0.483	1.167	0.838
	9	0.000	0.419	0.587	0.662	0.172	1.038	0.698
	10	0.000	0.349	0.393	0.551	0.057	0.875	0.566
	11	0.000	0.281	0.394	0.375	0.018	0.719	0.439
	12	0.000	0.220	0.207	0.303	0.005	0.608	0.351
	13	0.000	0.168	0.192	0.217	0.002	0.500	0.265
	14	0.000	0.126	0.065	0.162	0.000	0.364	0.184
	15	0.000	0.030	0.000	0.015	0.000	0.000	0.000

Date	Time(h)	P(mm)	NCDI Model			NCGAI model		
			QP(m³/s)	QO(m³/s)	Qregion.	QP(m³/s)	QO(m³/s)	Qregion.
1/10/97	1	0.000	0.899	0.000	0.724	0.068	0.000	0.423
	2	11.300	2.041	1.176	0.242	1.064	1.176	1.425
	3	19.400	2.499	3.079	1.251	2.464	3.079	3.093
	4	12.700	2.559	2.555	2.071	2.545	2.555	3.071
	5	8.700	2.404	2.078	2.228	1.724	2.087	2.630

6	1.000	2.146	1.511	2.069	0.904	1.511	2.035
7	0.600	1.851	1.020	1.697	0.400	1.020	1.497
8	0.500	1.559	0.872	1.335	0.156	0.872	1.199
9	0.000	1.289	0.732	1.071	0.056	0.732	0.970
10	0.000	1.051	0.568	0.853	0.019	0.568	0.765
11	0.000	0.848	0.415	0.677	0.006	0.415	0.590
12	0.000	0.677	0.357	0.531	0.002	0.357	0.481
13	0.000	0.537	0.301	0.428	0.001	0.301	0.392
14	0.000	0.423	0.247	0.342	0.000	0.247	0.315
15	0.000	0.332	0.194	0.275	0.000	0.194	0.249
16	0.000	0.259	0.118	0.217	0.000	0.118	0.178
17	0.000	0.201	0.046	0.163	0.000	0.046	0.114
18	0.000	0.155	0.035	0.116	0.000	0.035	0.085
19	0.000	0.120	0.023	0.088	0.000	0.023	0.064
20	0.000	0.092	0.012	0.065	0.000	0.012	0.045
21	0.000	0.030	0.000	0.015	0.000	0.000	0.000

Date	Time (h)	P(mm)	NCDI Model			NCGAI model		
			QP(m³/s)	QO(m³/s)	Qregion.	QP(m³/s)	QO(m³/s)	Qregion.
1/11/97	1	0.000	0.423	0.000	0.524	0.067	0.000	0.254
	2	10.600	1.896	1.168	0.123	0.800	1.168	1.289
	3	19.900	3.105	2.769	1.097	1.906	2.769	2.912
	4	8.100	3.604	3.143	1.976	2.364	3.143	3.557
	5	3.600	3.525	3.540	2.552	2.094	3.540	3.813
	6	0.200	3.114	2.788	2.784	1.514	2.788	3.247
	7	0.000	2.571	2.099	2.492	0.956	2.099	2.554
	8	0.000	2.022	1.358	2.102	0.547	1.358	1.847
	9	0.000	1.534	0.700	1.605	0.292	0.700	1.208
	10	0.000	1.132	0.337	1.157	0.147	0.337	0.778
	11	0.000	0.030	0.000	0.015	0.000	0.000	0.000

3 Catchment AP

Date	Time (h)	P (mm)	NCDI Model			NCGAI model		
			QP (m^3/s)	QO (m^3/s)	Qregion.	QP (m^3/s)	QO (m^3/s)	Qregion.
5/5/98	1	0.000	0.000	0.000	0.000	0.000	0.000	0.000
	2	0.400	0.001	0.000	0.000	0.002	0.000	0.001
	3	8.400	0.003	0.003	0.001	0.004	0.030	0.010
	4	7.500	0.005	0.006	0.003	0.005	0.006	0.006
	5	2.000	0.005	0.005	0.004	0.004	0.005	0.006
	6	0.000	0.004	0.004	0.004	0.003	0.004	0.005
	7	0.000	0.002	0.003	0.004	0.002	0.003	0.003
	8	0.000	0.001	0.002	0.003	0.001	0.002	0.002
	9	0.000	0.001	0.001	0.002	0.001	0.001	0.001
	10	0.000	0.030	0.000	0.015	0.000	0.000	0.000

Date	Time(h)	P(mm)	NCDI Model			NCGAI model		
			QP(m^3/s)	QO(m^3/s)	Qregion.	QP(m^3/s)	QO(m^3/s)	Qregion.
10/4/98	1	0.000	0.123	0.000	0.135	0.079	0.000	0.084
	2	10.600	0.932	1.168	0.051	0.945	1.168	1.066
	3	19.900	2.825	2.769	0.795	2.253	2.769	2.853
	4	8.100	3.450	3.143	1.974	2.794	3.143	3.626
	5	3.600	3.268	3.540	2.546	2.475	3.540	3.842
	6	0.200	2.657	2.788	2.814	1.789	2.788	3.209
	7	0.000	1.951	2.099	2.445	1.129	2.099	2.431
	8	0.000	1.333	1.358	1.998	0.647	1.358	1.674
	9	0.000	0.862	0.700	1.446	0.345	0.700	1.013
	10	0.000	0.535	0.337	0.976	0.174	0.337	0.590
	11	0.000	0.030	0.000	0.015	0.000	0.000	0.000

Date	Time(h)	P(mm)	NCDI Model			NCGAI model		
			QP(m³/s)	QO(m³/s)	Qregion.	QP(m³/s)	QO(m³/s)	Qregion.
7/14/99	1	0.000	0.006	0.000	0.005	0.001	0.000	0.003
	2	11.600	0.067	0.070	0.002	0.021	0.000	0.040
	3	16.900	0.137	0.161	0.041	0.065	0.070	0.126
	4	8.100	0.171	0.212	0.099	0.103	0.192	0.181
	5	10.600	0.166	0.130	0.119	0.118	0.160	0.173
	6	1.980	0.138	0.163	0.128	0.110	0.130	0.167
	7	0.200	0.104	0.091	0.132	0.089	0.163	0.145
	8	0.000	0.073	0.069	0.103	0.066	0.091	0.101
	9	0.000	0.048	0.049	0.085	0.046	0.069	0.074
	10	0.000	0.030	0.031	0.062	0.030	0.049	0.050
	11	0.000	0.019	0.016	0.044	0.018	0.031	0.032
	12	0.000	0.011	0.015	0.029	0.011	0.016	0.020
	13	0.000	0.014	0.014	0.020	0.006	0.015	0.017
	14	0.000	0.004	0.012	0.016	0.004	0.014	0.012
	15	0.000	0.002	0.011	0.010	0.002	0.012	0.009
	16	0.000	0.001	0.010	0.008	0.001	0.011	0.008
	17	0.000	0.001	0.009	0.006	0.001	0.010	0.007
	18	0.000	0.000	0.008	0.005	0.000	0.009	0.005
	19	0.000	0.000	0.006	0.003	0.000	0.008	0.004
	20	0.000	0.000	0.005	0.003	0.000	0.006	0.003
	21	0.000	0.000	0.004	0.002	0.000	0.004	0.003
	22	0.000	0.000	0.003	0.002	0.000	0.003	0.002
	23	0.000	0.000	0.002	0.001	0.000	0.002	0.001
	24	0.000	0.000	0.001	0.001	0.000	0.001	0.001
	25	0.000	0.030	0.000	0.015	0.000	0.000	0.000

Date	Time(h)	P(mm)	NCDI Model			NCGAI model		
			QP(m³/s)	QO(m³/s)	Qregion.	QP(m³/s)	QO(m³/s)	Qregion.
1/12/98	1	0.000	0.001	0.000	0.001	0.001	0.000	0.001
	2	10.600	0.017	0.000	0.001	0.021	0.000	0.010
	3	19.900	0.087	0.070	0.010	0.065	0.070	0.075
	4	8.100	0.153	0.192	0.056	0.103	0.192	0.174
	5	13.600	0.179	0.160	0.114	0.118	0.160	0.183

6	0.200	0.163	0.130	0.128	0.110	0.130	0.165
7	0.000	0.126	0.163	0.129	0.089	0.163	0.168
8	0.000	0.086	0.091	0.127	0.066	0.091	0.115
9	0.000	0.053	0.040	0.093	0.046	0.040	0.068
10	0.000	0.031	0.030	0.066	0.030	0.030	0.047
11	0.000	0.017	0.020	0.046	0.018	0.020	0.030
12	0.000	0.009	0.001	0.030	0.010	0.001	0.013
13	0.000	0.030	0.000	0.015	0.000	0.000	0.000

Date	Time(h)	P(mm)	NCDI Model			NCGAI model		
			QP(m³/s)	QO(m³/s)	Qregion.	QP(m³/s)	QO(m³/s)	Qregion.
5/5/98	1	0.000	0.000	0.000	0.001	0.017	0.000	0.004
	2	3.000	0.003	0.003	0.004	0.252	0.040	0.076
	3	7.200	0.005	0.005	0.065	0.761	0.400	0.309
	4	11.200	0.005	0.005	0.194	1.209	1.130	0.636
	5	1.800	0.004	0.004	0.321	1.379	2.250	0.989
	6	0.100	0.002	0.003	0.395	1.286	1.050	0.684
	7	0.000	0.001	0.002	0.403	1.048	0.900	0.588
	8	0.000	0.001	0.001	0.362	0.776	0.010	0.287
	9	0.000	0.030	0.000	0.015	0.000	0.000	0.000

Date	Time(h)	P(mm)	NCDI Model			NCGAI model		
			QP(m³/s)	QO(m³/s)	Qregion.	QP(m³/s)	QO(m³/s)	Qregion.
10/4/98	1	0.300	0.000	0.000	0.002	0.000	0.000	0.001
	2	5.000	0.003	0.001	0.000	0.004	0.001	0.002
	3	9.100	0.008	0.010	0.003	0.009	0.010	0.010
	4	1.200	0.009	0.008	0.007	0.010	0.008	0.010
	5	0.100	0.007	0.006	0.007	0.007	0.006	0.008
	6	0.000	0.004	0.004	0.007	0.003	0.004	0.005
	7	0.000	0.002	0.003	0.005	0.002	0.003	0.004
	8	0.000	0.001	0.002	0.003	0.001	0.002	0.002
	9	0.000	0.000	0.001	0.002	0.000	0.001	0.001
	10	0.000	0.030	0.000	0.015	0.000	0.000	0.000

Date	Time(h)	P(mm)	NCDI Model			NCGAI model		
			QP(m³/s)	QO(m³/s)	Qregion.	QP(m³/s)	QO(m³/s)	Qregion.
7/9/99	1	0.000	0.002	0.000	0.001	0.002	0.000	0.001
	2	2.600	0.007	0.006	0.001	0.006	0.006	0.007
	3	1.900	0.004	0.006	0.005	0.006	0.006	0.007
	4	0.000	0.007	0.002	0.004	0.004	0.002	0.005
	5	0.000	0.030	0.000	0.015	0.000	0.000	0.000

4 Catchment AR

Date	Time(h)	P(mm)	NCDI Model			NCGAI model		
			QP(m³/s)	QO(m³/s)	Qregion.	QP(m³/s)	QO(m³/s)	Qregion.
4/3/97	1	0.200	0.062	0.000	0.050	0.066	0.000	0.045
	2	16.700	0.256	0.315	0.032	0.172	0.315	0.273
	3	4.100	0.175	0.082	0.198	0.152	0.082	0.172
	4	0.000	0.058	0.069	0.110	0.093	0.069	0.100
	5	0.000	0.014	0.081	0.105	0.048	0.081	0.082
	6	0.000	0.003	0.012	0.063	0.022	0.012	0.028
	7	0.000	0.000	0.012	0.035	0.010	0.012	0.017
	8	0.000	0.000	0.011	0.021	0.004	0.011	0.012
	9	0.000	0.000	0.010	0.013	0.002	0.010	0.009
	10	0.000	0.000	0.009	0.008	0.001	0.009	0.007
	11	0.000	0.000	0.009	0.006	0.000	0.008	0.006
	12	0.000	0.000	0.008	0.004	0.000	0.008	0.005
	13	0.000	0.000	0.007	0.003	0.000	0.007	0.004
	14	0.000	0.000	0.006	0.003	0.000	0.006	0.004
	15	0.000	0.000	0.006	0.002	0.000	0.006	0.004
	16	0.000	0.000	0.005	0.002	0.000	0.005	0.003
	17	0.000	0.000	0.004	0.002	0.000	0.004	0.002
	18	0.000	0.000	0.003	0.002	0.000	0.003	0.002
	19	0.000	0.000	0.003	0.001	0.000	0.003	0.002
	20	0.000	0.000	0.007	0.001	0.000	0.007	0.004
	21	0.000	0.000	0.005	0.002	0.000	0.005	0.003
	22	0.000	0.000	0.002	0.002	0.000	0.002	0.001
	23	0.000	0.030	0.000	0.015	0.000	0.000	0.000

Date	Time(h)	P(mm)	NCDI Model			NCGAI model		
			QP(m³/s)	QO(m³/s)	Qregion.	QP(m³/s)	QO(m³/s)	Qregion.
4/4/97	1	2.000	0.017	0.000	0.012	0.018	0.000	0.012
	2	3.000	0.069	0.085	0.009	0.046	0.085	0.073
	3	5.500	0.047	0.026	0.053	0.041	0.026	0.048
	5	0.000	0.030	0.000	0.015	0.000	0.000	0.000

Date	Time(h)	P(mm)	NCDI Model			NCGAI model		
			QP(m³/s)	QO(m³/s)	Qregion.	QP(m³/s)	QO(m³/s)	Qregion.
4/5/97	1	16.100	0.014	0.000	0.110	0.010	0.000	0.034
	2	1.000	0.144	0.112	0.006	0.081	0.112	0.114
	3	0.200	0.204	0.238	0.112	0.129	0.238	0.230
	4	0.000	0.125	0.084	0.144	0.105	0.084	0.136
	5	0.000	0.049	0.048	0.106	0.060	0.048	0.078
	6	0.000	0.015	0.019	0.075	0.028	0.019	0.039
	7	0.000	0.030	0.000	0.015	0.000	0.000	0.000

Date	Time(h)	P(mm)	NCDI Model			NCGAI model		
			QP(m³/s)	QO(m³/s)	Qregion.	QP(m³/s)	QO(m³/s)	Qregion.
4/10/97	1	0.500	0.052	0.000	0.042	0.054	0.000	0.037
	2	2.000	0.563	0.441	0.027	0.456	0.441	0.482
	3	8.500	0.866	1.345	0.376	0.726	1.345	1.164
	4	10.500	0.810	0.783	0.741	0.591	0.783	0.927
	5	2.800	0.352	0.353	0.640	0.341	0.383	0.517
	6	0.000	0.118	0.221	0.447	0.160	0.221	0.292
	7	0.000	0.033	0.116	0.285	0.065	0.116	0.154
	8	0.000	0.008	0.091	0.165	0.024	0.091	0.095
	9	0.000	0.002	0.069	0.102	0.008	0.069	0.062
	10	0.000	0.000	0.049	0.061	0.003	0.049	0.041
	11	1.200	0.000	0.029	0.038	0.001	0.029	0.024
	12	0.800	0.000	0.012	0.023	0.000	0.012	0.012
	13	0.000	0.030	0.000	0.015	0.000	0.000	0.000

Date	Time(h)	P(mm)	NCDI Model			NCGAI model		
			QP(m³/s)	QO(m³/s)	Qregion.	QP(m³/s)	QO(m³/s)	Qregion.
6/19/97	1	0.000	0.003	0.000	0.245	0.001	0.000	0.062
	2	1.300	0.082	0.000	0.001	0.019	0.000	0.026
	3	0.800	0.318	0.013	0.087	0.096	0.013	0.132
	4	4.200	0.568	0.019	0.107	0.230	0.019	0.236
	5	11.700	0.673	0.207	0.226	0.367	0.207	0.420
	6	11.600	0.621	1.035	0.339	0.459	1.035	0.872
	7	7.700	0.484	1.973	0.585	0.485	1.973	1.375
	8	0.900	0.335	1.074	0.820	0.455	1.074	0.940
	9	0.000	0.211	0.111	0.612	0.391	0.111	0.359
	10	0.000	0.124	0.056	0.383	0.313	0.056	0.233
	11	0.000	0.069	0.015	0.276	0.237	0.015	0.153
	12	0.000	0.037	0.001	0.176	0.171	0.001	0.097
	13	0.000	0.030	0.000	0.015	0.000	0.000	0.000

Date	Time(h)	P(mm)	NCDI Model			NCGAI model		
			QP(m³/s)	QO(m³/s)	Qregion.	QP(m³/s)	QO(m³/s)	Qregion.
4/21/97	1	0.000	0.031	0.000	0.281	0.003	0.000	0.079
	2	2.000	0.062	0.100	0.009	0.044	0.100	0.079
	3	14.200	0.207	0.217	0.122	0.103	0.217	0.216
	4	3.100	0.183	0.176	0.134	0.106	0.176	0.194
	5	6.100	0.148	0.137	0.147	0.072	0.137	0.160
	6	2.700	0.114	0.112	0.123	0.038	0.112	0.125
	7	0.000	0.084	0.088	0.103	0.017	0.088	0.095
	8	0.000	0.061	0.065	0.078	0.007	0.065	0.069
	9	0.000	0.044	0.042	0.059	0.002	0.042	0.047
	10	0.000	0.031	0.037	0.041	0.001	0.037	0.037
	11	0.000	0.021	0.032	0.032	0.000	0.032	0.029
	12	0.000	0.015	0.026	0.024	0.000	0.026	0.023
	13	0.000	0.010	0.021	0.018	0.000	0.021	0.018
	14	0.000	0.030	0.000	0.015	0.000	0.000	0.000

Date	Time(h)	P(mm)	NCDI Model			NCGAI model		
			QP(m^3/s)	QO(m^3/s)	Qregion.	QP(m^3/s)	QO(m^3/s)	Qregion.
6/19/97	1	0.000	0.003	0.000	0.245	0.001	0.000	0.062
	2	1.300	0.082	0.000	0.001	0.019	0.000	0.026
	3	0.800	0.318	0.013	0.087	0.096	0.013	0.132
	4	4.200	0.568	0.019	0.107	0.230	0.019	0.236
	5	11.700	0.673	0.207	0.226	0.367	0.207	0.420
	6	11.600	0.621	1.035	0.339	0.459	1.035	0.872
	7	7.700	0.484	1.973	0.585	0.485	1.973	1.375
	8	0.900	0.335	1.074	0.820	0.455	1.074	0.940
	9	0.000	0.211	0.111	0.612	0.391	0.111	0.359
	10	0.000	0.124	0.056	0.383	0.313	0.056	0.233
	11	0.000	0.069	0.015	0.276	0.237	0.015	0.153
	12	0.000	0.037	0.001	0.176	0.171	0.001	0.097
	13	0.000	0.030	0.000	0.015	0.000	0.000	0.000

Date	Time(h)	P(mm)	NCDI Model			NCGAI model		
			QP(m^3/s)	QO(m^3/s)	Qregion.	QP(m^3/s)	QO(m^3/s)	Qregion.
4/21/97	1	0.000	0.031	0.000	0.281	0.003	0.000	0.079
	2	2.000	0.062	0.100	0.009	0.044	0.100	0.079
	3	14.200	0.207	0.217	0.122	0.103	0.217	0.216
	4	3.100	0.183	0.176	0.134	0.106	0.176	0.194
	5	6.100	0.148	0.137	0.147	0.072	0.137	0.160
	6	2.700	0.114	0.112	0.123	0.038	0.112	0.125
	7	0.000	0.084	0.088	0.103	0.017	0.088	0.095
	8	0.000	0.061	0.065	0.078	0.007	0.065	0.069
	9	0.000	0.044	0.042	0.059	0.002	0.042	0.047
	10	0.000	0.031	0.037	0.041	0.001	0.037	0.037
	11	0.000	0.021	0.032	0.032	0.000	0.032	0.029
	12	0.000	0.015	0.026	0.024	0.000	0.026	0.023
	13	0.000	0.010	0.021	0.018	0.000	0.021	0.018
	14	0.000	0.030	0.000	0.015	0.000	0.000	0.000

Date	Time(h)	P(mm)	NCDI Model			NCGAI model		
			QP(m³/s)	QO(m³/s)	Qregion.	QP(m³/s)	QO(m³/s)	Qregion.
4/25/97	1	0.000	0.017	0.000	0.211	0.010	0.000	0.060
	2	7.400	0.221	0.200	0.007	0.154	0.200	0.195
	3	9.900	0.427	0.433	0.197	0.357	0.433	0.462
	4	8.800	0.364	0.755	0.306	0.369	0.755	0.637
	5	1.300	0.202	0.092	0.421	0.250	0.092	0.264
	6	0.000	0.087	0.025	0.212	0.131	0.025	0.120
	7	0.200	0.031	0.010	0.166	0.058	0.010	0.069
	8	0.000	0.030	0.000	0.015	0.000	0.000	0.000

Date	Time(h)	P(mm)	NCDI Model			NCGAI model		
			QP(m³/s)	QO(m³/s)	Qregion.	QP(m³/s)	QO(m³/s)	Qregion.
6/7/97	1	0.000	0.079	0.000	0.050	0.136	0.000	0.066
	2	4.100	0.757	0.500	0.054	0.659	0.500	0.617
	3	0.500	1.005	1.500	0.492	0.793	1.500	1.322
	4	0.100	0.575	0.450	0.838	0.565	0.450	0.719
	5	0.000	0.030	0.000	0.015	0.000	0.000	0.000

Date	Time(h)	P(mm)	NCDI Model			NCGAI model		
			QP(m³/s)	QO(m³/s)	Qregion.	QP(m³/s)	QO(m³/s)	Qregion.
6/15/97	1	0.000	0.149	0.000	0.152	0.245	0.000	0.137
	2	8.100	1.402	0.900	0.099	1.191	0.900	1.123
	3	1.800	1.823	2.710	0.911	1.432	2.710	2.397
	4	0.800	1.019	0.620	1.516	1.021	0.620	1.199
	5	0.500	0.368	0.054	0.893	0.560	0.054	0.482
	6	0.200	0.102	0.029	0.624	0.263	0.029	0.262
	7	0.000	0.030	0.000	0.015	0.000	0.000	0.000

Date	Time (h)	P (mm)	NCDI Model			NCGAI model		
			QP (m^3/s)	QO (m^3/s)	Qregion.	QP (m^3/s)	QO (m^3/s)	Qregion.
6/15/97	1	0.000	0.029	0.000	0.310	0.027	0.000	0.092
	2	4.500	0.444	0.300	0.014	0.425	0.300	0.371
	3	3.000	1.008	1.001	0.370	0.985	1.001	1.091
	4	5.000	1.020	2.083	0.752	1.018	2.083	1.739
	5	0.700	0.676	0.813	1.123	0.689	0.813	1.028
	6	0.000	0.347	0.020	0.733	0.361	0.200	0.415
	7	0.000	0.150	0.086	0.463	0.160	0.086	0.236
	8	0.000	0.057	0.005	0.282	0.063	0.005	0.103
	9	0.000	0.030	0.000	0.015	0.000	0.000	0.000

5 Catchment AQ

Date	Time (h)	P (mm)	NCDI Model			NCGAI model		
			QP (m^3/s)	QO (m^3/s)	Qregion.	QP (m^3/s)	QO (m^3/s)	Qregion.
4/3/97	1	0.000	0.008	0.000	0.005	0.010	0.000	0.006
	2	0.400	0.013	0.000	0.005	0.149	0.000	0.042
	3	0.500	0.319	0.320	0.042	0.344	0.320	0.336
	4	0.700	0.351	0.430	0.247	0.355	0.430	0.453
	5	0.000	0.253	0.230	0.294	0.241	0.230	0.312
	6	0.000	0.142	0.070	0.243	0.126	0.070	0.163
	7	0.000	0.067	0.040	0.158	0.056	0.040	0.090
	9	0.000	0.030	0.000	0.015	0.000	0.000	0.000

Date	Time (h)	P (mm)	NCDI Model			NCGAI model		
			QP (m^3/s)	QO (m^3/s)	Qregion.	QP (m^3/s)	QO (m^3/s)	Qregion.
4/5/97	1	0.000	0.020	0.000	0.024	0.036	0.000	0.020
	2	2.600	0.383	0.000	0.014	0.427	0.000	0.206
	3	5.700	1.098	0.670	0.208	1.018	0.970	0.991
	4	0.100	1.421	1.890	0.700	1.262	1.890	1.791
	5	0.400	1.212	1.210	1.195	1.118	1.210	1.486
	6	0.000	0.802	0.650	1.060	0.808	0.650	0.993
	7	0.000	0.448	0.450	0.864	0.510	0.450	0.680
	8	0.000	0.220	0.280	0.617	0.292	0.280	0.422
	9	0.000	0.100	0.130	0.414	0.156	0.130	0.232
	10	0.000	0.030	0.000	0.015	0.000	0.000	0.000

Date	Time (h)	P (mm)	NCDI Model			NCGAI model		
			QP (m³/s)	QO (m³/s)	Qregion.	QP (m³/s)	QO (m³/s)	Qregion.
4/7/97	1	0.000	0.021	0.000	0.019	0.040	0.000	0.020
	2	8.500	0.398	0.000	0.015	0.479	0.000	0.223
	3	17.100	1.172	0.500	0.224	1.142	0.050	0.772
	4	6.000	1.560	2.120	0.707	1.416	2.120	1.981
	5	4.400	1.368	1.210	1.330	1.254	1.210	1.593
	6	1.200	0.932	0.630	1.135	0.907	0.630	1.058
	7	0.700	0.536	0.060	0.950	0.572	0.060	0.544
	8	1.200	0.273	0.060	0.576	0.328	0.060	0.324
	9	0.600	0.127	0.060	0.403	0.175	0.060	0.206
	10	1.400	0.055	0.050	0.234	0.088	0.050	0.119
	11	0.480	0.023	0.050	0.149	0.042	0.050	0.078
	12	0.600	0.009	0.050	0.087	0.020	0.050	0.054
	13	1.200	0.003	0.040	0.057	0.009	0.040	0.037
	14	1.300	0.001	0.040	0.035	0.004	0.040	0.030
	15	0.800	0.000	0.040	0.025	0.002	0.040	0.027
	16	0.300	0.000	0.040	0.019	0.001	0.040	0.025
	17	0.800	0.000	0.030	0.017	0.000	0.030	0.019
	18	0.300	0.000	0.030	0.012	0.000	0.030	0.018
	19	0.000	0.000	0.030	0.012	0.000	0.030	0.018
	20	0.000	0.000	0.030	0.011	0.000	0.030	0.018
	21	0.000	0.000	0.020	0.010	0.000	0.020	0.013
	22	0.000	0.000	0.020	0.008	0.000	0.020	0.012
	23	0.000	0.000	0.020	0.008	0.000	0.020	0.012
	24	0.000	0.000	0.010	0.007	0.000	0.010	0.007
	25	0.000	0.000	0.010	0.004	0.000	0.010	0.006
	26	0.000	0.000	0.010	0.004	0.000	0.010	0.006
	27	0.000	0.030	0.000	0.015	0.000	0.000	0.000

Date	Time (h)	P (mm)	NCDI Model			NCGAI model		
			QP(m³/s)	QO (m³/s)	Qregion.	QP (m³/s)	QO (m³/s)	Qregion.
4/9/97	1	0.000	0.001	0.000	0.001	0.003	0.000	0.001
	2	3.400	0.023	0.000	0.001	0.036	0.000	0.015
	3	3.100	0.073	0.090	0.015	0.086	0.090	0.089
	4	1.100	0.107	0.160	0.063	0.107	0.160	0.149
	5	0.300	0.104	0.150	0.097	0.095	0.150	0.149

6	0.000	0.078	0.110	0.103	0.068	0.110	0.117
7	0.000	0.049	0.080	0.088	0.043	0.080	0.085
8	0.000	0.028	0.050	0.069	0.025	0.050	0.055
9	0.000	0.014	0.030	0.048	0.013	0.030	0.034
10	0.000	0.007	0.010	0.031	0.007	0.010	0.016
11	0.000	0.003	0.010	0.018	0.003	0.010	0.011
12	0.000	0.001	0.010	0.012	0.001	0.010	0.008
13	0.000	0.001	0.010	0.007	0.001	0.010	0.007
14	0.000	0.030	0.000	0.015	0.000	0.000	0.000

Date	Time(h)	P(mm)	NCDI Model			NCGAI model		
			QP(m³/s)	QO(m³/s)	Qregion.	QP(m³/s)	QO(m³/s)	Qregion.
11/9/97	1	0.000	0.054	0.000	0.045	0.068	0.000	0.042
	2	8.100	0.488	0.200	0.031	0.572	0.200	0.373
	3	0.100	0.849	1.000	0.326	0.913	1.000	1.022
	4	2.300	0.757	0.400	0.698	0.744	0.400	0.750
	5	2.200	0.479	0.340	0.557	0.430	0.340	0.536
	6	0.000	0.247	0.160	0.487	0.202	0.160	0.314
	7	0.000	0.111	0.090	0.291	0.083	0.090	0.166
	8	0.000	0.045	0.040	0.193	0.031	0.040	0.087
	9	0.000	0.017	0.030	0.102	0.011	0.030	0.047
	10	0.000	0.006	0.020	0.063	0.003	0.020	0.028
	11	0.000	0.002	0.010	0.033	0.001	0.001	0.012
	12	0.000	0.030	0.000	0.015	0.000	0.000	0.000

Date	Time(h)	P(mm)	NCDI Model			NCGAI model		
			QP(m³/s)	QO(m³/s)	Qregion.	QP(m³/s)	QO(m³/s)	Qregion.
4/23/97	1	0.000	0.016	0.000	0.016	0.038	0.000	0.018
	2	0.850	0.326	0.060	0.014	0.456	0.060	0.229
	3	1.700	1.008	0.700	0.215	1.088	0.700	0.928
	4	3.600	1.415	1.160	0.702	1.349	1.160	1.447
	5	0.000	1.311	2.020	1.035	1.195	2.021	1.895
	6	0.000	0.943	0.610	1.307	0.864	0.610	1.084
	7	0.000	0.573	0.111	0.863	0.545	0.111	0.551
	8	0.000	0.308	0.009	0.634	0.312	0.009	0.318
	9	0.000	0.030	0.000	0.015	0.000	0.000	0.000

Date	Time(h)	P(mm)	NCDI Model			NCGAI model		
			QP(m^3/s)	QO(m^3/s)	Qregion.	QP(m^3/s)	QO(m^3/s)	Qregion.
6/19/97	1	0.000	0.009	0.000	0.006	0.014	0.000	0.007
	2	1.100	0.206	0.080	0.006	0.206	0.080	0.144
	3	2.000	0.745	0.250	0.124	0.624	0.250	0.498
	4	14.500	1.230	0.750	0.406	0.991	0.750	1.032
	5	3.000	1.345	2.180	0.774	1.131	2.180	1.902
	6	6.100	1.145	1.070	1.266	1.054	1.070	1.401
	7	2.700	0.823	0.500	1.011	0.859	0.500	0.923
	8	0.000	0.525	0.040	0.862	0.636	0.040	0.526
	9	0.000	0.305	0.030	0.553	0.438	0.030	0.339
	10	0.000	0.166	0.030	0.409	0.285	0.030	0.230
	11	0.000	0.085	0.030	0.258	0.177	0.030	0.145
	12	0.000	0.042	0.020	0.175	0.106	0.020	0.091
	13	0.000	0.020	0.020	0.107	0.062	0.020	0.057
	14	0.000	0.009	0.020	0.069	0.035	0.020	0.038
	15	0.000	0.004	0.020	0.043	0.019	0.020	0.026
	16	0.000	0.002	0.010	0.028	0.011	0.010	0.015
	17	0.000	0.001	0.010	0.016	0.006	0.010	0.011
	18	0.000	0.000	0.010	0.011	0.003	0.010	0.009
	19	0.000	0.000	0.010	0.007	0.002	0.010	0.007
	20	0.000	0.030	0.000	0.015	0.000	0.000	0.000

Date	Time(h)	P(mm)	NCDI Model			NCGAI model		
			QP(m^3/s)	QO(m^3/s)	Qregion.	QP(m^3/s)	QO(m^3/s)	Qregion.
6/20/97	1	0.300	0.413	0.030	0.102	0.810	0.030	0.346
	2	17.900	2.416	1.940	0.313	2.160	1.940	2.192
	3	0.000	2.511	2.390	1.655	1.943	2.390	2.722
	4	0.000	1.300	0.520	1.789	1.218	0.520	1.337
	5	0.000	0.473	0.200	1.173	0.640	0.200	0.672
	6	0.000	0.140	0.040	0.776	0.303	0.040	0.325
	7	0.000	0.030	0.000	0.015	0.000	0.000	0.000

Date	Time(h)	P(mm)	NCDI Model			NCGAI model		
			QP(m^3/s)	QO(m^3/s)	Qregion.	QP(m^3/s)	QO(m^3/s)	Qregion.
7/10/97	1	2.300	0.255	0.000	0.200	0.340	0.000	0.199
	2	4.100	3.045	1.580	0.149	2.873	1.500	2.287
	3	9.800	5.202	5.010	1.925	4.579	5.010	5.431
	4	3.900	3.891	2.450	3.735	3.723	2.450	4.062
	5	0.000	1.895	0.720	2.997	2.147	0.720	2.120
	6	0.000	0.712	0.130	2.124	1.006	0.130	1.026
	7	0.000	0.225	0.070	1.211	0.411	0.070	0.497
	8	0.000	0.063	0.050	0.708	0.152	0.050	0.256
	9	0.000	0.016	0.030	0.369	0.052	0.030	0.124
	10	0.000	0.004	0.010	0.201	0.017	0.010	0.061
	11	0.000	0.030	0.000	0.015	0.000	0.000	0.000